CRUISE REPORT

Vent Discovery and Petrological Sampling of the Lau Back-Arc Basin

R/V Kilo Moana Cruise KM 0417

September 10 – October 15, 2004

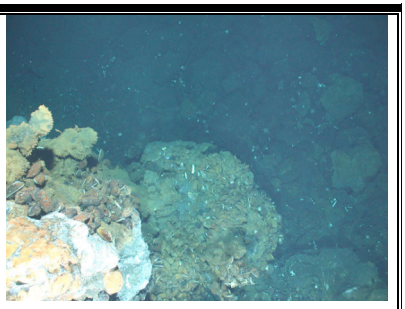

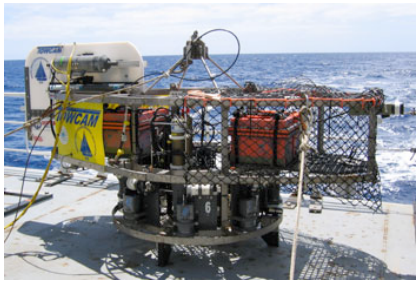

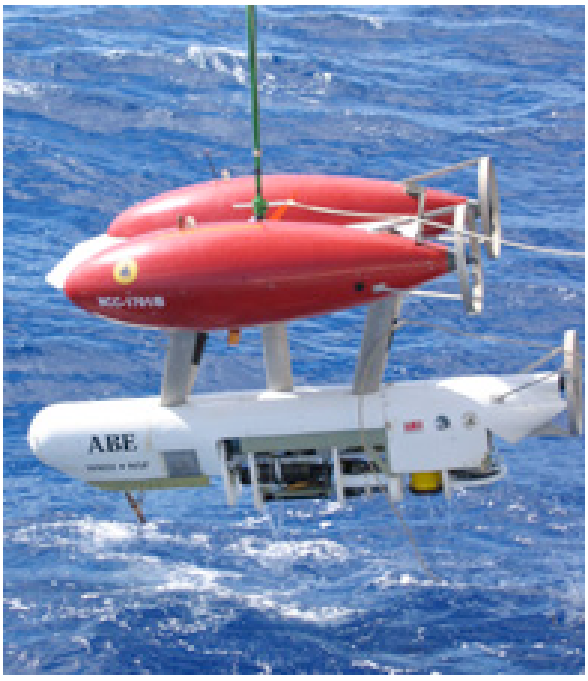

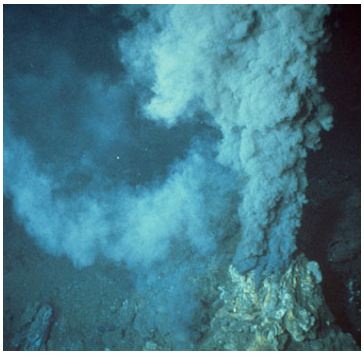

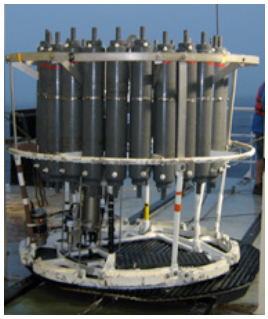

TABLE OF CONTENTS

TABLE OF FIGURES

LIST OF TABLES

LIST OF APPENDICES

ACKNOWLEDGEMENTS

This cruise could only take place through the planning efforts of dozens of people in the ridge community who participated in workshops and developed the vision that was to be realized by the series of four cruises. Our cruise in particular was based on the data collected by the Martinez cruise, and the maps and water column information they collected and made available to us were the essential precursor for all of our investigations. The Ridge 2000 planning office also made substantial efforts in supporting this program in many ways, including development of relations with the Republic of Tonga and support and implementation of the education and outreach effort. All the programs depend on the support of the National Science Foundation, and the engaged program management of David Epp.

Science at sea depends on the effective management of ship operations, and we were helped in all aspects of our program by the Hawaii Institute of Geophysics, who made special efforts to make sure the diverse and particular aspects of our program could be accomplished. At sea, Captain Gray Drewry and the crew of Kilo Moana were consistently supportive and helpful in all science operations, well beyond what was required. Gabe Foreman and Kuhio Vellalos had to maintain 24 hour readiness for deck operations, and all the station work was dependent on their help and participation.

We recognize and appreciate all this work by others that enabled our program.

Responsibilities of Personnel*

Chief Scientist:	Charles Langmuir[1]
ABE Group:	Dana Yoerger[2], Al Bradley[2], Rod Catenach[2], Mike Jakuba[2]
Water Column, CTD's and Water Chemistry:	Chris German[3], Doug Connelly[3], Ralf Pren[3], John Breier[4], Amy Townsend[4]-Small, Craig Aumack[4], Charlotte Goddard[5]
Rock Sampling and Processing:	Charles Langmuir[1], Peter Michael[6], Paul Asimow[7], Elizabeth Gier[1], Stephane Escrig[1], Antoine Bezos[1], Andrew Matzen[6], Tiffany Ying[1]
Rock Chemical Analysis:	Susan Woods[1]
TowCam Operations:	Dan Fornari[2], Tim Shank[2]
Multibeam Bathymetry and Sidescan:	Margo Edwards[8]
GIS Development:	Andrew Matzen[6], Margo Edwards[8]
Biology:	Tim Shank[2]
Watch Leaders:	Dan Fornari[2], Chris German[3], Peter Michael[6], Tim Shank[2]
Education and Outreach:	Kristen Kusek[9]
On Shore PI's:	Hedy Edmonds[4], Steve Goldstein[10], Dave Graham[5]

1. Department of Earth & Planetary Sciences, Harvard University, 20 Oxford Street, Cambridge, MA 02138
2. Woods Hole Oceanographic Institution, Co-op Building MD#16, Woods Hole, MA 02543
3. Southampton Oceanography Center, Empress Dock, Southampton, SO14 3ZH, UK
4. Marine Science Institute, University of Texas at Austin, 750 Channel View Drive, Port Aransas, TX 78373
5. College of Oceanic Atmospheric Sciences at Oregon State University, 104 COAS Admin Building, Corvallis, OR 97331

6. Department of Geosciences, University of Tulsa, 600 S. College Ave., Tulsa, OK 74101
7. Geology & Planetary Sciences, Caltech, 1200 E. California Blvd., Pasadena, CA 91125
8. School of Ocean & Earth Science & Technology, University of Hawaii, 1680 East-West Road, POST 802, Honolulu, HI 96822
9. Ridge 2000, Penn State University, Department of Biology, 208 Mueller Lab, University Park, PA 16802
10. Lamont-Doherty Earth Observatory, Columbia University, P.O. Box 1000 61 Route 9W, Palisades, NY 10964

* Email contacts for personnel as of early 2005 are given in Appendix 17 of this report.

INTRODUCTION

Cruise KM0417 was the second leg of a four cruise exploratory investigation of the spreading centers of the Lau Basin, in order to develop an integrated study site for the Ridge 2000 (R2K) program. An integrated study site has the aim of studying the ridge formation process "from mantle to microbe", including the processes of melt generation in the mantle, the creation of the solid ocean crust, the interaction of volcanic systems with seawater to create hydrothermal vents, and the biological communities and water column plumes that arise from these vents. To carry out these studies requires finding vent sites that provide the environment for life.

The scientific excitement about the Lau Basin in general, and the Eastern Lau Spreading Center (ELSC) in particular is that the ELSC lies at varying distance from the volcanic front of the Tonga Arc as one proceeds along its length.

Finding and investigating vents is not a trivial task—vent fields of 100m on a side may exist only every hundred km or so along the ridge, so their discovery is a bit like finding a needle in a haystack. The four cruises are carrying out a staged approach to vent discovery and exploration. The first cruise, carried out by R/V Kilo Moana in April, 2004 (Fernando Martinez, chief scientist), obtained high resolution maps of the ridge axis, and also towed a group of miniature autonomous plume recorders (MAPRs) that gave an indication of optical backscatter in the water column along the entire length of the axis. The MAPR data identified regions of the ridge where hydrothermal activity was likely to exist, and narrowed the search to a number of regions of about 2km by 8km. These data were provided to us prior to publication for planning purposes for our expedition, and were indispensable to the success of our program.

The primary job of KM0417 was to find and map the vents, which would then be investigated in detail by hydrothermal chemists and biologists on cruises three and four, to take place in 2005. In a pre-cruise meeting, we met with scientists from the previous leg in order to assimilate and discuss the map and MAPR data that they had collected. This meeting, attended by the chief scientists of all four cruises, as well as the principal investigators of KM0417, identified five target sites along the length of the Eastern Lau Spreading Center that were proposed to be the focus of our expedition. A sixth site would be selected as well, time permitting, and indeed we were able to investigate six sites during KM0417. The aim was to find at least two, and perhaps as many as four, vent fields. Ideally one of the vent fields would be hosted on basalt rock at greater depths in the northern parts of the study area, and another would be on andesitic rock at shallow depths in the south. This would then provide a diversity of environments to act as a "natural experiment" to understand the effects of depth and crustal composition on the vent systems and their associated biological communities. The site map for the Lau Basin and a map indicating the six target sites is given as Figure 1-A.

The second major task of KM0417 was to carry out regional rock sampling of the ridge and off-axis seamounts in order to better define the composition of the ocean crust and understand the mantle and volcanic processes that give rise to the crustal diversity. While plumes in the water column were already investigated in cruise 1, and hydrothermal activity would be investigated in ever greater detail on cruises three and four, KM0417 was the sole cruise with the aim of crustal composition, and therefore this aim was given a high priority in the review and cruise planning process.

CRUISE PLAN

The pioneering aspect of KM-0417 was the attempt to use autonomous underwater vehicle technology to find hydrothermal vents. While AUV's had been used in known vent areas previously, no previous cruise had undertaken a systematic and phased approach to vent exploration. Because this approach was unproven and of high risk, we also had on board the conventional methods of CTD's and towed camera systems if for some reason the AUV methodology proved unsuccessful.

The Autonomous Benthic Explorer (ABE) run by the Woods Hole Oceanographic Institution was our exploration vehicle, and it was used in three different phases that corresponded with increasing refinement of our vent search. On arrival at each of our six target sites, we carried out CTD "Tow-yos" in order to confirm the plumes identified by the MAPR surveys and to determine the current depth of the plume, usually some 200-300 meters above the bottom. ABE was then deployed in Phase I to map the plume at this depth, and sometimes at two different depths. There was a trade-off between the amount of area that could be covered, the line spacing flown by ABE, generally 100 - 200m, and how many different depths could be investigated. This aspect of the survey was to identify where the plume was most intense, and the aim was also to use chemical sensors on ABE to help determine distance within the plume to the likely plume source. Because we were not able to obtain the full suite of chemical sensor data, we had to rely on other sensors and perturbations in depth to estimate where the plume intensity was largest.

The plume data collected roughly 200 meters off the bottom in Phase 1 were then used to define a smaller region for Phase II. Phase II was carried out at 30-60 meter line spacings, 50 meters above the bottom. The aim of Phase II was to intersect the buoyant stem of the plume, as seen in clear "hits" in optical backscatter, Eh sensor and upward deflections of the vehicle path. Phase II also used the SM2000 system to produce very high resolution maps of the sea floor.

The combination of the geological information from the maps, the "hits" in the water column data, and estimates of water movement from other ABE measurements was to enable estimates of exact vent locations on the sea floor. These hypothetical locations were then the targets of Phase III, where ABE flew 5 meters off the bottom taking pictures of the sea floor, with the aim of revealing specific vent locations and animal communities.

As a supplement to this process, we had the towed camera system, TowCam, also run out of Woods Hole Oceanographic Institution. TowCam is able to identify the youngest region of the sea floor—often optimal for vent locations—and also has higher resolution photographic capability than ABE. Therefore TowCam was useful in both reconnaissance mode, and as a final step of high photographic resolution of vent sites.

Because ABE is an autonomous vehicle, during its deployment it was possible to obtain rock samples nearby, and during battery charges and transit between sites it was possible to obtain more regional coverage. Thus rock sampling and ABE deployment were highly synergistic, particularly because the percussion coring method takes only an hour of ship time, and delays in ABE deployment or dive time could be accommodated by the sampling program.

PRINCIPAL RESULTS

We steamed out of Fiji to the northern end of our study area, and carried out a series of Phase I surveys as we headed south along the ELSC. The Phase I dives are summarized in the ABE section of the report. There was a planned rendezvous with the Japanese Sweep-Vents cruise in the southernmost part of our study region, the Valu Fa area. The Japanese planned dives with the Shinkai 6500, and were anxious to learn of our results prior to their dive program. The time constraints meant we had to be efficient in the Phase I part of our program in order to have completed our surveys of Valu Fa prior to the Japanese dive program.

At site 2, near 20° 19'S, we had the good fortune of having a TowCam run that extended to just outside the area being surveyed by ABE, and discovered hydrothermal venting in the center of the rift valley. This site was later named "TowCam" and served as the focus for Phase II and III dives in the region.

The most likely site in the south was a series of vigorous plumes identified on several earlier cruises, that seemed to be centered on the eastern limb of the overlapping spreading center located near 22° 10'S. We carried out three ABE dives in this region, creating two dimensional maps of the plume in the water column, and high resolution SM2000 maps of the sea floor. In order not to duplicate effort, we provided the Japanese with all our data, and suggested dive waypoints for their first dive in the region. The Shinkai 6500 followed the dive track, and just beyond our last way-point they discovered a vigorous hydrothermal field, named "Mariner." The maps and observations of the Japanese are being made available to the subsequent Lau cruises. While our expedition did not find and photograph this site, the ABE data contributed to its discovery.

We also carried out ABE dives, CTD Tow-yos and TowCam runs at site 6, located on the shallowest point along the western limb of the same overlapping spreading center. There was a strong plume in the water column at a depth of 1450 meters, suggesting hydrothermal activity at a depth of 1650-1700 meters, a depth found only at the summit of the western limb of the overlapper. This plume was seen in the MAPR data of the Martinez cruise and in CTD tow-yos undertaken prior to our cruise. CTD casts confirmed the presence of the plume, and localized its presence to near the summit of the western limb. A TowCam run, however, found only discolored sediment and no significant hydrothermal activity. Three subsequent dives by the Japanese also did not find active hydrothermal venting at site 6. Nothing that was found in this location, however, would account for the location and depth of the hydrothermal plumes, therefore sites may exist there that remain undiscovered.

Following the rendezvous with the Japanese and discovery of the Mariner vent field, we headed north and returned to site 2, where we had a known vent. Because of the complexities of the water column data that we encountered at Site 5, we planned a dive that would include portions at all three depths encompassed by Phases I-II-III in order to see how well the data from one level in the water column was reflected at the others. This dive was only partially successful because equipment problems led to a lack of optical backscatter and Eh data.

The Phase I data at sites 1 and 3 indicated clear interception of active plumes in the water column, and therefore we concentrated on these sites to discover new vent fields. The Phase I-II-III sequence for these sites succeeded as envisaged, and we

discovered two active vent fields, the "Kilo Moana" vent field near 20° 03'S, and the "ABE" vent field near 20° 46'S.

Thus our work (with ABE and TowCam) and the collaborative effort with the Japanese led to the discovery of four hydrothermal fields spanning the entire range of spreading parameters along the ELSC, and accomplished the objectives laid out in the Ridge 2000 planning documents.

We also were able to occupy more than two hundred sampling stations, with most of the sampling done during ABE dives, ABE battery recharge and occasional ABE down time. Sixty-two dredges and one hundred forty-five rock cores led to the most completely sampled back-arc spreading center. Locations and descriptions are given in Appendices 1 – 5. This sampling was guided by on-board geochemical data, which allowed us to identify the regions of principal geochemical gradients and to sample them more densely. The on-board data also demonstrated that the "ABE" vent field occurred on andesitic host rock, while "Towcam" and "Kilo Moana" were hosted on basalt. Therefore the three sites in the northern region encompassed most of the range of rock compositions that makes the Lau Basin of particular interest for subsequent hydrothermal and biological investigations.

Having successfully accomplished our objectives, at the end of the cruise we undertook additional exploration of the Fonualei Rifts spreading center. This spreading center has a similar natural setting to the ELSC, since it begins at its southern extremity very close to the Tonga arc, and is progressively more distant from the arc towards the north. The angle of the spreading center to the arc is greater than for the ELSC. We occupied 25 sampling stations on the Fonualei Rifts, and identified several sites of intense plumes in the water column. Data from the Fonualei Rifts was provided to cruises headed by Richard Arculus and the Koreans, who were undertaking cruises to this region shortly after the end of our mission.

Site locations for the hydrothermal surveys and a map of our sample locations are presented in Figure 1-A and 1-B. The cruise track for the expedition with multibeam data is shown in Figure 1-C. Appendix 13 ("Cruise Plan") gives a detailed log of each day's events.

This cruise had several significant successes. It was the first time that ABE had been used in a three phase targeted exploration mode for hydrothermal vent discovery. Discovery of three new vent fields and contribution to a fourth in a single cruise where a major sampling program also was accomplished is unprecedented. We generated the most comprehensive basement sampling of a back-arc basin that has yet been accomplished, and obtained the largest and highest quality chemical data set at sea on the collected rocks. These accomplishments could only take place with the participation and expertise of the entire scientific party and officers and crew of the Kilo Moana.

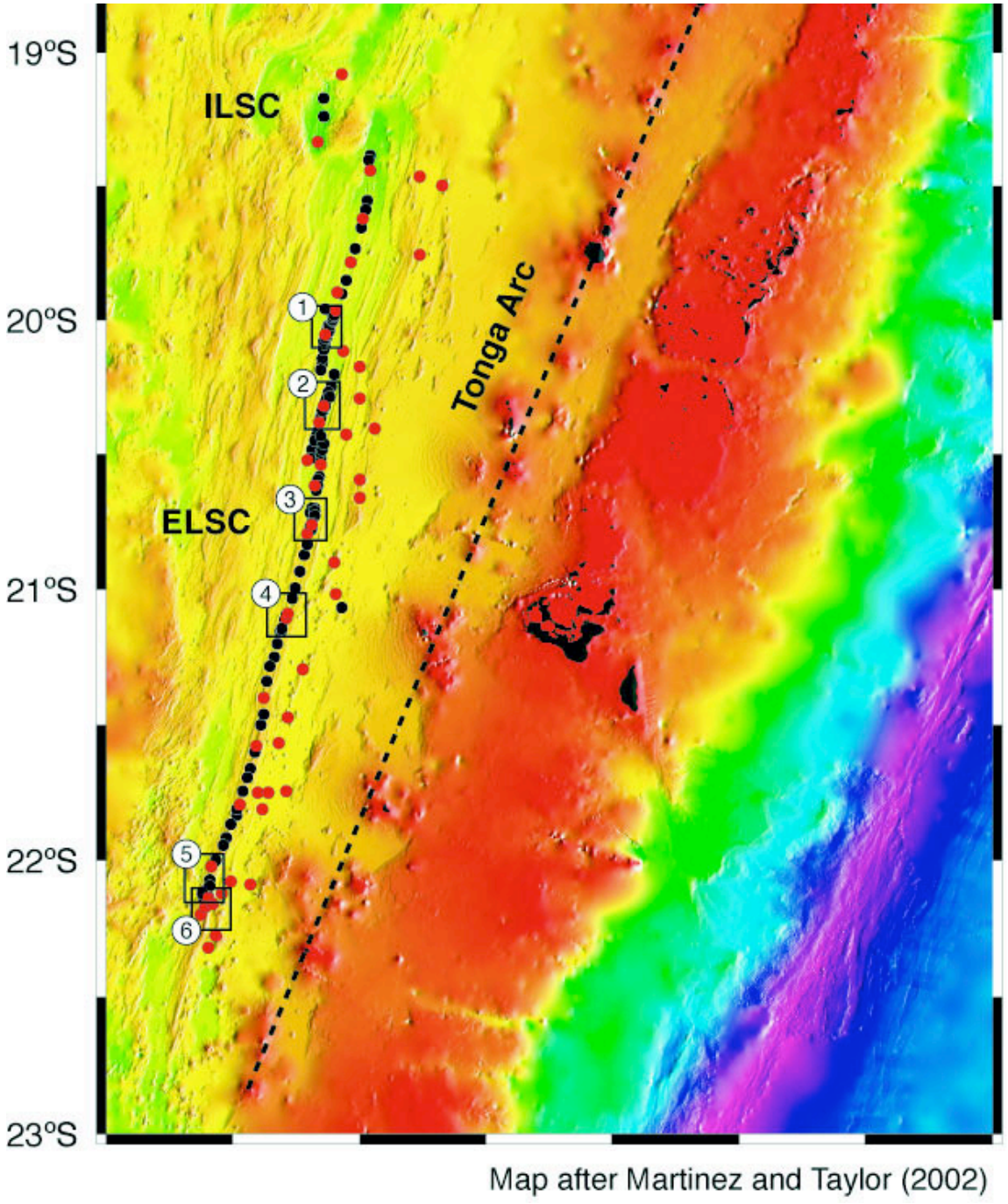

Figure 1A: Map of the Eastern Lau Spreading Center (ELSC)
(from Martinez and Taylor (2002) with sample locations recovered during KM0417. Solid red circles are dredge locations. Black circles are rock locations. Numbered boxes indicate the six locations where ABE investigations of hydrothermal activity were undertaken

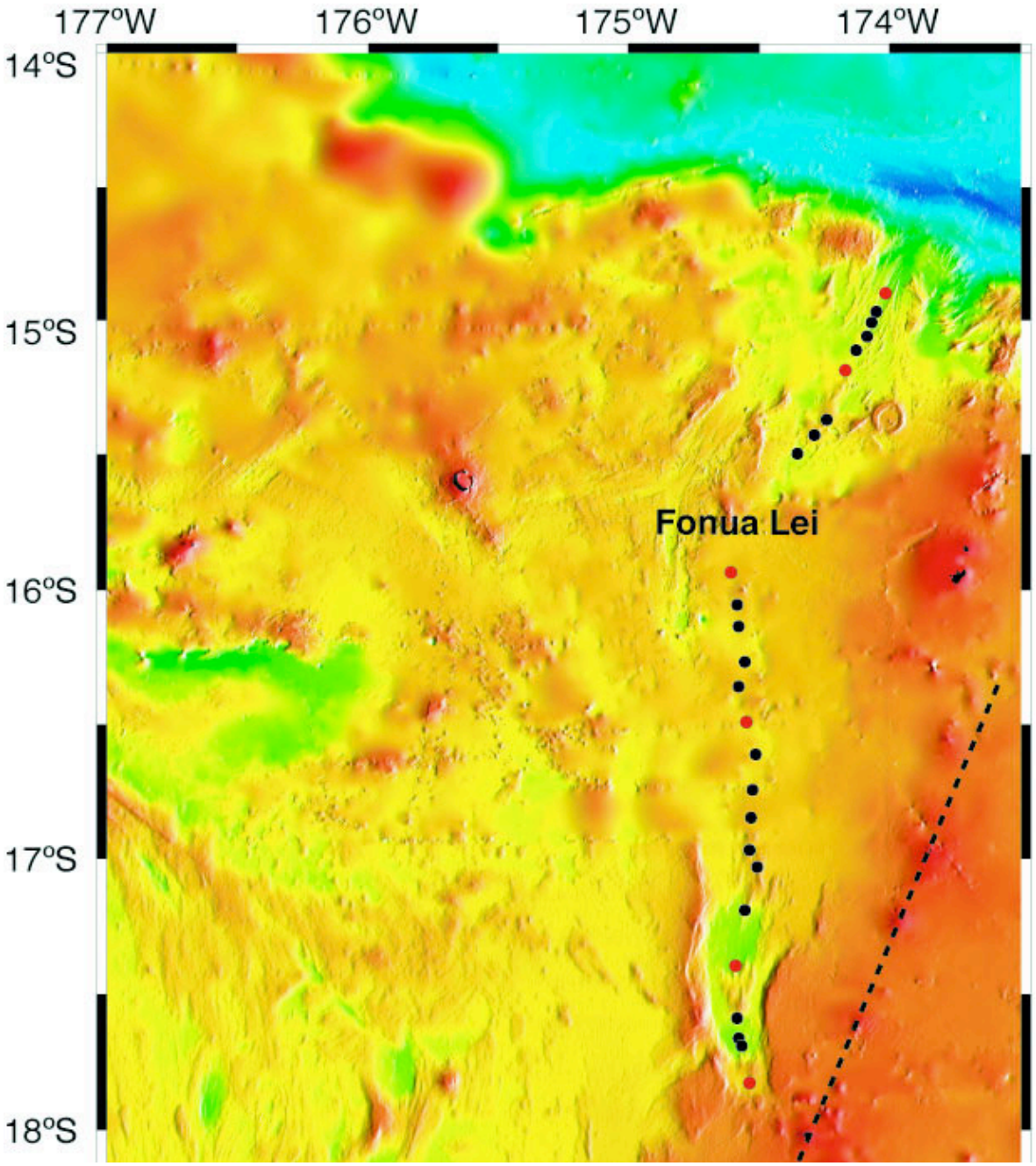

Figure 1B: Map of northern Lau Basin
(from Martinez and Taylor (2002) with sample locations recovered during KM0417. Solid red circles are dredge locations. Black circles are rock locations.

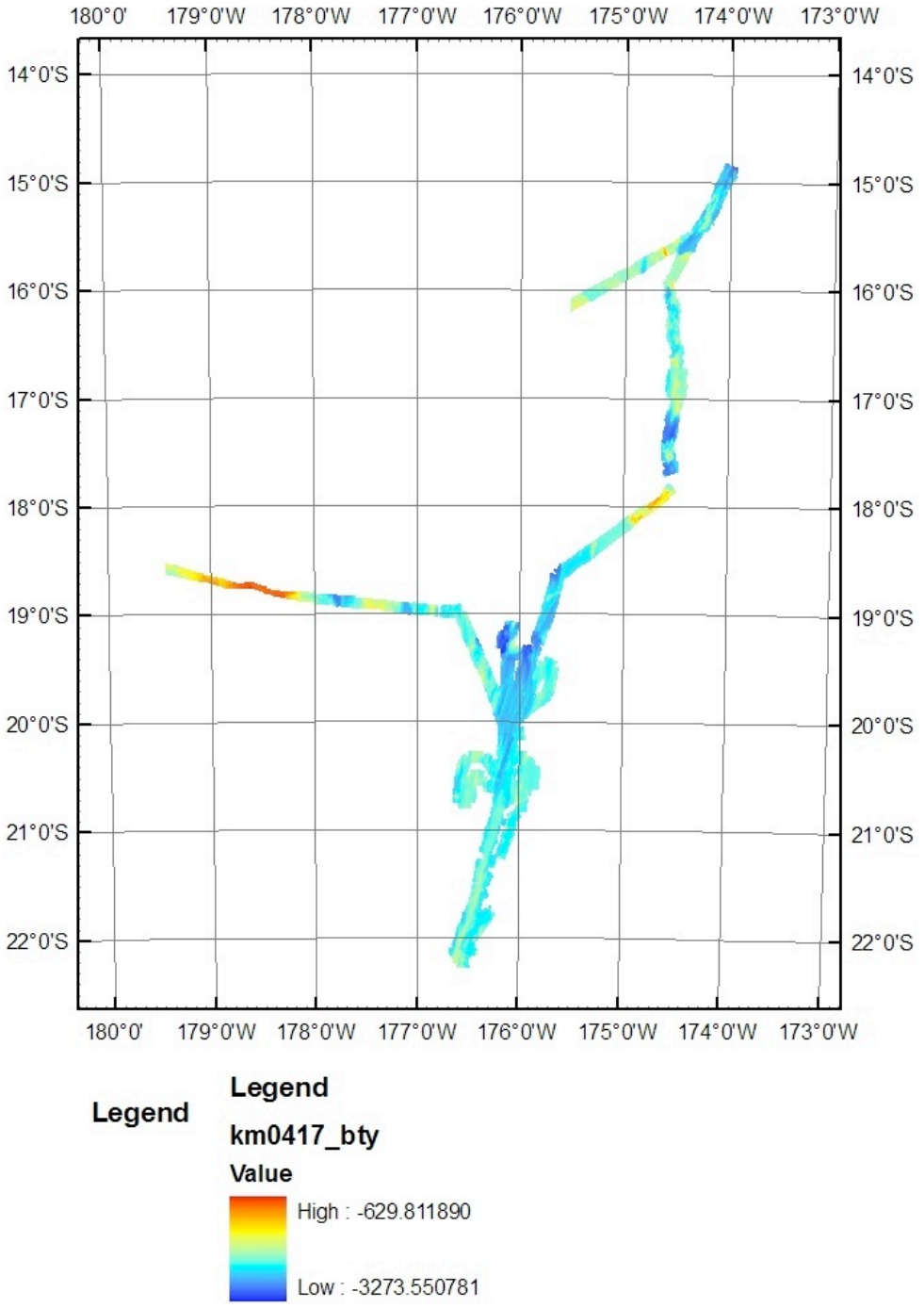

Figure 1C: Cruise track for KM0417. Kilo Moana departed Fiji and headed east to the Eastern Lau Spreading Center (ELSC), proceeding first to the south for ABE Phase 1 investigations, then returning north for Phases II and III. After the conclusion of work on the ELSC, the ship headed northeast to the Fonaolei Rifts, and then headed west to return to FIji.

ABE Operations

Site 1

ABE made 4 dives at Site 1, a phase, dive, 1 phase 2 dive, and two phase 3 dives. The phase 1 and phase 2 dives permitted us to locate the rising plume in the nonbuoyant layer, then refine our estimate based on both water column data and bathymetry. In phase 3, we photographed the site over two dives, although the first of the phase 3 dives was compromised by a software error. On the second phase 3 dive (ABE141), we covered the target site exceeding 50% coverage with 5 meter line spacing. At the end of the phase 3 survey, ABE executed an additional grid pattern at a spot chosen autonomously by the vehicle software during the dive. The adaptive survey algorithm utilized temperature and eH data combined with a clustering algorithm to determine the most attractive location for the final survey.

The phase 1 dive at site 1 (ABE126) covered 25.5 km of tracklines over 12.1 hours, starting in the northeast corner, with tracks progressing from north to south. Figure ABE1.1 shows the trackline coverage of the Phase 1 dive (ABE126), Phase 2 dive (ABE137), and the successful Phase 3 dive (ABE141). The phase 1 tracks were run at constant depth (2350 decibars) with 200 meter track spacing. The phase 2 tracks were run with bottom-following engaged and set to 50 meters. The tracks were spaced at 35 meters, but were run interlaced, so the vehicle completed one full pass over the area in the first half of the survey. The phase 3 tracks were run at 5 meters height with 5 meter track spacing, as was the adaptive survey. Figure ABE1.2 shows a closeup view of the Phase 2 and Phase 3 tracklines.

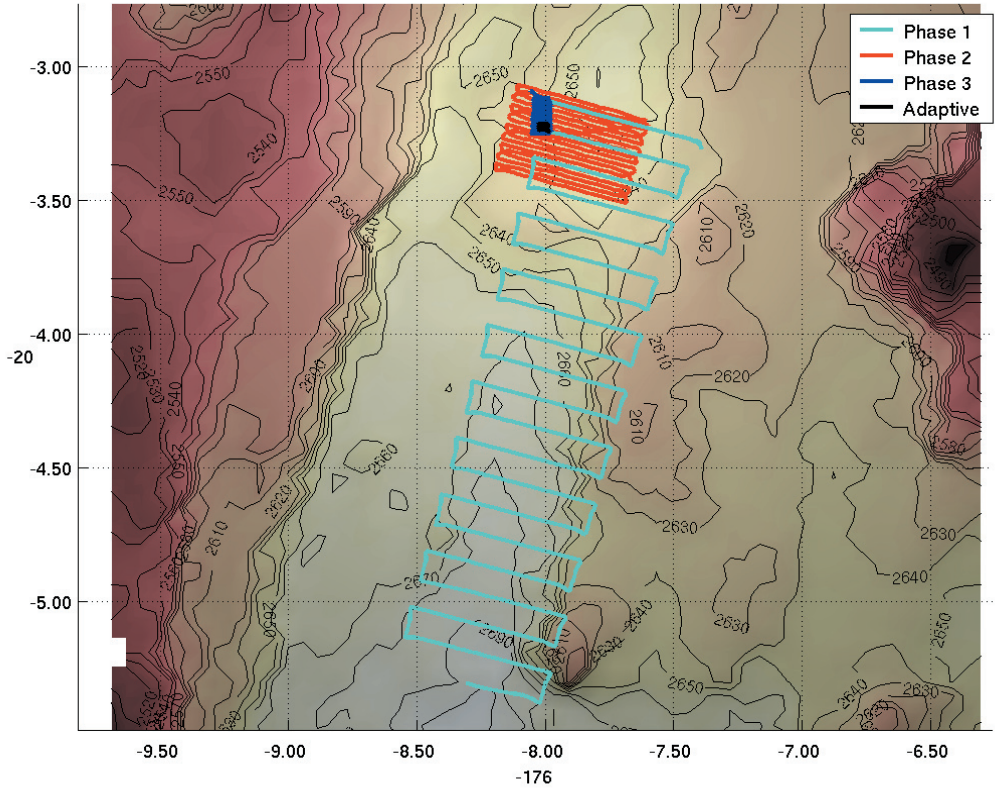

Figure 2 - ABE1.1*: This plot shows the tracklines from the phase1, 2, and 3 ABE dives over site 1. The tracklines are superimposed over EM120 bathymetry.*

The location and depth of the phase 1 dive were both critical choices. The area was chosen using mapper data from the Martinez cruise, CTD data from our cruise, and the DSL120 and EM120 sonar data. Geological interpretations suggested the area should be moved to the south, the CTD and mapper data suggested positioning it to the north. In hindsight, the CTD data indicated the vent locations best. Figure ABE1.3 shows that the depth was chosen correctly. The plot shows the vehicle's depth as a function of time, with the color indicating the strength of optical backscatter. The vehicle passed through a zone of high optical backscatter at the survey depth (2350 decibars), then a less intense zone deeper. Optical backscatter intensity diminishes throughout the dive as the vehicle moves south.

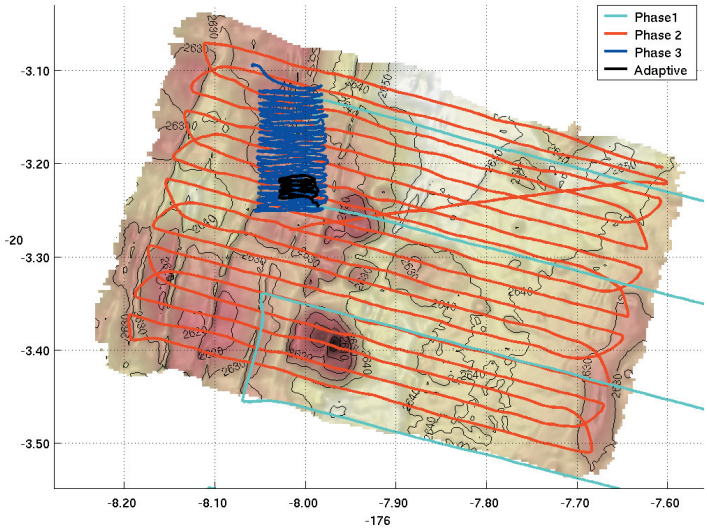

***Figure 3 - ABE1.2**: This figure shows a closeup of the phase 2 and 3 tracklines shown over the nearbottom multibeam bathymetry gathered by ABE on the phase 2 dive.*

***Figure 4 - ABE1.3**: This plot shows optical backscatter superimposed on pressure as a function of time. It shows the vehicle's descent after it reaches 2000 decibars, the vehicle rising off the seafloor to the assigned survey height, the survey, and finally the vehicle's ascent. These data show that the survey depth was well-chosen as well as the possible presence of a less intense, deeper nonbuoyant layer.*

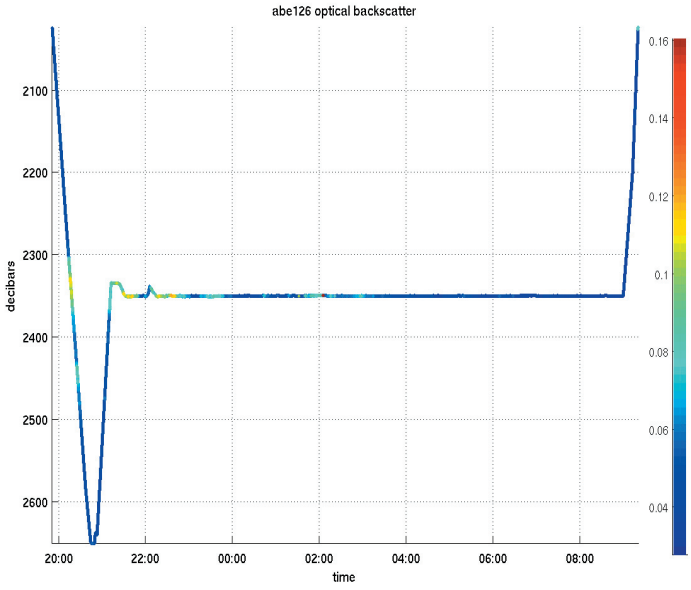

Figure ABE1.4 shows the spatial distribution of optical backscatter, eH, and temperature anomalies. Each sensor shows the presence of a plume in the northeast corner, with optical backscatter showing higher intensity, eH showing a downward transitions (from warm to cool colors), and a temperature increase.

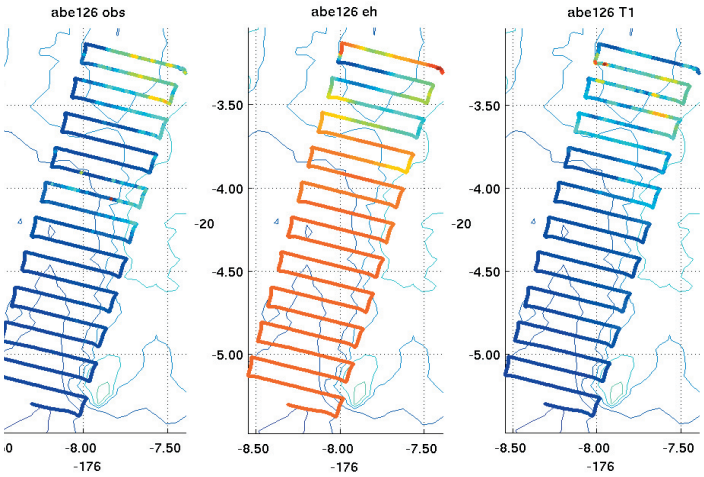

***Figure 5 - ABE1.4**: These plots show the spatial distribution of optical backscatter, eH, and temperature anomalies throughout dive 126. They all show the presence of a plume in the northeast corner, with optical backscatter showing higher intensity, eH showing a downward transitions (from warm to cool colors), and a temperature increase.*

The most prominent event in the phase 1 survey occured just after the vehicle turned to the east on the second trackline. This event is shown in figure ABE1.5, which plots the vehicle depth, eH, optical backscatter, and temperature over a 1.5 hour period. Although the vehicle's commanded depth remained constant, the vehicle rose over 10 meters just after 22:00, which is consistent with the vehicle encountering a rising plume that its thrusters were unable to overcome. This occured simultaneously with a drop in eH and a temperature increase of about 200 millidegrees. Although optical backscatter does not show a simultaneous rise, the spatial plot (ABE1.4) shows a substantial area of higher optical backscatter closeby to the east.

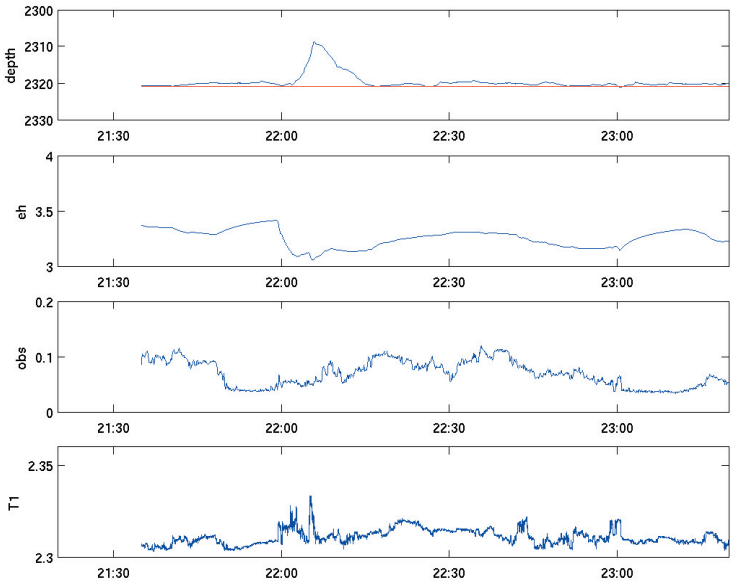

***Figure 6 - ABE1.5**: This plot shows the vehicle depth, eH, optical backscatter, and temperature over a 1.5 hour period. Although the vehicle's commanded depth remained constant, the vehicle rose over 10 meters just after 22:00. This occured simultaneously with a drop in eH and a temperature increase of about 200 millidegrees*

The spot where ABE was pushed up with simultaneous indicators of eH and temperature was used to locate the phase 2 survey, which was done on ABE137. On this dive, ABE ran tracklines spaced at 35 meters with tracklines run first at 70 meter spacing then interlaced. We adopted this strategy to ensure that we got complete bathymetric coverage even if the vehicle did not complete the entire survey (it did).

The phase 2 data from dive 137 yielded water column data showing a plume source nearby. As shown in figure ABE1.6, the vehicle's sensors observed downward eH transitions along with increases in optical backscatter and temperature (up to 400 millidegrees) in a zone less than 200 meters across. The presence of these tracers on adjacent tracks confirms that our 35 meter trackspacing was adequate.

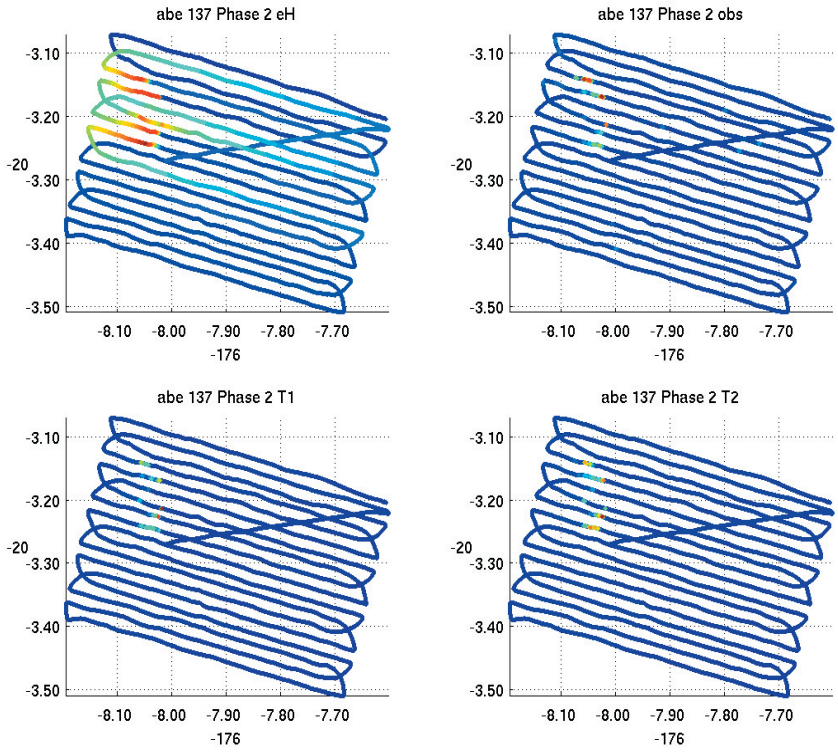

Figure 7 - ABE1.6*: This plot shows eH, optical backscatter, and the readings from both ABE's temperature sensors. The eH downward transitions, increases in optical backscatter, and temperature increases all occur at nearly the same spots.*

The phase 2 dive produced a high quality bathymetric map after postprocessing the compass, transponder navigation and doppler navigation data. The resulting map shows. The completed map is shown in figure ABE1.7. Using the Fledermaus program, we were able to find spires in the resulting bathymetry, as shown in figure ABE1.8. We used this position to site both the phase 3 ABE dives as well as Tow Cam runs.

The phase3 survey was planned based on the simultaneous tracer hits from the phase 2 survey along with the spires observed in the bathymetry. This yielded a survey box about 200 meters by 100 meters. ABE dive 140 targeted an area about twice as wide with 5

meter spaced tracklines in three blocks. To help prevent ABE from flying into the fissures seen in the bathymetry, tracklines were chosen to cross the fissures across axis. Additionally, a “hard floor” was imposed on the bottom following algorithm just below the lip of the fissures (2627 meters). As the bathymetry was produced by ABE, we had a high degree of confidence in the validity of that depth, with the largest uncertainty coming from tides.

ABE140 had significant problems. A software error concerning the doppler navigation data was the primary cause. We had changed the doppler settings to provide exclusively bottom track pings, doubling our update rate for navigation data by eliminating the water track pings. Unfortunately the real-time code that parses the doppler data failed in this mode, and that failure went undetected by the state estimation module that uses the resulting velocity data to update the vehicle position. As a result, when ABE did not receive consistent transponder fixes, its estimate of its position would wander off rapidly at a constant rate. So ABE did not fly its assigned trackelines well. Since ABE was lost much of the time, it did not complete many tracklines successfully (37 out of 96). We had programmed ABE to back up for one minute if it did not reach the end of a trackline successfully. On two occasions, was descending a steep slope when the trackline timeout occurred, and it backed into the slope for over a minute. These collisions fed into ABE’s bottom following algorithm (backup if you are too close), increasing the collision with the seafloor even more. On one occasion, the vehicle’s tailcone was torn free, although it dangled from the vehicle by its cable. ABE completed the assigned tracklines and took several thousand bottom images in the assigned area using only the two top aft thrusters. ABE also completed the adaptive survey, it had sufficient LBL fixes when the best spot was detected and during the resulting survey to complete the experiment. Fortunately, we noticed the dangling tailcone before recovery, and we used the ship’s small boat to remove the tailcone and dummy off the live electrical connector before the vehicle was lifted from the water.

The vehicle suffered some significant damage. The thruster’s oil compensation system was contaminated by seawater and its connector had been exposed to seawater when live. The connector on the endcap block had been cracked and slightly loosened. This permitted a small amount of water to seep in and damage several nearby connectors (including the connector for the compass). Repairs and software improvements were completed in 24 hours.

ABE141 went according to plan. It repeated the tracklines on the east side of the survey area, taking over 4000 color bottom photos. The vehicle repeated the adaptive survey, continously updating the position is judged most appropriate for the final targeted survey. It finally chose the same point as on the previous dive. It successfully completed a 50x50 meter survey with 5 meter spaced lines over the spot. Figure ABE1.9 shows the footprints of the resulting camera images based on an estimate of the vehicle position, the vehicle height off bottom, and the heading. Footprints are shown for photos taken at a height of 10 meters of less. Note that no footprints are shown directly over the fissures, as the vehicle was forbidden to descend into them and the resulting heights exceeded 10 meters.

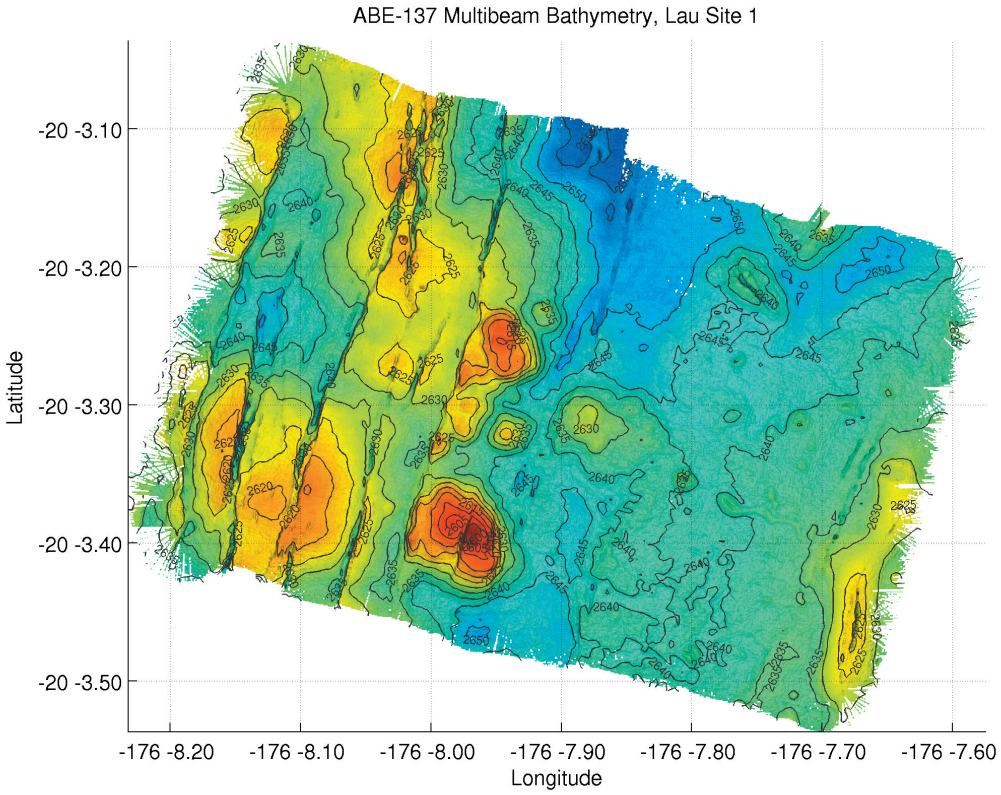

***Figure 8 - ABE1.7**: The bathymetric map produced with data from ABE137.*

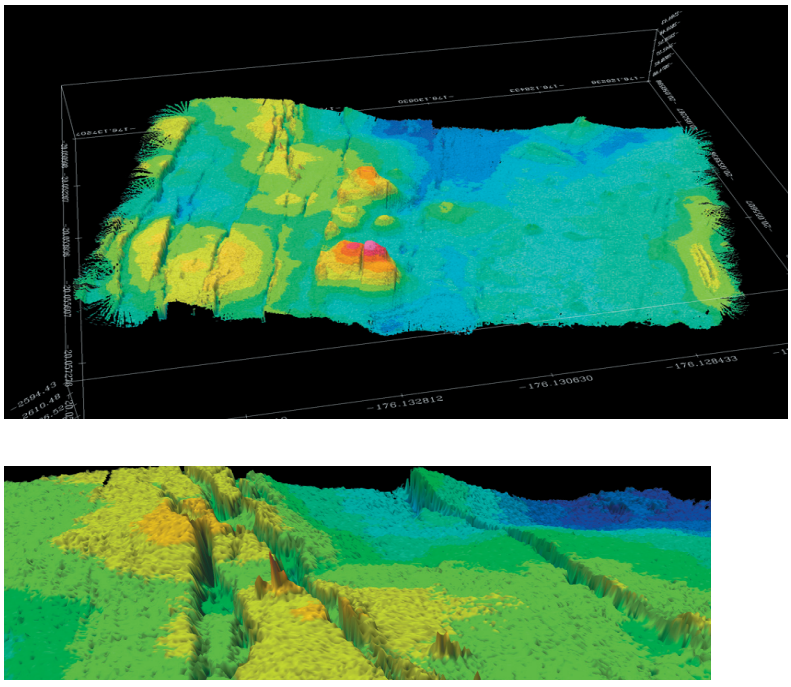

***Figure 9 - ABE1.8**:*

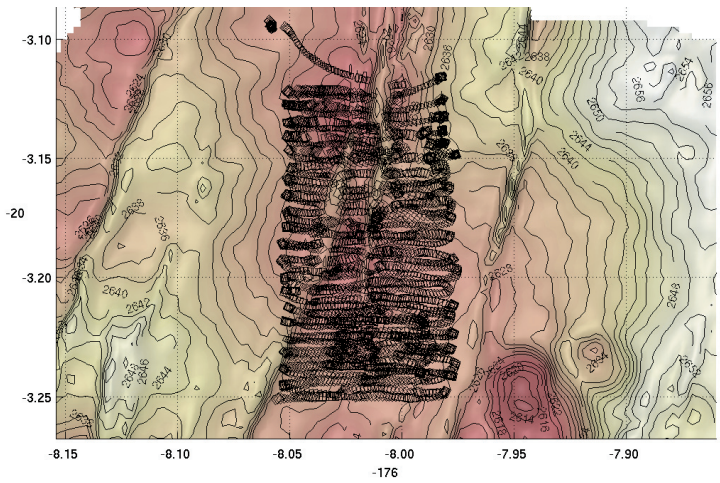

***Figure 10 - ABE1.9**: This plots shows the footprint of all images taken during ABE141 at heights of 10 meters or less.*

Site 2

At Lau site 2 (20 19S, 176 8W) we also pursued a successful strategy of phases 1 through 3, although we were able to jump ahead a bit due to an early siting of an active vent with Tow Cam. Figure ABE2.1 shows the tracklines from all 3 phases. ABE126 performed a phase 1 survey, ABE135 performed a short phase 1 survey to fill the area to the north, then did a phase 2 survey. ABE138 made a phase 3 survey with the color camera.

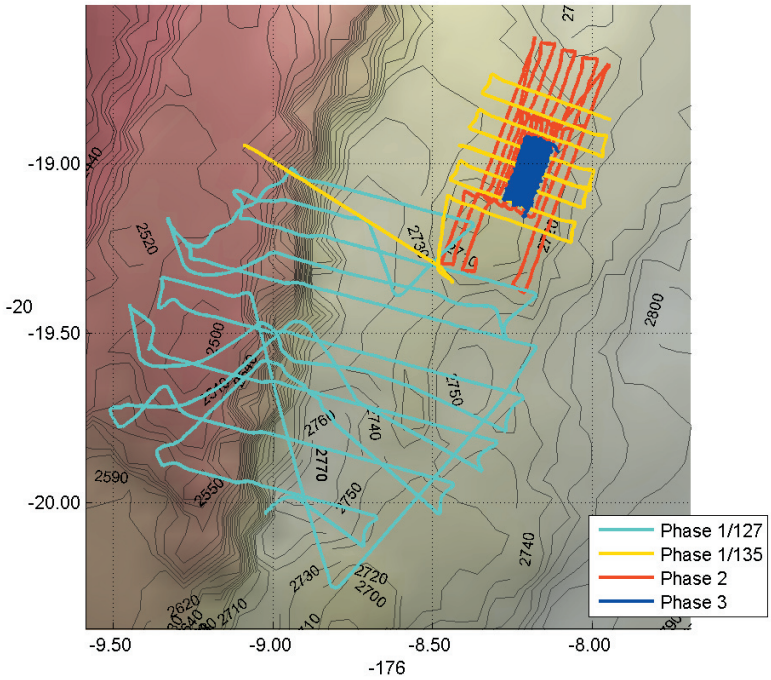

***Figure 11 - ABE2.1**: This plot shows the tracklines of all dives at site2. The first phase 1 dive, ABE127, had a problem with navigation, tracklines running westbound had poor LBL navigation and the state estimator was improperly processing the doppler navigator data which caused poor deadreckoning.*

The first phase 1 dive at Site 2, ABE127, had some avigation problems but nevertheless provided us with sufficient clues to pin down the vent site. ABE had a problem processing data from its doppler navigator, and the result was that its internal position es-

timate would not advance when no dvl data was available. When LBL fixes were plentiful, this was of little consequence. But for periods with no LBL fixes, the software would not propagate the estimated position forward, resulting in poor trackfollowing until good fixes arrived.

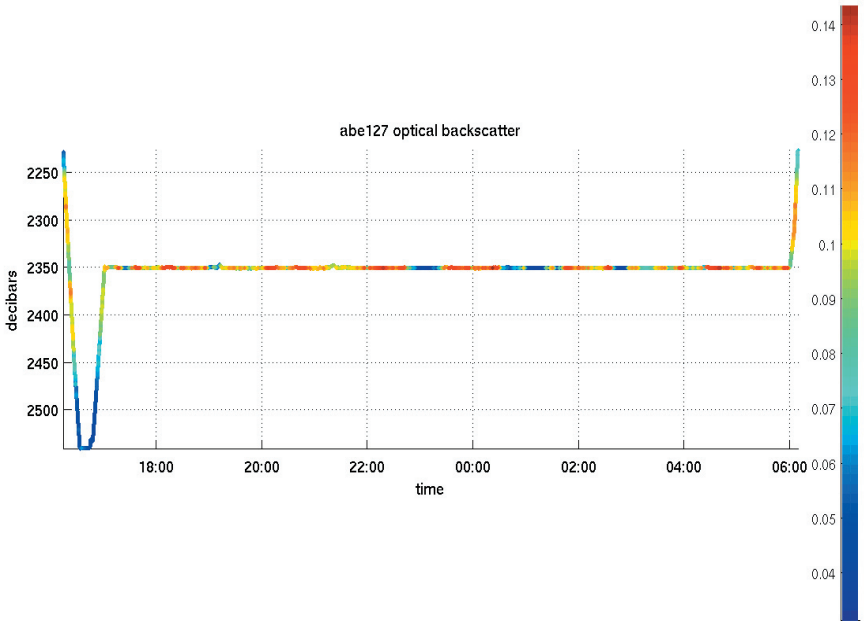

Figure 12-ABE2.2*: For dive 127, the vertical profile of optical backscatter obtained on the vehicle's descent. The layer is approximately 200 meters thick and much weaker than at the previous site.*

Figure ABE2.2 shows that the optical backscatter profile was much different from the first site. The nonbuoyant layer was thicker and more complicated, and our chosen depth may have fallen between two distinct layers.

Figure 13 - ABE2.3*: This plot shows data from the realtime navigation display on the ship used to track ABE in realtime. The vertical excursion shown here was observed in realtime. Due to the correspondance of the position of the vertical excursion with the underlying geology shown in the DSL-120 maps, a Tow Cam run was made immediately along the axis based on this point. This Tow Cam run identified a vent site.*

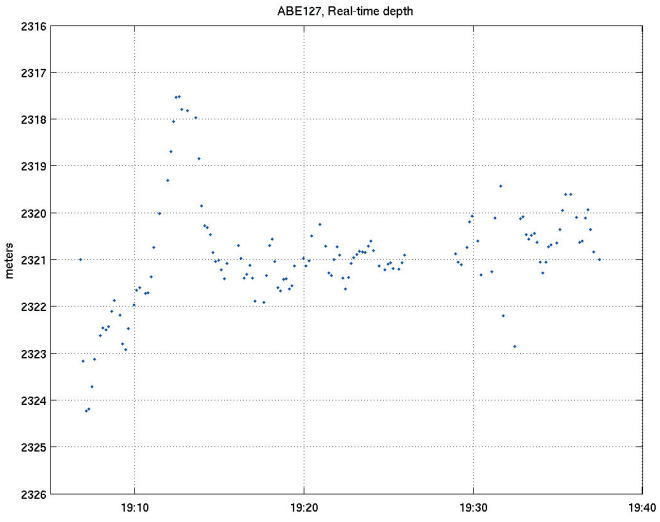

Good fortune allowed us to jump ahead with our Phase1-3 strategy. On an early trackline of the Phase 1 survey, we observed that the vehicle rose 5 meters while on a long straight trackline (figure ABE2.3). The ship was doing a dredge at the time, so its motion did not distort the tracking. This excursion was observed to lie over the central rifts in the volcanoes of the rift valley, as seen in the DSL120 bathymetric and backscatter maps. Based on this correlation, the evenings plan was changed to include a Tow Cam run over the central rift. North of the ABE survey site, Tow Cam observed temperature rises, optical backscatter increases, and sampled warm water that smelled of sulfide. Tow cam images revealed a black smoker.

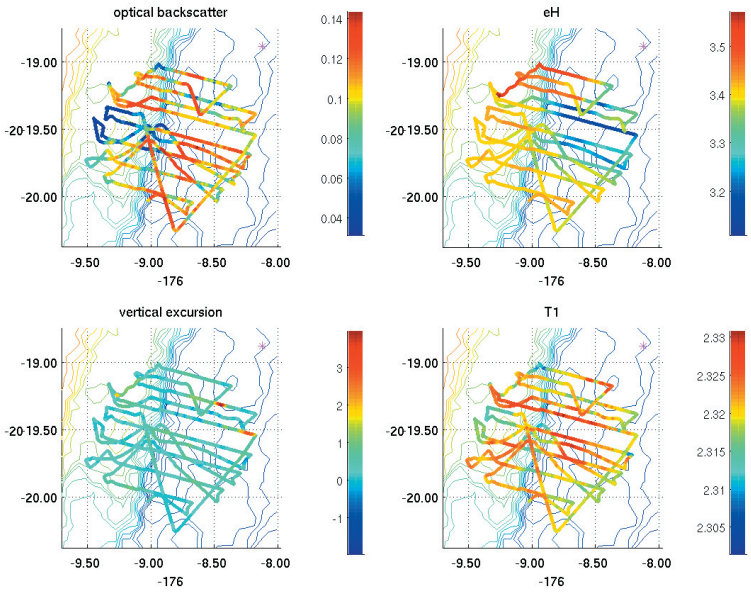

Figure 14 - ABE2.4*: These 4 panels show optical backscatter, eH, vertical excursion, and temperature for the phase 1 survey on ABE127. The vertical excursions show the clearest view of rising plume water, eH shows some consistent downgoing signals in the same area, but temperature and optical backscatter did not produce any clear indicators at the same spot.*

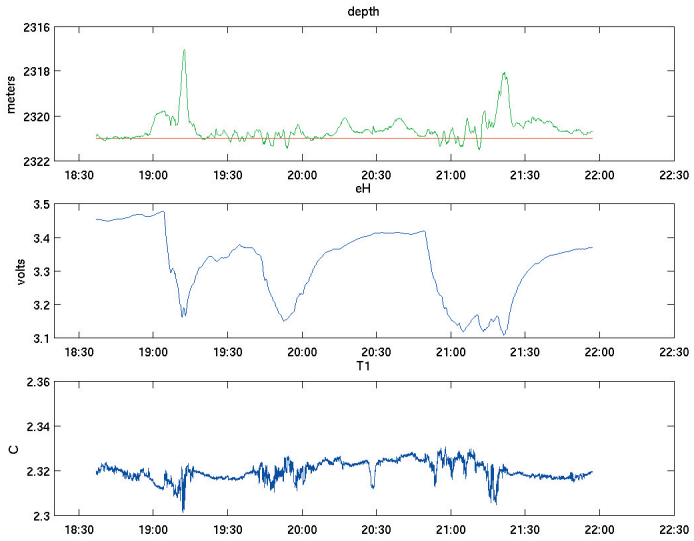

Figure 15 - ABE2.5*: The first vertical excursion (t = 19:10) corresponded to a drop in eH but also seemed to correlate with a drop in temperature. The second vertical excursion occured in a region of lowered eH.*

Figure ABE2.4 shows optical backscatter, eH, vertical excursion, and temperature for the phase 1 survey. emperature and optical backscatter did not correlate with the vertical excursions, although both excursions occured in a region of lowered eH signal, and the first, largest excursion corresponded to a sharp drop in the eH signal (see figure ABE2.5).

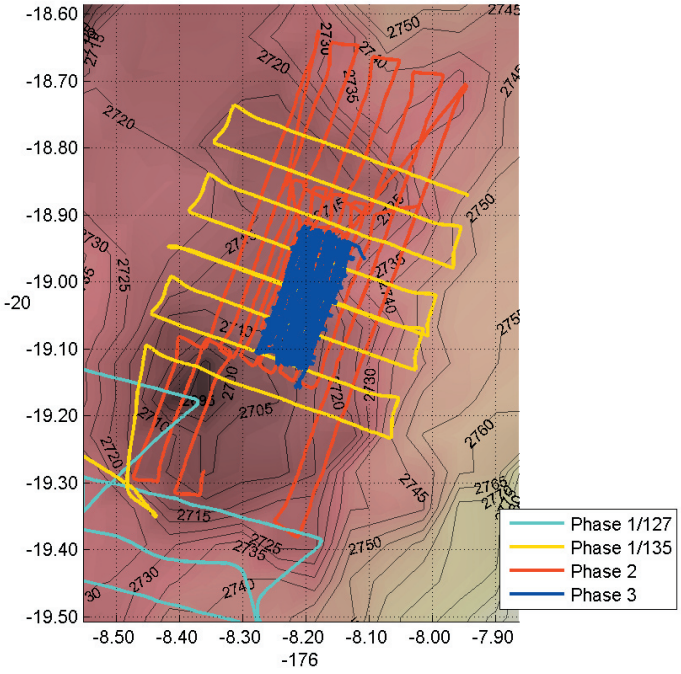

Figure 16 - ABE2.6*: Tracklines for phase 2 and phase 3 were centered on the spot identified by Tow Cam as an active vent.*

Figure 17 - ABE2.7*: The phase 2 survey identified an area around the Tow Cam site with temperatures up to 4C.*

On dive 135, ABE did an additional phase 1 survey above the Tow Cam site, then dropped down for a phase 2 survey, which included a 10m high survey over the Tow Cam field. These tracklines are shown in figure ABE2.6. We had hoped to clarify the relationship betweent the vertical xcursions, temperature, eH and optical backscatter with a phase 1 survey as part of ABE135, but a failure in ABE's analog sensing system (bad cable) made eH and optical backscatter unavailable for that dive.

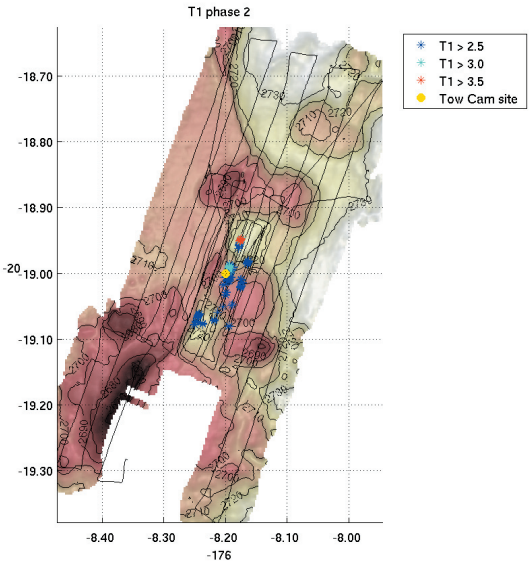

The phase 2 survey over the Tow Cam site showed temperature rises up to 4C (see figure ABE2.7). These data showed temperature hits over an area about 300 meters by 100 meters.

Figure ABE2.8 shows the nearbottom multibeam map made using data from ABE135. The gap in the south occured because ABE ran out of battery power when starting that section.

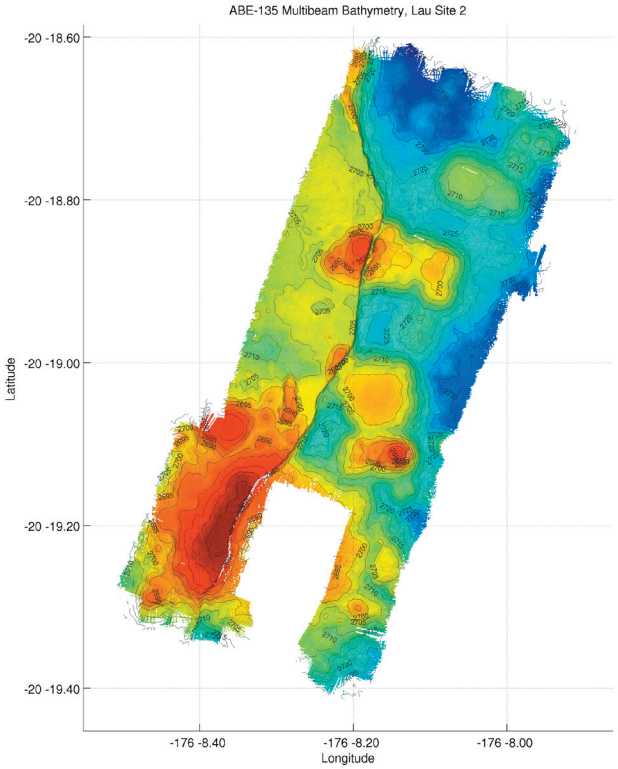

The phase 3 survey run in ABE138 centered on the area defined by the temperature hits registered in the phase 2 survey. Figure ABE2.9 shows the camera footprint plot for the photo survey, tracklines were spaced at 5 meters over an area 350 by 150 meters. Crossing lines spaced 20 meters were also executed. Approximately 10000 photos were taken over 14 hours of survey.

***Figure 18 - ABE2.8**: This plot shows the bathymetric map made with ABE for site 2.*

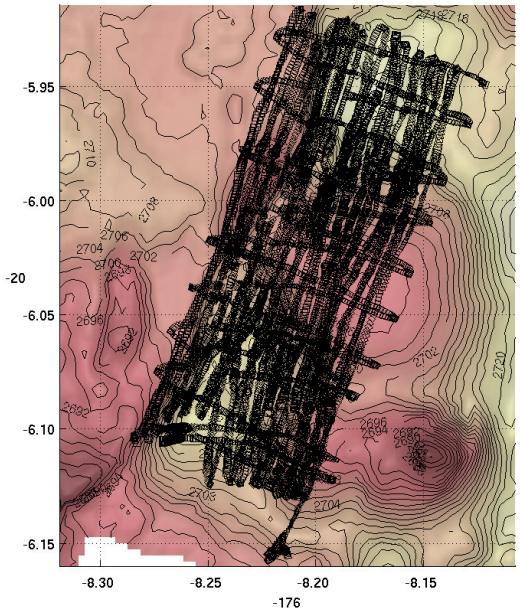

***Figure 19 - ABE2.9**: Camera footprint plot for ABE138, the phase 3 dive at site 2. The plot shows camera footprints for all photos taken at a height of 10 meters or less.*

Site 3

Site 3 followed our intended progression of phases. Results from the phase 2 ABE survey allowed us to target a Tow Cam dive precisely onto the vent sites, enabling us to further pinpoint the phase 3 ABE survey.

Figure ABE3.1 shows the tracklines from all three phases at Site 3. The extent of the lenting discovered required the long, extended phase 3 survey in three blocks.

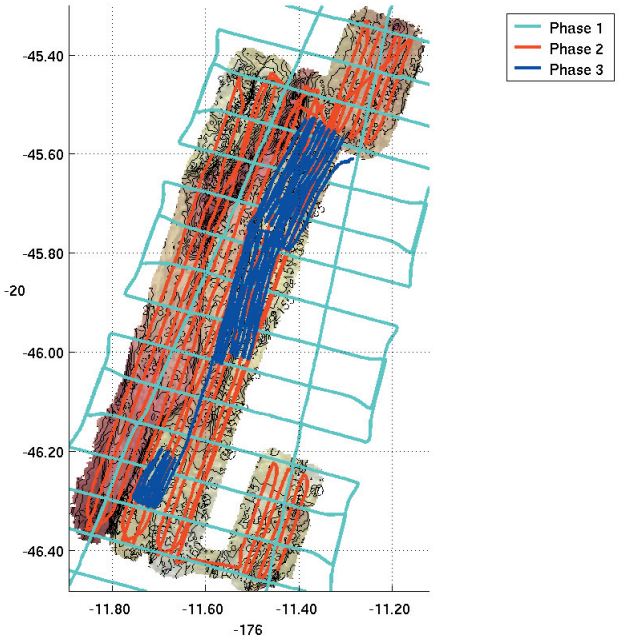

***Figure 20 - ABE3.1**: This figure shows all three phases at Site 3.*

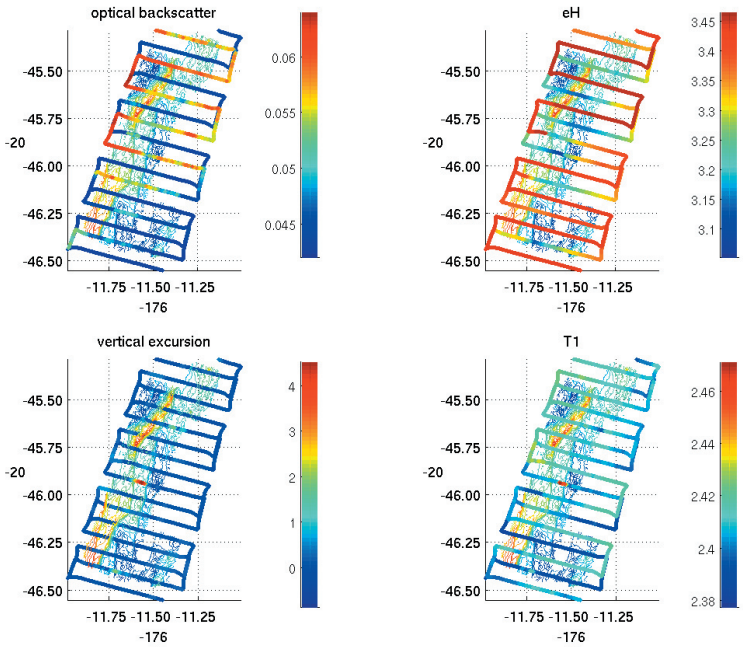

***Figure 21 - ABE3.2**: The phase 1 survey at Site 1 showed a number of spots where the vehicle rose vertically, optical backscatter changed, the eH voltage dropped, and the temperature rose*

The phase 1 survey gave very solid indications of plume activity. The survey was conducted at two pressures, 1900 and 1980 decibars. The deeper survey showed much more activity than the shallower survey. The optical backscatter data gathered on ABE's descent and ascent on the phase 1 dive (ABE128) showed that the deeper survey was well positioned, but that the layer with high optical backscatter seen in the CTD at 1900 decibars was not present at least at the site at which ABE descended (figure ABE3.3). The deeper survey produced multiple, simultaneous indications by vertical excursions,eH signals, and temperature increases, as shown in figure ABE3.4.

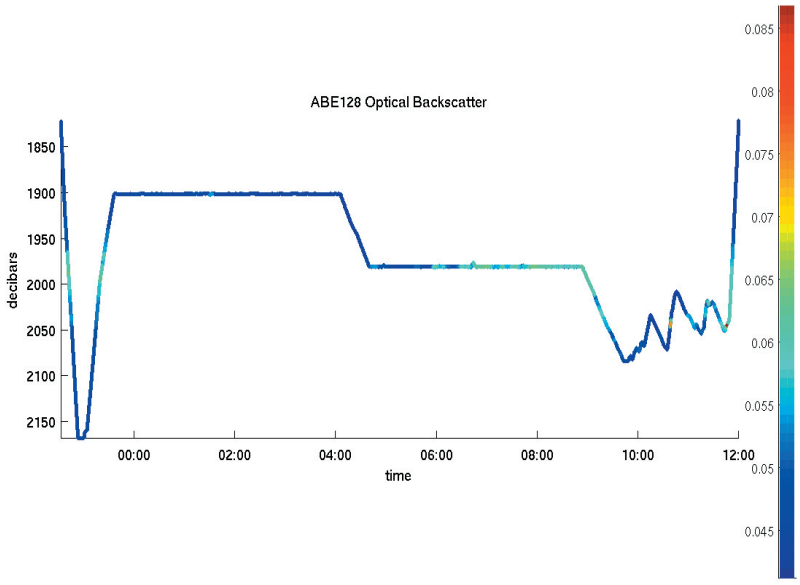

***Figure 22 - ABE3.3**: The optical backscatter profile gathered by ABE on its descent showed little activity at the upper survey height (1900 decibars), but the lower survey (1980 decibars) was positioned properly.*

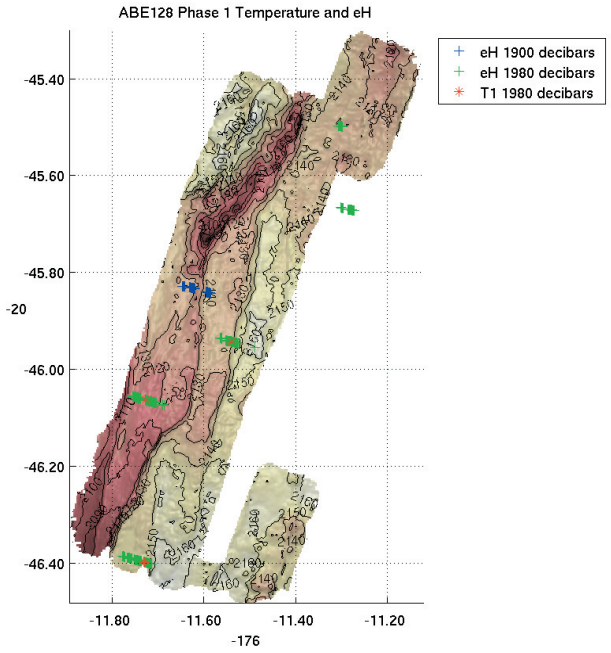

***Figure 23 - ABE3.4**: The upper phase 1 survey (1900 decibars) showed little activity, but the lower survey (1980 decibars) showed several coincident temperature and eH events. These were used to plan the phase 2 survey.*

The phase 2 survey produced more refined indications of plume activity than did phase 1. ABE registered vertical excursions in at least two spots, even though discerning such motions is more difficult when the vehicle is following the terrain. In both cases, the vehicle was pushed up while descending at full down thrust, making the presence of a vertical current very apparent. The vertical excursions were coincident with eH, temperature, and backscatter indications, as shown in figure ABE3.5.

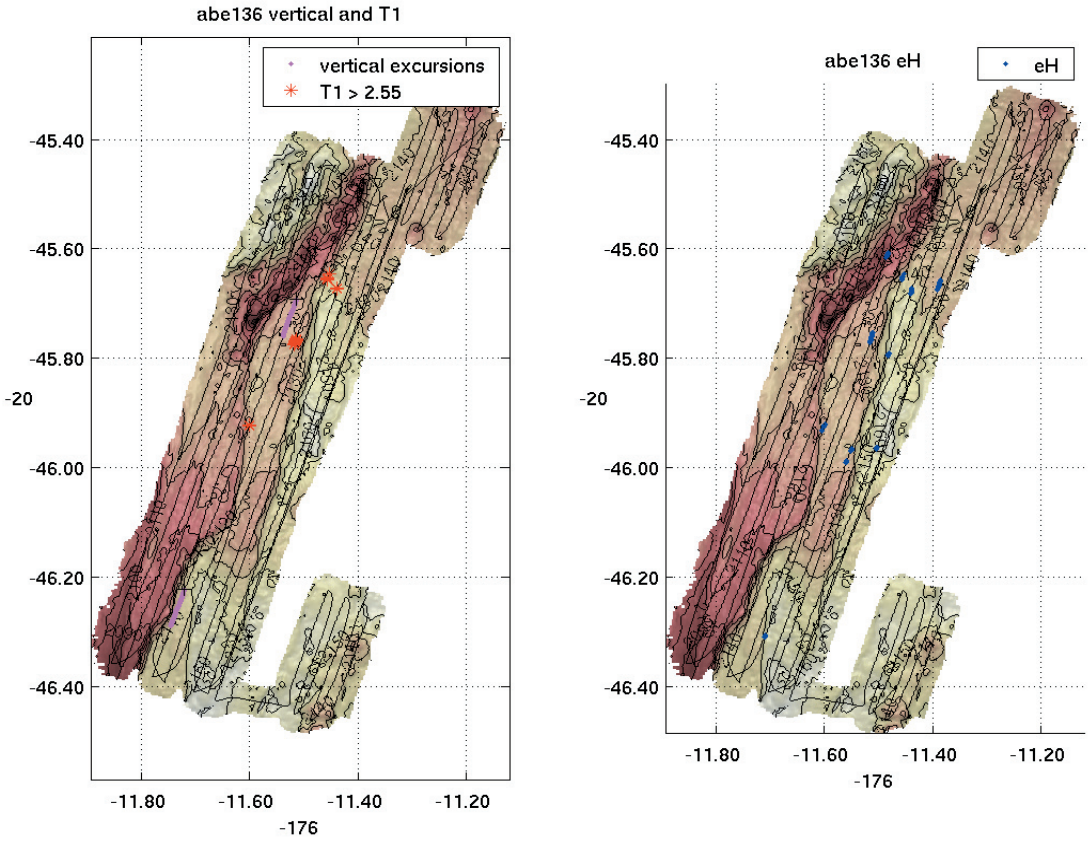

Figure 24 - ABE3.5*: The phase 2 survey showed activity in several spots. Vertical excursions were more difficult to determine since the vehicle was constantly driving up or down to follow the terrain, but at least two were spotted (vehicle going up under full down thrust) which corresponded to both temperature and eH hits.*

The bathymetric map produced by ABE136 data, shown in figure ABE3.6, provides a detailed context for the vent observations. Following postprocessing of the navigation data, the sonar data was gridded at 1 meter. This map was also used to help plan the phase 3 ABE dive (ABE139) and runs with Tow Cam.

The phase 3 tracklines were chosen with the benefit of the phase 1 data as well as definitive sitings of plume activity from Tow Cam. The phase 3 camera footprints along with points where high temperatures were measured are shown in figure ABE3.7. With 10 meter spacing, the areas were covered by less than 50%, but the larger spacing was required to complete the areas in the alloted time.

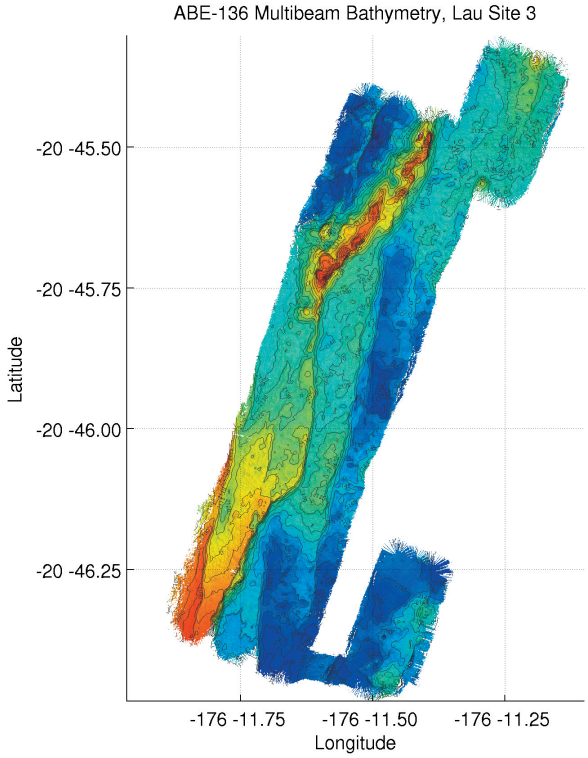

Figure 25 - ABE3.6*: This plot shows the multibeam bathymetry produced from the ABE136 data. This map was used to plan the phase 3 ABE and Tow Cam dives.*

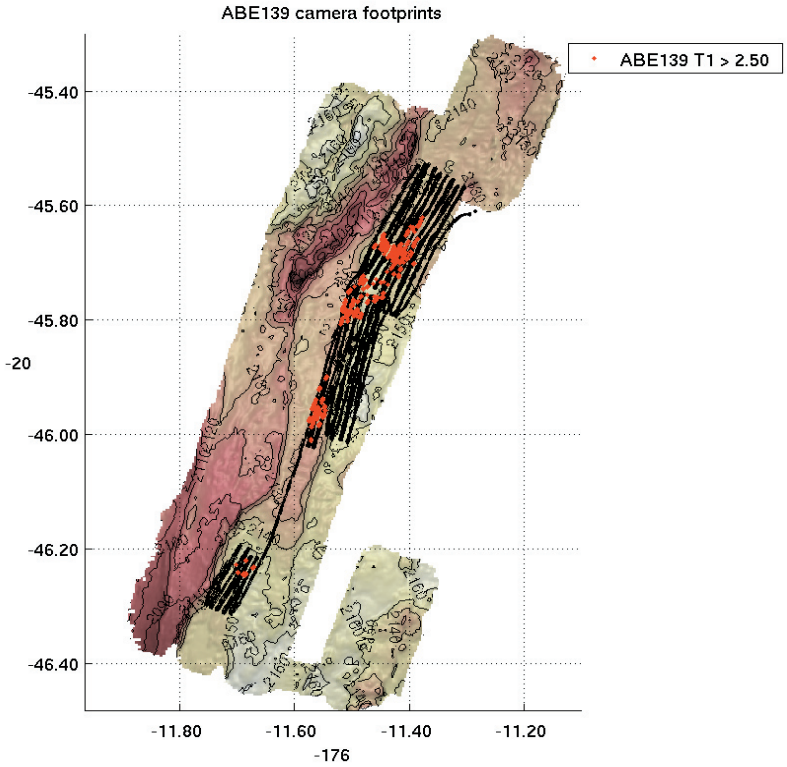

Figure 26 - ABE3.7: *The camera survey focussed on three areas identified from the phase 2 and Tow Cam data. These areas were covered with 10 meter spaced tracklines. The plot shows the camera footprints along with all points where temperatures greater than 2.5C were observed.*

Site 4

We made one dive at site 4, which was abandonded afterwards. The dive (ABE129) included a phase 1 survey and part of a phase 2 survey. The phase 1 survey found multiple, aligned changes in optical backscatter, eH, and temperature but spotted no vertical excursions. These signals were not seen in the lower, phase 2 portion.

Figure ABE4.1 shows the tracklines of the phase 1 and phase 2 surveys. On the first two tracklines of the phase 2 survey, ABE was descending to the proper phase 2 depth.

The phase 1 data (see figure ABE4.2) showed multiple hits on temperature, eH, and optical bacscatter that correlated well between tracklines. These were deemed to be caused by interactions with the bathymetry and were not believed to originate from plumes. The magnitude of these tracer signals was substantial and uniform, as shown in figure ABE4.3.

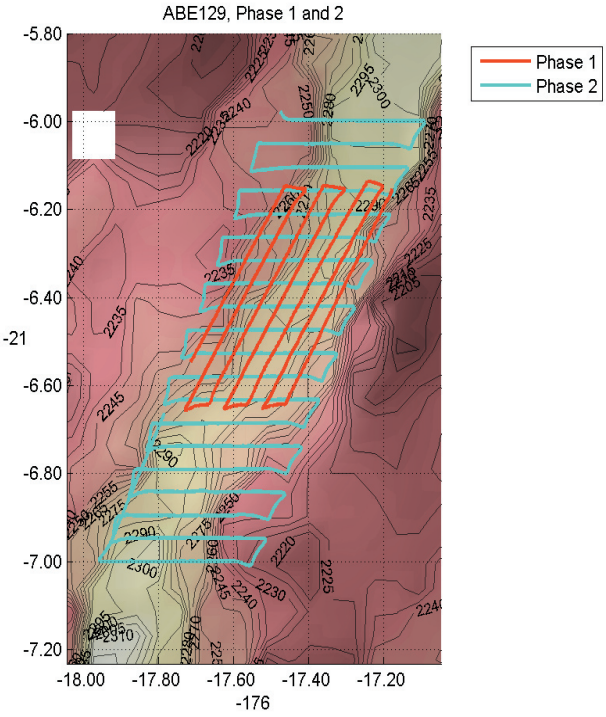

***Figure 27 - ABE4.1**: ABE dive 129 did both phase 1 and phase 2 work at site 4.*

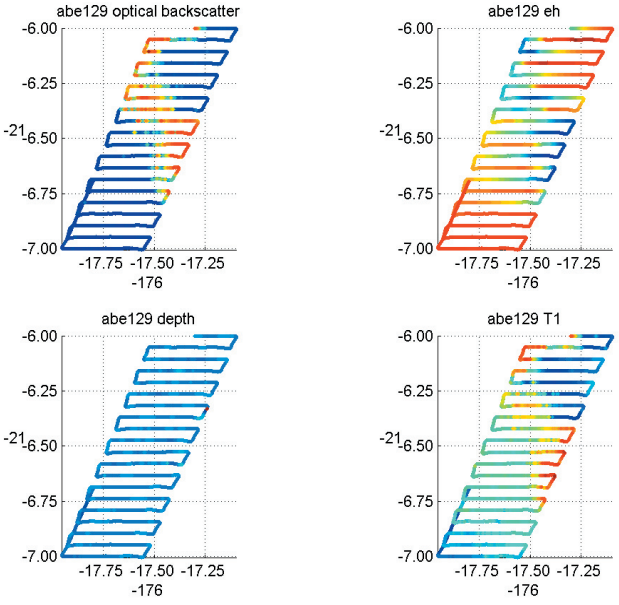

***Figure 28 - ABE4.2:** These plots show optical backscatter, eH, depth excursion, and temperature for the phase 1 dive at site 4, ABE129. We observed a line of all indicators with the exception of depth excursion*

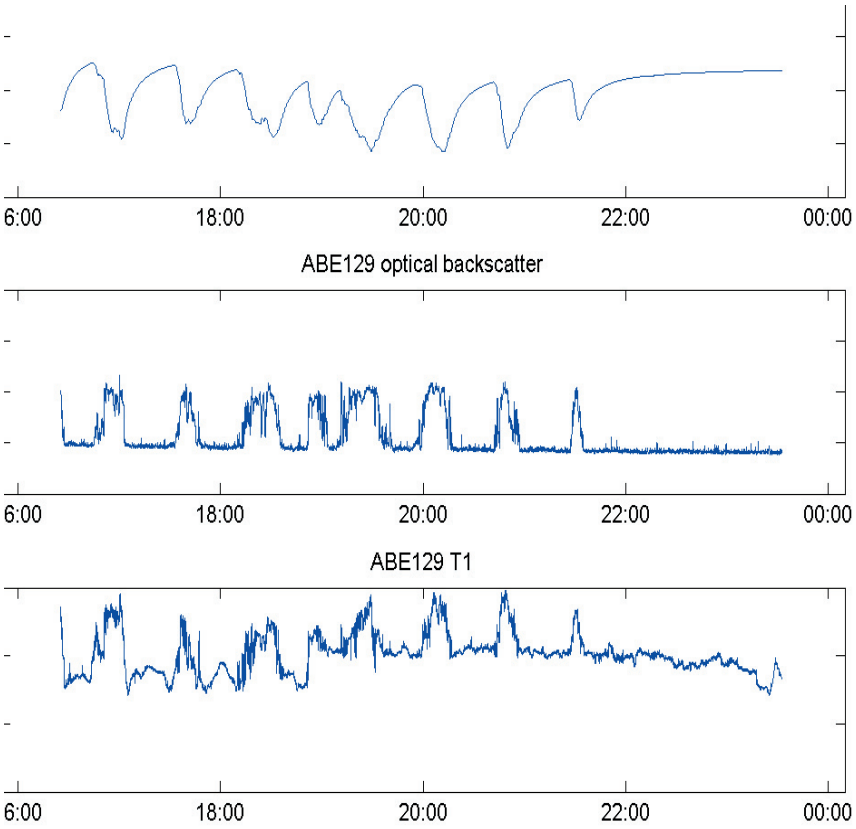

Figure 29 - ABE4.3*: This figure shows that the optical backscatter, eH, and temperature signals correlate and are of substantial magnitude.*

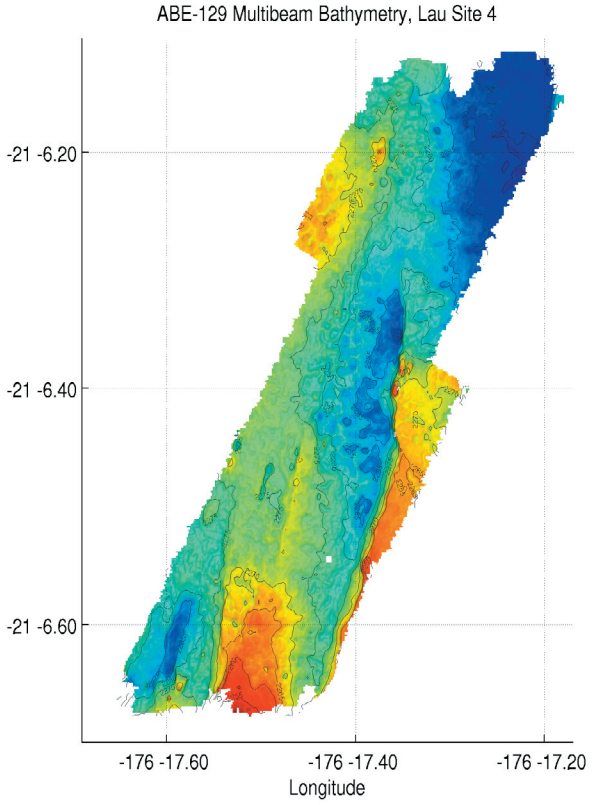

Figure 30 - ABE4.4*: This plot shows the bathymetry gathered at the end of the phase 1 dive at site4.*

ABE data produced a bathymetric map of the area, shown in figure ABE4.4.

The phase 2 data showed little activity in terms of the plume tracers. As shown in figure ABE4.5, the only changes in the plume tracers occured as ABE began to descend from the phase1 survey height, no substantial signals were seen after that.

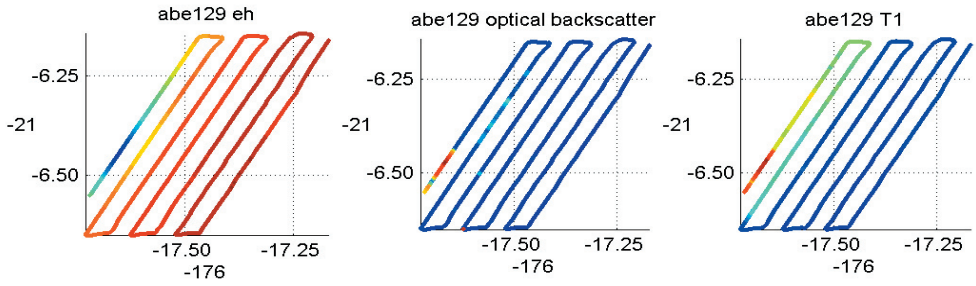

Figure 31 - ABE4.5*: The phase 2 survey saw only one significant event, a simultaneous eH, temperature, and optical backscatter hit just as the vehicle began to descend from the phase 1 depth. No more substantial plume signals were seen.*

Site 5

We made 3 ABE dives at site 5. The first, dive 131, made phase 1 surveys at three different pressures. The second, ABE133, did a phase 2 survey, and the final dive, ABE134 did a phase 2 survey followed by a phase 3 survey with ABE's monochrome camera. These dives are summarized in figure ABE5.1.

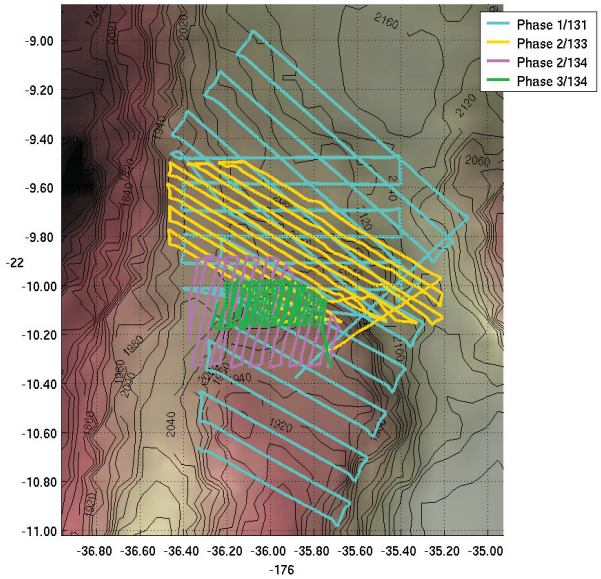

Figure 32 - ABE5.1*: We made 3 ABE dives at site 5. The first, ABE131, did a phase 1 survey at 3 different pressures. The second, ABE133, did a phase 2 survey. The final dive, ABE134, did a phase 2 survey then a phase 3 survey with the monochrome camera.*

The deep (1900 decibar) phase 1 survey portion of dive 131 showed some substantial activity in optical backscatter, eH, and temperature on the final, southwest tracklines (see figure ABE5.2). Depth excursions were also seen in the southeast side.

The mid-level survey (1820 decibars, figure ABE5.3) showed correlated increases in optical backscatter, reductions in eH voltage, and depth excursions on the western side of the survey.

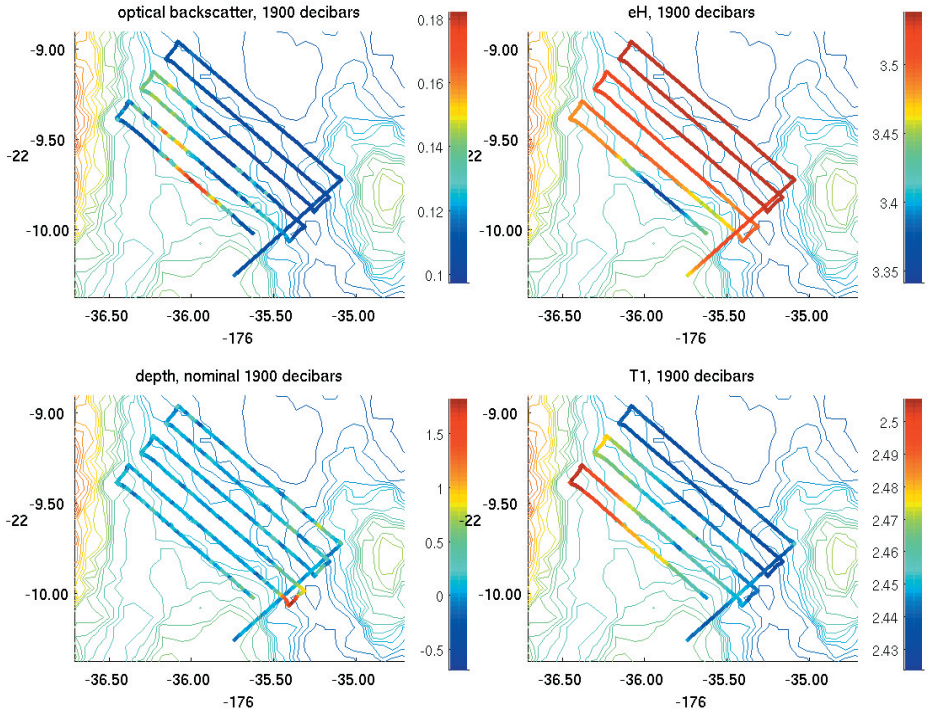

Figure 33 - ABE5.2*: The deep phase 1 survey (1900 decibars) showed coincident changes in optical backscatter, eH, and temperature on the final line to the southeast. It also showed substantial depth excursions to the southeast.*

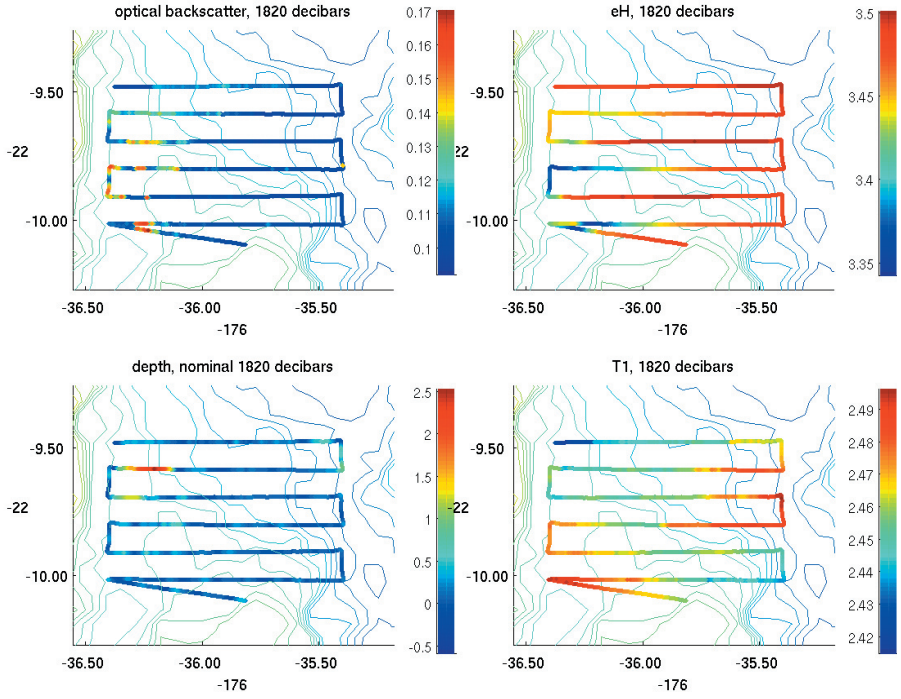

Figure 34 - ABE5.3*: The mid level phase 1 survey (1820 decibars) showed optical backscatter, eH, and depth excursion events to the west.*

The highest survey (1630 decibars, figure ABE5.4) showed correlated eH changes, depth excursions, and temperature changes to the south.

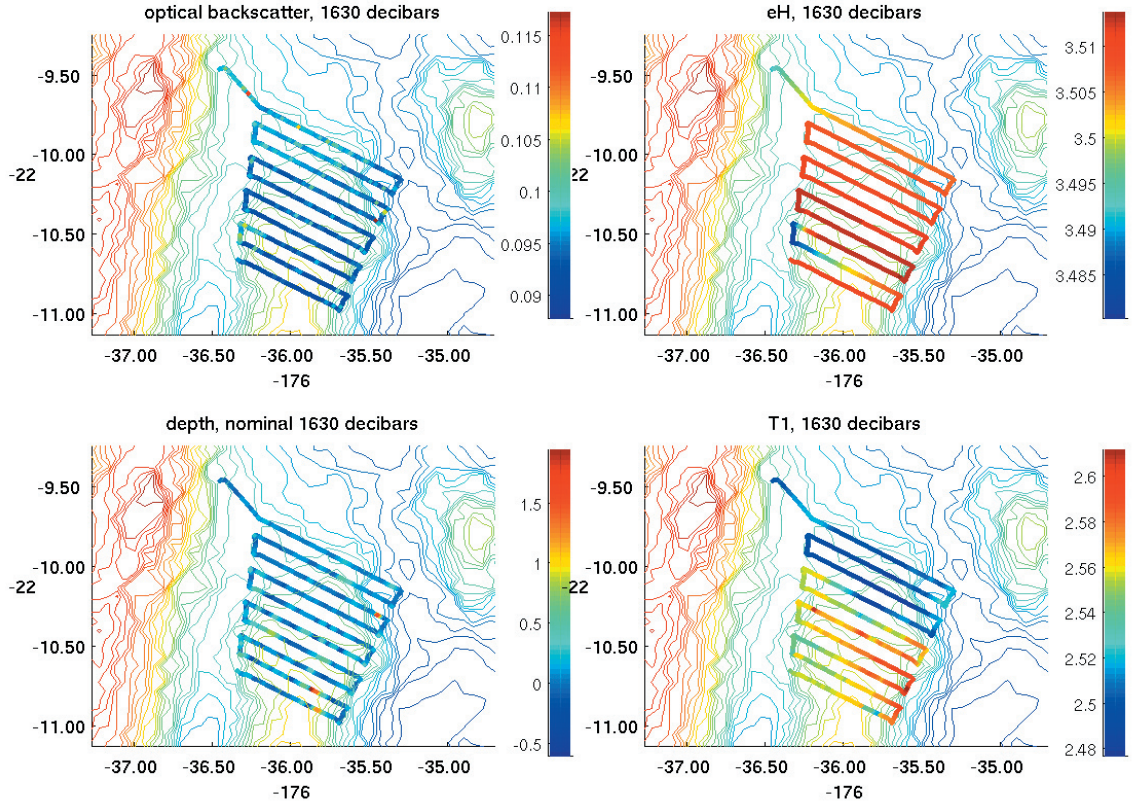

Figure 35 - ABE5.4*: The shallow phase 1 survey (1630 decibars) showed fluctuations in temperature, eH, and depth to the south.*

The optical backscatter record from the entire 131 dive (figure ABE5.5) showed substantial turbidity corresponding to the deep and mid-level surveys, but that the increase in backscatter observed with the CTD at 1630 decibars was no longer present.

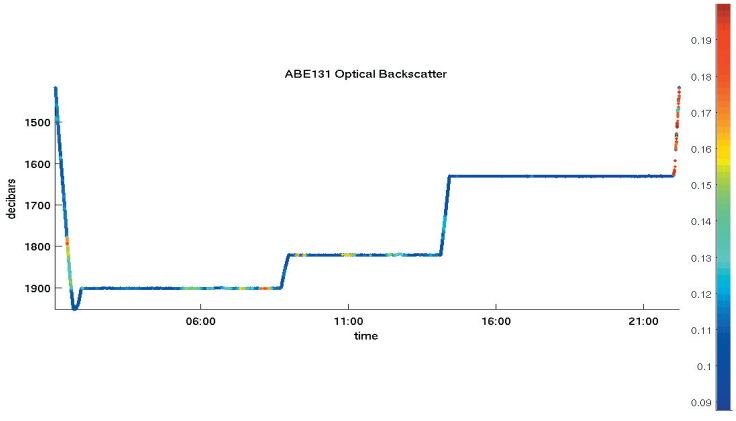

Figure 36 - ABE5.5*: This figure shows the vehicle depth as a function of time, with the color indicating intensity of the optical backscatter signal. There was no strong indication of a layer at 1630 decibars as had been observed in the CTD. The optical backscatter sensor became fouled at the very end of the run, producing the strong signal on ascent.*

The phase 2 survey done on ABE 133 showed activity in the eH, optical backscatter, and temperature sensors at the southern extent of the survey, shown in figure ABE5.6. While more difficult to determine because the vehicle was bottom-following, these events also showed vertical excursions. These signals were in the vicinity of the activity seen in the deep portion of dive 131.

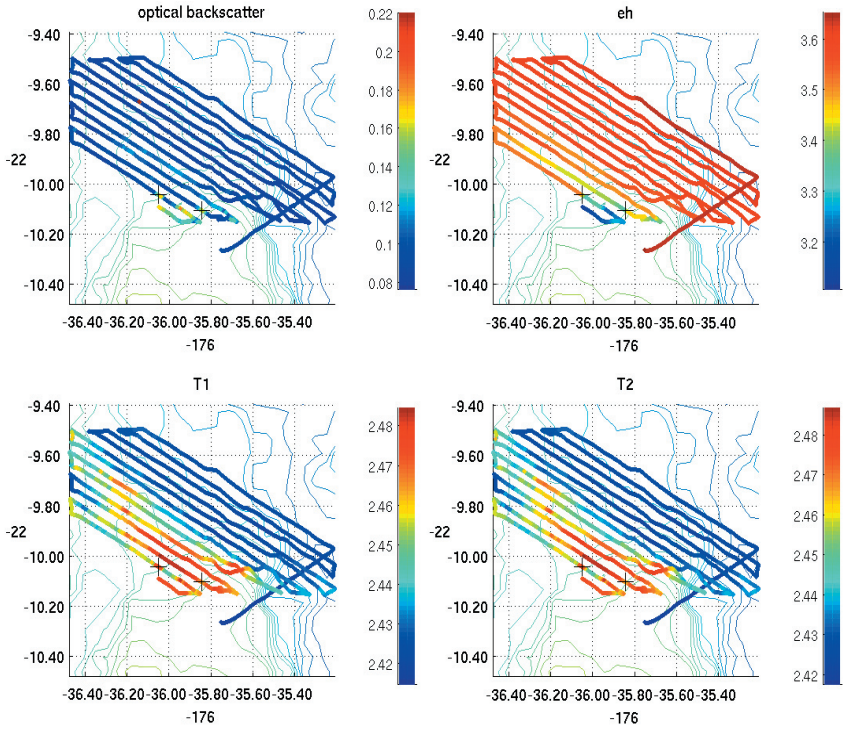

***Figure 37 - ABE5.6**: The phase 2 survey showed activity in the eH, optical backscatter, and temperature sensors at the southern extent of the survey. While more difficult to determine because the vehicle was bottom-following, these events also showed vertical excursions.*

***Figure 38 - ABE5.7**: The phase 2 element of dive 134 showed some temperature increases, but these did not correlate with changes in either eH or optical backscatter.*

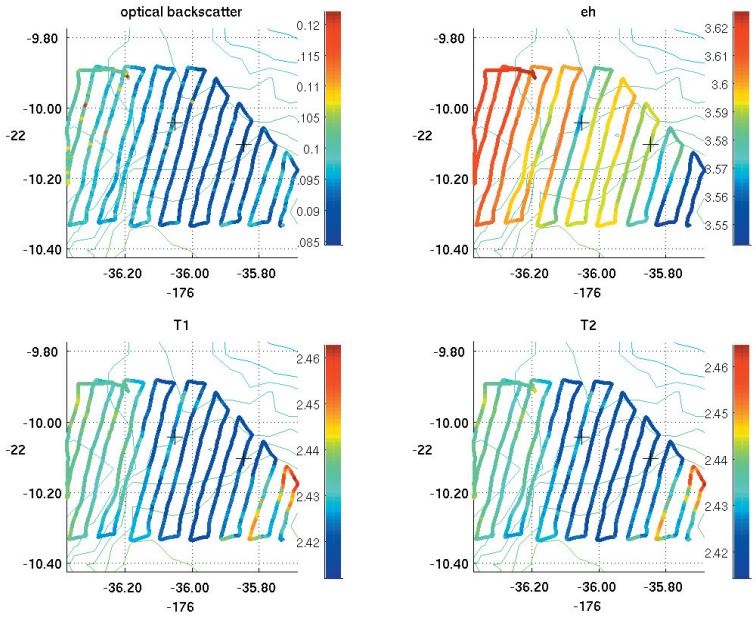

The phase 2 portion of ABE134 showed an increase in temperature at the eastern edge, but this did not correlate with changes in eH or optical backscatter (see figure ABE5.7). The tracklines for ABE135 overlapped
with the lines from ABE133, but the same events were not seen. The temperature increases were over 300 meters to the east of the events seen in ABE133.

The phase 3 portion of ABE134 showed a substantial band of activity in temperature, eH, and optical backscatter to the west, as seen in figure ABE5.8. These changes were not seen in the overlapping phase 2 lines of the same dive, but they did correlate spatially with the most notable events in ABE133.

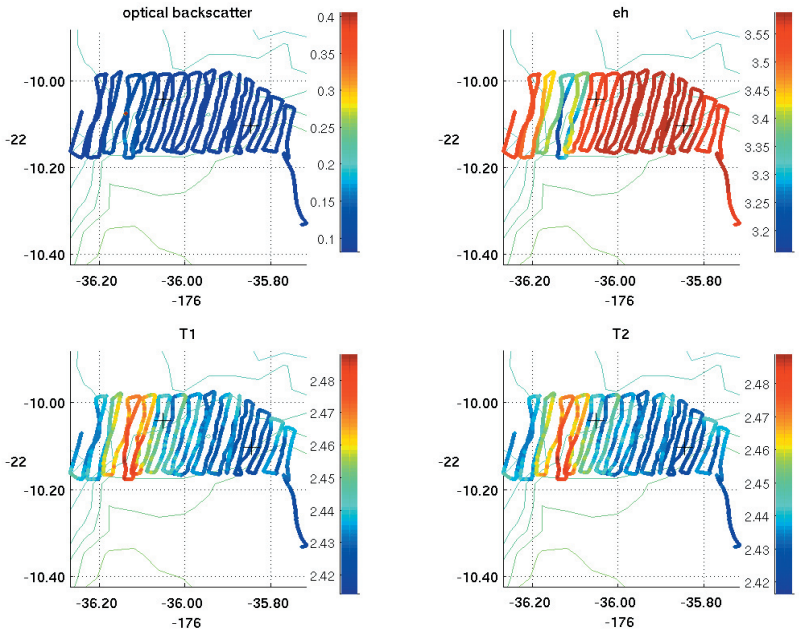

Figure 39 - ABE5.8*: The phase 3 portion of dive 134 showed some increases in temperture on 4 tracklines, which correlated with changes in eH and an increase in optical backscatter.*

The bathymetric map of the site assembled from dives 133 and 134 is shown in figure ABE5.9. This map used both SM2000 multibeam data from dive 133 and Imagenex scanning sonar from dive 134.

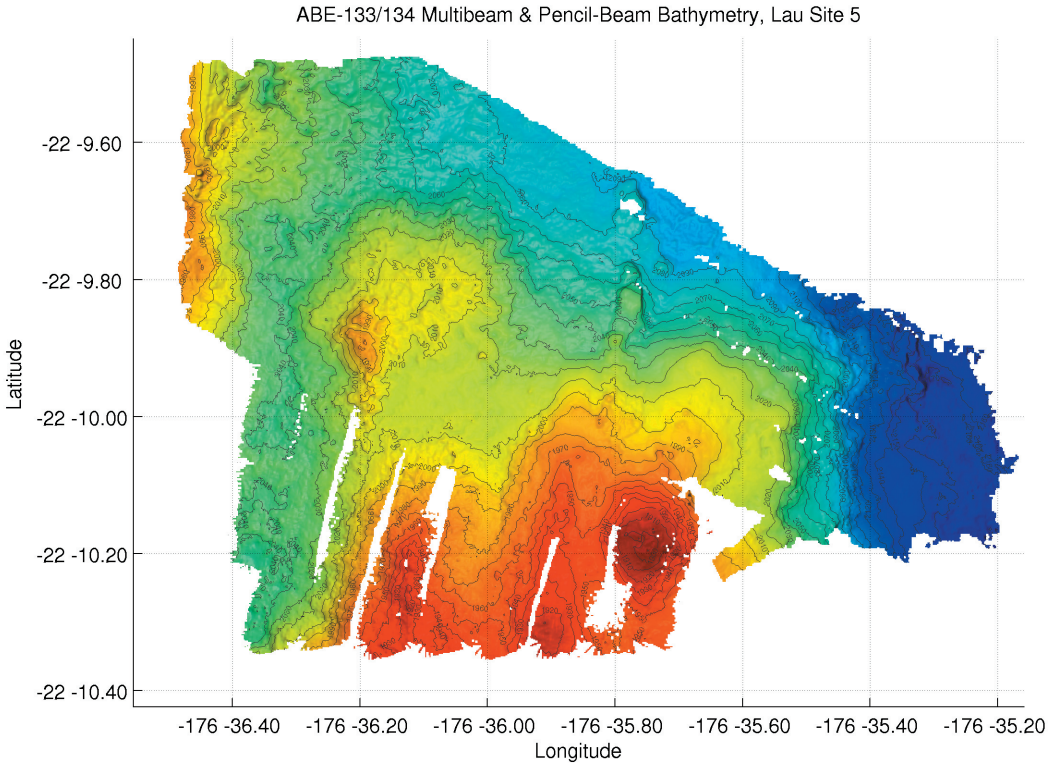

Figure 40 - ABE5.9*: This figure shows the bathymetry produced on ABE 133 and 134. The 133 data came from the SM2000 multibeam, the 134 data came from the Imagenex mechanically-scanned sonar.*

Site 6

ABE made one dive at site 6, located about 6 km to the northwest of site 5. As shown in figure ABE6.1, this dive included both phase 1 and phase 2 elements.

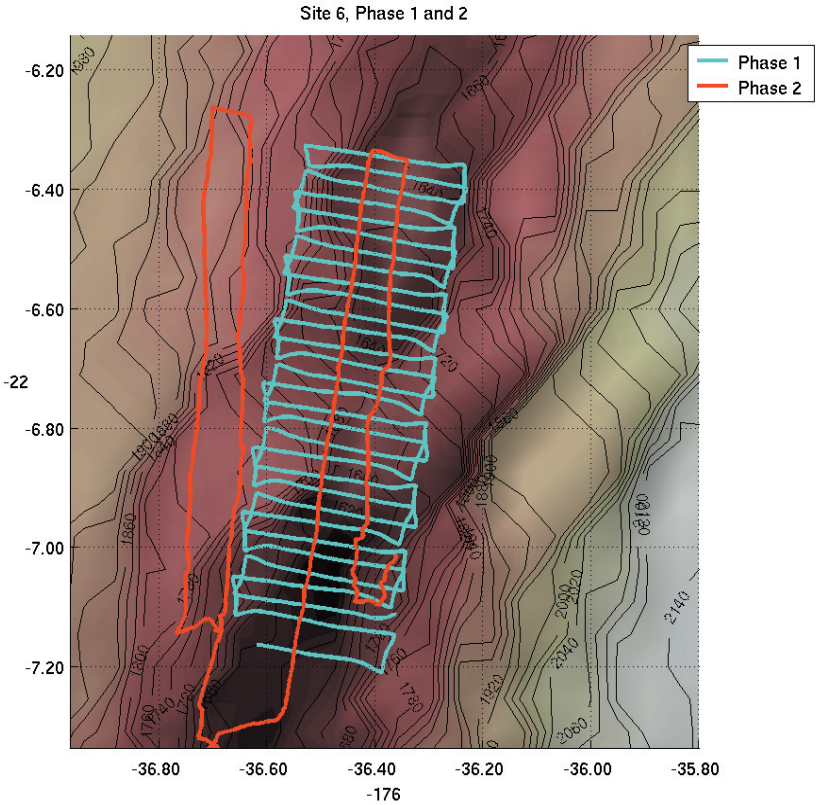

Figure 41 - ABE6.1*: ABE made one dive at site 6, which included both a phase 1 and a phase 2 survey.*

The phase 1 portion of dive 132 showed some correlated changes in optical backscatter and eH in the southeast corner as well as some strong temperature increases to the north, see figure ABE6.2. The temperature increases to the north did not correlate with either optical backscatter or eH changes.No vertical excursions were observered in the phase 1 data.

The phase 2 survey had a problem with the transponder navigation for the first two lines, when the direct path to the transponders was obscured by terrain. These lines were navigated after the dive using surface bounces. Due to compass errors, the two tracklines without LBL navigation were deflected to the west. During one of those lines, the vehicle saw a large vertical excursion of 10 meters (at 03:10), but his was not correlated with temperature, eH, or optical backscatter.

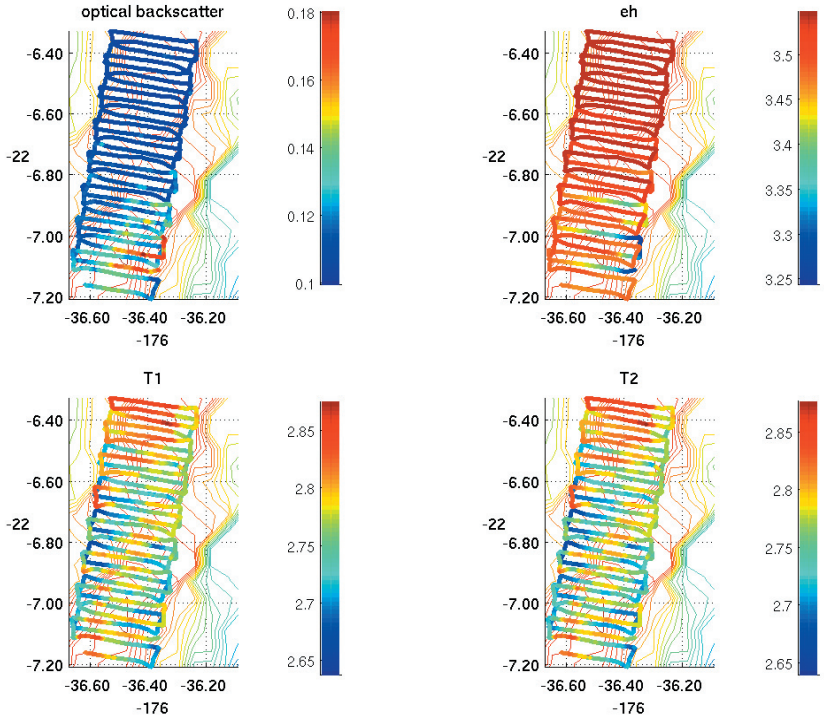

Figure 42 - ABE6.2*: The phase 1 survey at site 6 showed increases in optical backscatter and drops in eH in the southeast corner, and uniform fluctuations in temperature across the ridge.*

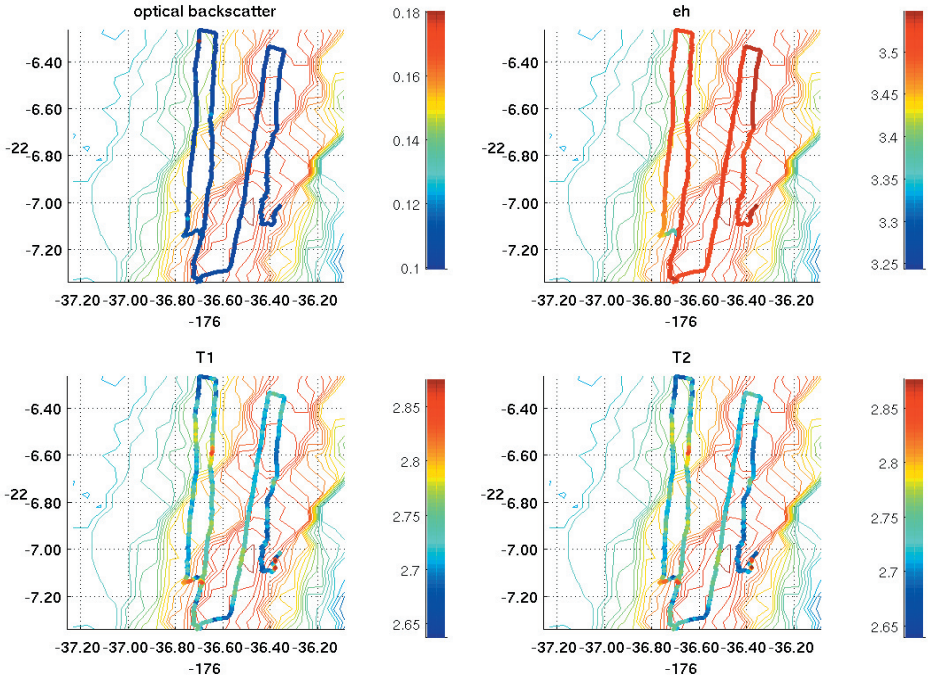

Figure 43 - ABE6.3: *The phase 2 portion of dive 132 showed some correlated temperature and eH activity while descending at the beginning (southwest corner), but little activity otherwise.*

Table 1: Transponder Positions

Site 1

lau1 xpndr a: NOAA8.5H reply freq: 8.50 release code: H on off: A/B serial number: 42543 Sept 15, 2004 surveyed: -20 -3.3619 -176 -8.6308 2428.9 Status: deployed	lau1 xpndr b: NOAA 9.5E reply freq: 9.50 release code: E on off: A/B serial number: 59645 Sept 15, 2004 surveyed: -20 -4.8891 -176 -9.1092 2458.1 Status: deployed

Site 2

lau2 xpndr a: NOAA 10.0G reply freq: 8.50 release code: G on off: B/D serial number: 42418 Oct 1, 2004 surveyed: -20 -19.4905 -176 -9.1932 2337.2 Status: deployed	lau2 xpndr b: NOAA 9.5E reply freq: 9.50 release code: E on off: B/D serial number: 50665 Oct 1,2004 surveyed: -20 -20.0171 -176 -7.1974 2367.2 Status: deployed
lau2 xpndr c: UNC 10.0D reply freq: 10.00 release code: D on off: none? serial number: 48518 Sept 16, 2004 surveyed: -20 -20.3144 -176 -10.3261 2221.0 status: recovered Oct 7, 2004	lau2 xpndr d: UNC 11.5f reply freq: 11.50 release code: F on off: A/B serial number: 65871 Sept 16, 2004 surveyed: -20 -18.6553 -176 -9.9063 2207.6 Status: Recovered Oct 7, 2004

Site 3

lau3 xpndr a: NOAA 8.5F reply freq: 8.50 release code: F on off: B/D serial number: 63588 Sept 19, 2004 surveyed: -20 -47.0237 -176 -10.6523 2029.4 status: deployed	lau3 xpndr b: UNC 9.5C reply freq: 9.50 release code: C on off: A/B serial number: 45361 Sept 17, 2004 surveyed: -20 -45.5734 -176 -10.1658 2071.0 status: deployed

Site 4

lau4 xpndr a: ABE 8.5F reply freq: 8.50 release code: F on off: none serial number: 68264 Sept 20, 2004 surveyed: -21 -6.9085 -176 -16.6004 1947.9 Status: deployed	au4 xpndr b: ABE 9.5C reply freq: 9.50 release code: C on off: none serial number: 69599 Sept 20, 2004 surveyed: -21 -5.8584 -176 -16.1415 1973.8 Status: Deployed

Site 5: All site 5 transonders were recovered

au6 xpndr a: NOAA 8.5G reply freq: 8.50 release code: G on off: B/D serial number: 42418 Sept 24, 2004 surveyed: -22 -7.9432 -176 -36.7371 1506.8 Status: recovered	lau5 xpndr b: reply freq: 9.50 release code: E on off: B/D serial number: 50665 Sept 22, 2004 surveyed: -22 -11.1050 -176 -35.9033 1689.8 Status: recovered
lau5 xpndr c: ABE 10.0B reply freq: 10.00 release code: B on off: none serial number: 68243 Sept 22, 2004 surveyed: -22 -10.5805 -176 -37.1193 1550.0 Status: recovered	lau6 xpndr d: ABE 11.5F reply freq: 11.50 release code: F on off: none serial number: 67591 Sept 24, 2004 surveyed: -22 -7.2291 -176 -34.8208 1349.8 Status: recovered

CTD Operations & Water Column Analyses

When high-temperature hydrothermal vents are emitted from the deep seafloor they are buoyant and can rise hundreds of meters above the seafloor before reaching a level of neutral buoyancy. Because these fluids are chemically quite distinct from non-hydrothermal seawater a range of chemical reactions take place as these fluids mix, turbulently, within the buoyant hydrothermal plume: a range of minerals precipitate (sulfides, oxides) which are swept up with the ascending fluid to generate a particle-laden, chemically-enriched fluid layer that can be detected kilometers away from an active vent-site. For this reason, tow-yo'ing of CTDs has become a standard method for the detection and location of seafloor hydrothermal vent-sites – at least to within a few hundreds of meters. In this cruise, exactly that form of exploration was used to commence operations subsequently taken on by ABE during Phase I and Phase II dives (see elsewhere). Following those more comprehensive plume surveys, not readily achievable from a CTD package deployed from a surface ship, additional vertical lowerings of the CTD system were conducted toward the end of Phase II studies, to collect best possible samples for inter-comparison of plume geochemistries among the different sites visited during our cruise and to provide maximum input on likely vent-fluid composition to the wider R2K community.

Operational information

The CTD system used throughout the cruise was the ship's own SeaBird 9/11+ CTD-rosette system equipped with 24 x 10L Niskin bottles. The hydrographic team successfully completed 23 full-depth CTD casts (~87.5 hours of operation), 1 test cast, and only had 2 aborted casts. After the initial test deployment we discovered that only 20 of 24 Niskin bottles were functional. The 4 remaining bottles, Niskins 3, 4, 8 , and 18, had the top and bottom cap O-rings replaced, the spigots changed (with O-rings) changed, and the discs replaced. These bottles were then acid washed and re-commissioned. During the cruise, simple maintenance was also conducted on Niskins 2, 5-6, 8-10, 13, 15, 17, and 22. This includes replacement and/or resetting O-rings, spigot O-ring replacement, and resealing end caps. The lanyard on Niskin 4 snapped during operation and was replaced as well. Of the two aborted casts, only one was do to equipment malfunction. Cast #19 was aborted and redone after repositioning the ship to a more promising site while Cast #17 was aborted in response to extremely high modular error counts, an indication of faulty signals coming up the wire. Several tests indicated a bad termination, a loose connection that lead to seawater leaking and subsequent communication problems between the CTD itself and the deck unit. Once the faulty connection was identified and the cable termination redone (less than one hour), no further communication problems occurred.

The carousel and water sampler were also replaced after cast #12. During cast #11, Niskin 19 came on deck in its open position. The processed data showed that Niskin 19 had been triggered, indicating a potential signaling problem to that bottle position. Once the water sampler was removed, it was discovered that solenoid 19 on the carousel was slightly ruptured, most likely hampering the electronic signal between the carousel and water sampler. Furthermore, a ruptured solenoid is a potential leak source that would lead to a ruined carousel and may result in a damaged CTD. Accordingly, the spare

carousel was taken from storage and all its solenoids were cleaned thoroughly. Afterwards, the complete carousel/water sampler combination on the rosette was replaced with the ship's spare units. The units remained on the CTD and are operating properly. The carousel taken off the CTD has been cleaned and placed into storage with its water sampler. A full report of the problems encountered with the CTD and steps taken in response has been placed with STAG Gabe Foreman, aboard ship.

There were several auxiliary instruments connected to the CTD in addition to the standard Seabird CTD sensors. Both an SBE 43 Oxygen Sensor and a Seapoint Fluorometer were attached to the rosette prior to the cruise and several pieces of equipment were added to the system after departure. First, a WetLabs LBSS backscattering sensor was fixed to the frame and connected to auxiliary port 6 in the CTD. We also attached a Benthos 2110-2 Altimeter to several auxiliary ports but could not convert the voltage readout to practical units (meters above bottom) because we lacked the altimeter's control file. As a replacement, we attached a bottom contact switch with 7 meters slack and routinely affixed a pinger to the bottom of the frame. Additionally, an acoustic pinger was attached to the rosette frame for all near-bottom sampling operations (CTD 12 onwards).

Of the total of 23+1 CTD operations conducted during the cruise, all except 2 were completed along the Eastern Lau Spreading Centre. The exceptions were an off-axis background station (CTD 23) and a final CTD station (CTD 24) above the southern Fonualei Ridge to ground-truth one of several sets of optical back-scatter signal obtained from MAPR deployments on Rock Cores 125-145 and Dredges 57-62.

Phase I Operations (Exploratory Tow-Yo's)

Within the ELSC, a series of Phase I tow-yo's were conducted, working from North to South, as follows:

• In Area 1, the coverage obtained from optical back-scatter data on the CTD system were sufficient to deduce that the primary source of venting lay between parallel tow-lines CTD 01and CTD 02, probably closer to CTD 02. This information was used to help constrain the choice of survey area for ABE Phase I diving.

• In Area 2, the absence of a third CTD line was sufficient only to deduce that a strong source existed north of CTD 04 (CTD 05 was south of CTD 04). The source identified by these CTDs may be the vent-sites subsequently located farther north.

• In Area 3, no directional information was obtained but it was recognized that at least two separate plumes existed at different depths and the ABE Phase I dive was adjusted accordingly.

• In Area 4 no directional information, nor data on the temporal variability of the non-buoyant plume's depth was obtained. ABE subsequently flew a short mission at a constant depth, ca. 50m deeper than the non-buoyant plume.

• In Area 5 a long tow-yo parallel to the ridge-axis revealed extremely strong plume signals at three different depths at the north end of the Vai Lili Ridge segment (CTD 08). A subsequent cross-axis tow-yo (CTD 09) from the northern Vai-Lili Ridge toward the White Church segment revealed strongest plume signals – the strongest observed on the CTD throughout the entire cruise – immediately north of the Vai Lili Ridge, close to the crossing point with CTD 08.

• In Area 6 a first cross-axis tow-yo (CTD 10), north of a target AVR (axial volcanic ridge) revealed a modest plume that was stronger to the East than to the West of the ridge-summit. Subsequent tow-yo CTD11, just south of CTD 10 again found evidence for a strong plume dispersing North and East away from the summit but strongest optical backscatter signals were observed distant from the target AVR, overlying the much deeper seafloor, east of the White Church ridge-segment.

Table 2: CTD-TOW-YO LOCATIONS

			Latitude-(^{0}S)		Longitude -(^{0}W)
Area 1	CTD 01: Start	20	2.660	176	8.070
	CTD 01: End	20	3.548	176	7.035
	CTD 02: Start	20	3.182	176	8.222
	CTD 02: End	20	4.070	176	7.238
	CTD 03: Start	20	3.704	176	8.327
	CTD 03: End	20	4.964	176	6.748
Area 2	CTD 04: Start	20	19.490	176	9.301
	CTD 04: End	20	20.230	176	7.460
	CTD 05: Start	20	19.392	176	9.235
	CTD 05: End	20	20.760	176	7.550
Area 3	CTD 06: Start	20	47.541	176	11.755
	CTD 06: End	20	44.093	176	11.325
Area 4	CTD 07: Start	21	6.495	176	17.598
	CTD 07: End	21	6.807	176	17.483
Area 5	CTD 08: Start	22	13.353	176	37.066
	CTD 08: End	22	8.623	176	34.913
	CTD 09: Start	22	10.147	176	35.733
	CTD 09: End	22	8.768	176	36.779
Area 6	CTD 10: Start	22	6.483	176	35.636
	CTD 10: End	22	6.499	176	37.157
	CTD 11: Start	22	6.715	176	37.013
	CTD 11: End	22	6.911	176	34.946

Phase II Operations: Detailed Plume Sampling

During Phase II operations in the ELSC area, detailed sampling was attempted at 5 of 6 locations with greater success to the North than to the South. Station locations occupied during this stage of the cruise were generally occupied from South to North as listed below. The detailed list of water samples collected is given in Appendix 10.

Table 3: CTD-Vertical Casts

			Latitude-(^{0}S)		Longitude -(^{0}W)
Area 6	Start: CTD 12	22	7.098	176	36.381
	End: CTD 12	22	6.006	176	36.327
Area 5	CTD 13	22	9.907	176	35.947
Area 3	CTD 16	20	46.232	176	11.710
	CTD 17	20	45.918	176	11.533
	CTD 18	20	45.667	176	11.464
	CTD 20	20	45.654	176	11.470
Area 2	CTD14	20	19.008	176	8.190
	CTD 15	20		176	8.165
	CTD 21	20	19.055	176	8.252
Area 1	Start: CTD 22	20	3.096	176	8.012
	End: CTD 22	20	3.255	176	8.008

• In Area 6, CTD 12 was lowered to the seafloor at a site targeted from ABE dive signals (physical and chemical sensors) without any site of active seafloor venting being characterized. Because no strong optical backscatter signal was obtained, the CTD was tow-yo'd north along the target Axial Volcanic Ridge with no apparent change in proximity to vent-source.

• In Area 5, CTD 13 was lowered close to the intersection of CTD tow-yo's 08 and 09. There was no indication of active venting in the immediate vicinity.

• Area 4 was not returned to during Phase II operations.

• In Area 3 a series of 4 CTD stations were occupied from South to North following various ABE targets but without any active source of venting on the seafloor being confirmed. Strong optical back-scatter signals were observed in all stations (CTDs 16-18, 20) but no buoyant plume signals were obtained. CTD 19 was an aborted cast in this area.

• In Area 2, CTD 14 was lowered directly above the TowCam- identified vent-site in this area and a buoyant hydrothermal plume was intercepted and sampled. No buoyant plume signals were identified at either of two further stations occupied based upon ABE Phase II data (CTDs 15, 21).

• In Area 1, there was only time for a single CTD station, despite the wide range of targets available. Consequently, a short tow-yo was conducted starting from above already-imaged (TowCam) vent-sites to an area characterized by strongest ABE Phase II anomalies. At the end of the cast a buoyant plume was intercepted and sampled.

In addition to the above stations, were CTD 23 and CTD 24:

CTD 23 (off-axis background station) was occupied at 18° 39'S, 175° 38'W.

CTD 24 (Fonua Lei Ridge) was occupied at 17° 01.39'S 174° 30.14'W.

In Situ Chemical Sensors

The SOC *in situ* chemical sensors are the result of a collaborative effort between the Ocean Engineering Division, the Challenger Division for Seafloor Processes and the School of Ocean and Earth Sciences. The instruments are a further development on those devised by Johnson and co-workers at Moss landing laboratory, CA (Johnson et al, 1986; Chin et al., 1992). The sensors are designed to determine the presence and concentration of dissolved iron II and manganese II.

The sensors employ a method of unsegmented continuous flow analysis. The sample stream is inoculated with a reagent, the combined solutions are mixed and pass into a cell where the intensity of color is determined using an LED as light source and a photodiode with light to frequency converter (TAOS) as detector. Changes in intensity of the light transmitted through the cell are proportional to the color development and hence concentration of analyte in question. The system has a series of valves that switch the system from pumping sample to a blank solution and a standard. The use of 'on-board' standard and blank, corrects for any effect that pressure and temperature can have on the colorimetric system. The iron system depends on the colorimetric reaction between Ferrozine (3-(-2-pyridyl)-5,6,-diphenyl-1,2,4-triazine-p-p'-disulphonic acid) and iron II.

Unfortunately due to an error in chemical delivery the manganese system was inoperable for this cruise, and the iron sensor was operated in a less than ideal mode. The pump system configuration on the iron sensor and insufficient chemical resulted in the system being used with lower concentrations of ferrozine. The result of this is a decrease in the resolution of the system, with a resulting deterioration in detection limit.

The iron sensor was deployed on a total of 15 ABE dives and 2 CTD casts. This resulted in a total of 275 hours of in situ operation. There were constant modifications to the system as the cruise progressed, and a great deal of high quality data was obtained that will merit further in-depth study. Although useful data was only obtained from the very final CTD cast of KM0417, the experience gained was invaluable for an excellent series of deployments with the ABE AUV just 4 months later aboard RRS Charles Darwin cruise CD169.

Shipboard & Shorebased Chemical Analyses

Water samples were collected from 23 CTD casts and 4 TOWCAM runs for shipboard analysis of methane and hydrogen gas concentrations and pH. Shipboard measurement of these quantities is critical because it minimizes potential loss or dilution of sample gas due to leakage. Because of problems with reliability (see earlier) Niskin bottles were typically fired in duplicate resulting in 10 to 12 discrete, replicated samples per cast, hence over 250 discrete replicated water samples for the cruise. Typically, duplicate samples of methane and hydrogen were drawn from each of the Niskin sampling-bottles and analyzed on board for a total of approximately 500 methane and hydrogen analyses during the cruise. One pH measurement was made for each Niskin bottle fired for a total again of 500 analyses for the cruise.

Samples for methane and hydrogen gas analysis were collected from Niskin bottles using gas-tight syringes. The samples were then equilibrated to room temperature in a water bath. After temperature equilibration a helium head space was added and the

mixture shaken to strip the dissolved methane and hydrogen gases into the helium headspace. The headspace gases were then injected into a SRI gas chromatograph which has both a flame ionization detector (FID) and a pulse discharge detector (PDD). Hydrogen is detected by the PDD while methane is detected by both the FID and the PDD. The methane and hydrogen concentration of each water sample were then determined by preparing a standard curve using known methane and hydrogen concentrations and comparing the GC signals from these standards to those of the samples. Though final results of the methane and hydrogen analysis are not yet available, the general findings are 1) Lau Basin hydrothermal vent fluids contain methane and, in some cases, hydrogen gas significantly enriched above that of background seawater, 2) the buoyant plumes sampled contained several orders of magnitude higher gas concentrations than the associated non-buoyant plumes, and 3) the highest concentrations of methane and hydrogen gas measured on this cruise occurred at CTD casts 14 and 22.

Samples for pH were collected from Niskin bottles and equilibrated to room temperature in a water bath. After equilibration, the temperature and voltage response of each sample was taken using a pH electrode. For each set of pH samples, the pH electrode response was calibrated with standards of known pH. Determination of pH in this manner not only provided valuable information concerning hydrothermal plume chemistry as well as an immediate indication of Niskin bottle leaks that would have otherwise gone undetected.

Additional samples were collected, processed, and stored for shore based analysis of ^{3}He, methane stable carbon isotope composition, Fe and Mn concentration, and plume particulate characterization by XRF and SEM. Water samples for ^{3}He were collected and stored in copper tubing. Although insufficient reagents were delivered to the ship to permit at sea Fe or Mn determinations, samples for shorebased Fe and Mn analysis were collected throughout the cruise and stored according to trace metal clean protocols. On vertical PHASE II profiles, samples for methane stable carbon isotope analysis were collected and sealed in gas tight bottles. Similarly, on vertical PHASE II profiles, samples for plume particulates were collected, filtered, stored and dried.

MAPR Operations

In collaboration with Ed Baker of NOAA we had with us at sea Miniature Autonomous Plume Recorders (MAPR's) that could be attached to dredges and rock cores to record depth, temperature and light transmission in the water column. The Martinez cruise had completed an underway survey of the water column using a string of five MAPR's at different depths on the wire above and below their deep towed survey vehicles. Since regional water coverage was already completed for the ELSC, we used MAPR's only when necessary to help locate the vent sites within the target areas. When we were trying to establish in more detail the gradient of a plume over a vent site in the target area we would attach MAPR's to the wire during rock cores. This approach was used at site 5.

We also did some work outside the survey area of Martinez et al, and in these locations MAPR's were used routinely on both dredges and rocks cores We obtained new water column data for the intra-Lau spreading center, north of the Martinez coverage. Most of the new MAPR coverage took place on the Fonua Lei Rifts, where we discovered multiple sites with distinct vigorous water column plumes. These results are the first indication of substantial hydrothermal activity for this spreading center.

Table 8 gives the locations of all MAPR deployments. The complete MAPR data are included as Appendix 14 in the CD attached to this report. Profiles of nephelometer voltage for the deeper part of the water column for every MAPR deployment are shown in Figure 44.

Figure 44: Deep water column profiles of nephelometry voltage recorded by the MAPR's

RC 003

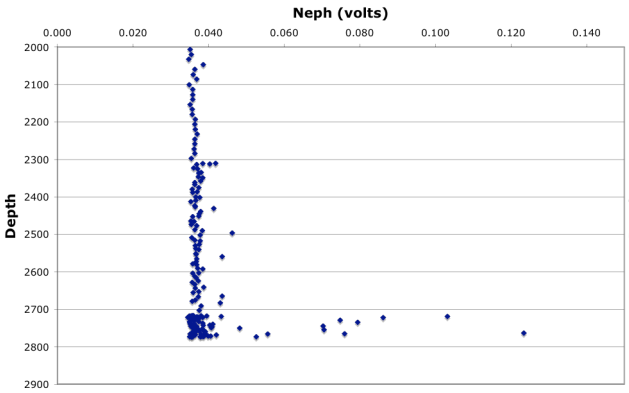

RC 004

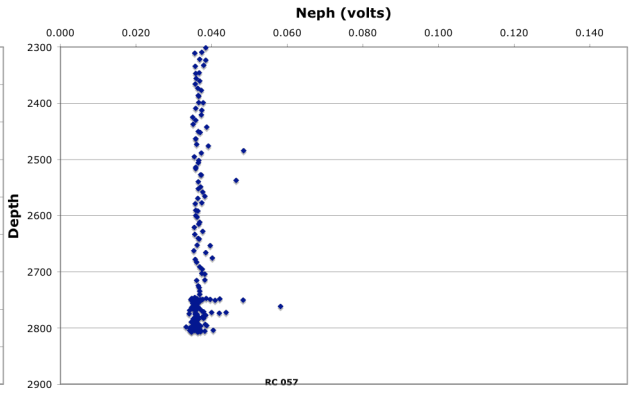

RC 057

DR 004

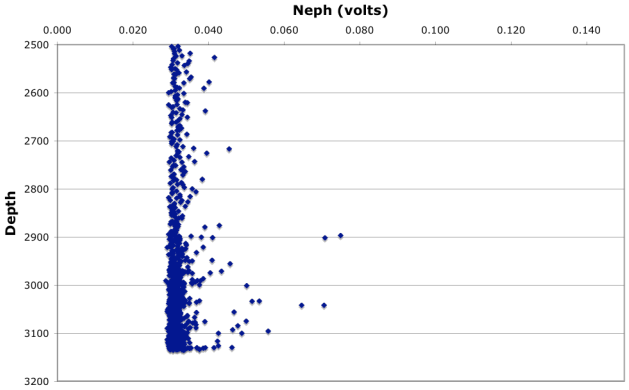

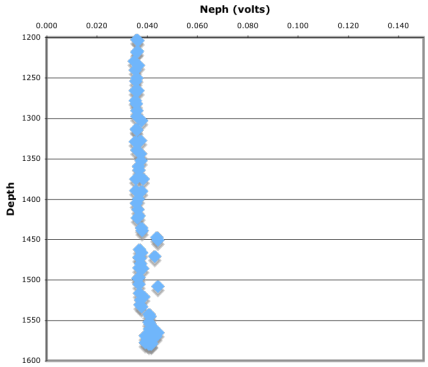

RC 059

RC 058

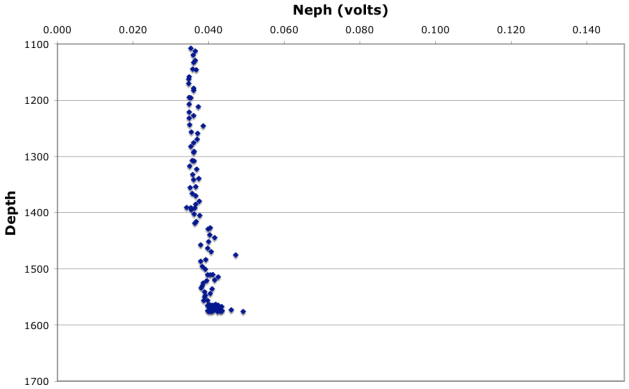

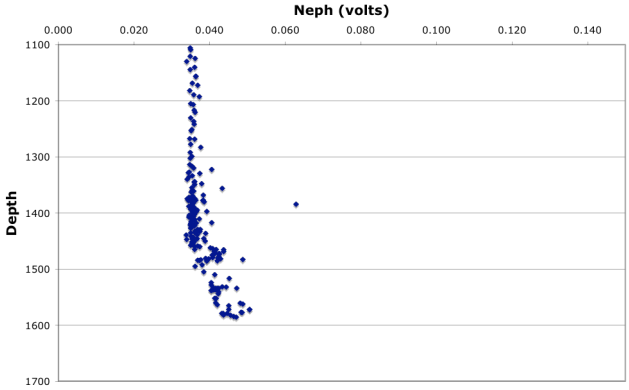

RC 091

RC 075

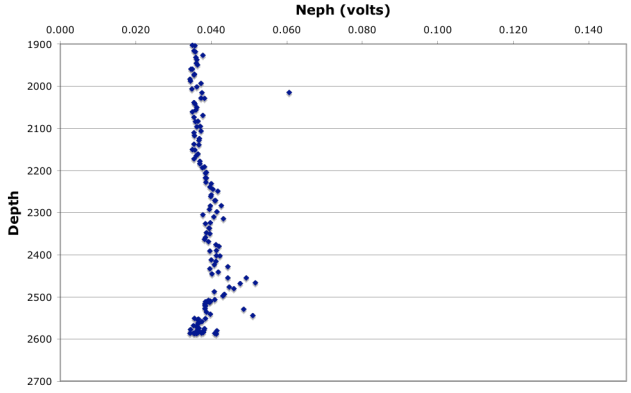

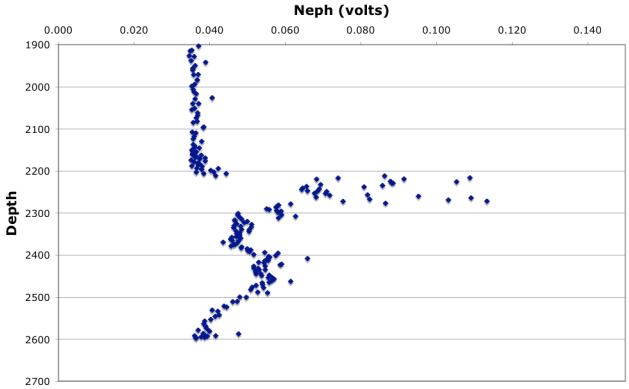

RC 125

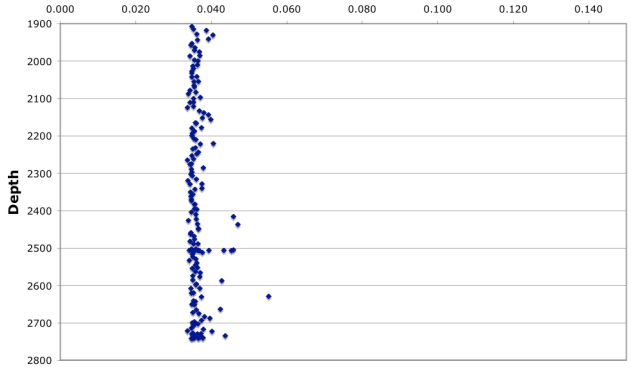

RC 126

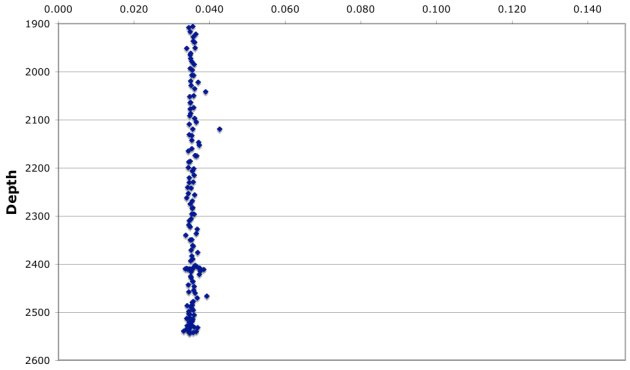

RC 127

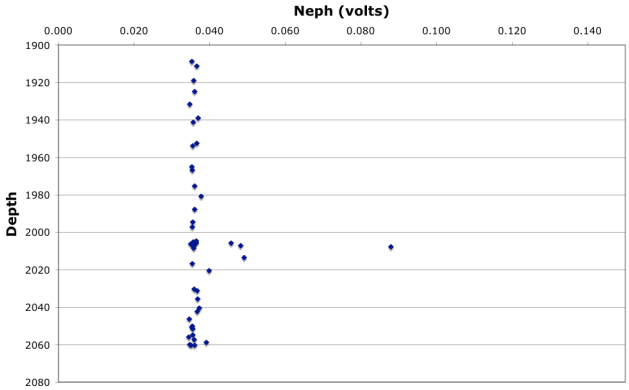

DR 058

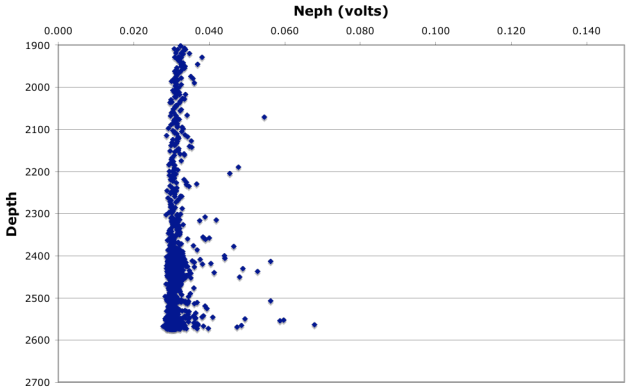

RC 128

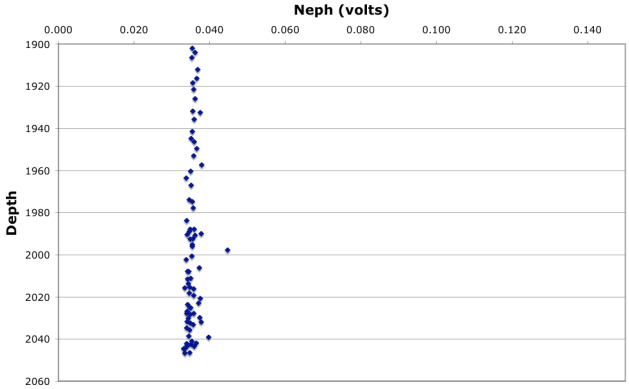

RC 129

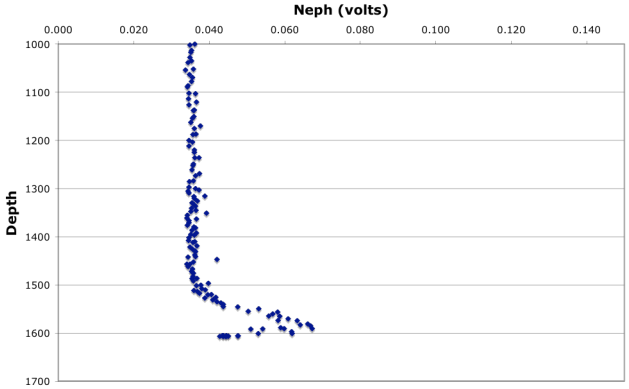

RC 130

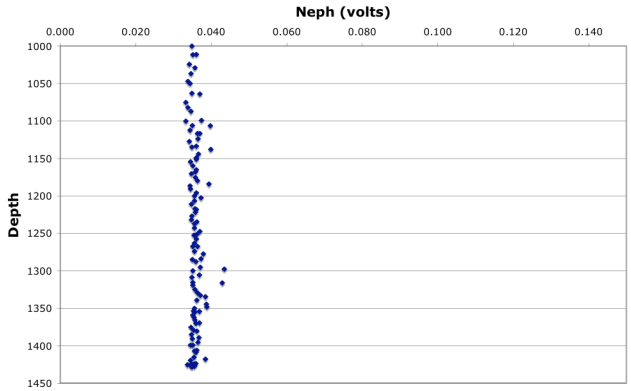

RC 131

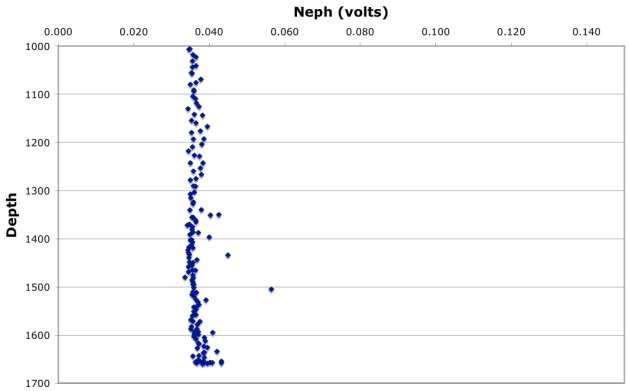

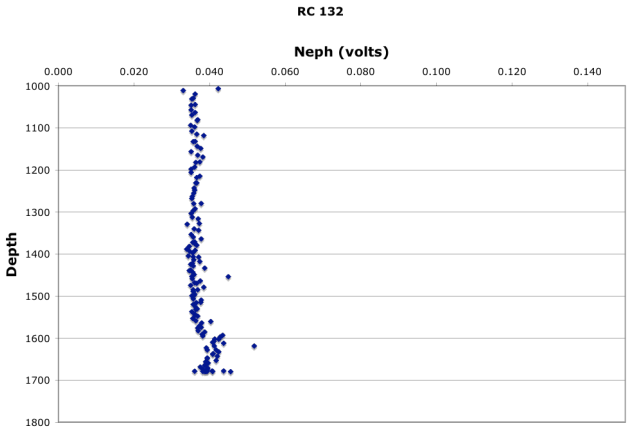
RC 132
Neph (volts)
0.000
0.020
0.040
0.060
0.080
0.100
0.120
0.140
Depth
1000
1100
1200
1300
1400
1500
1600
1700
1800

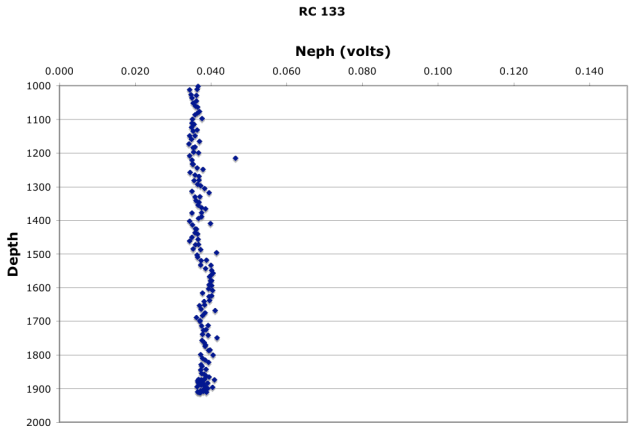
RC 133
Neph (volts)
0.000
0.020
0.040
0.060
0.080
0.100
0.120
0.140
Depth
1000
1100
1200
1300
1400
1500
1600
1700
1800
1900
2000

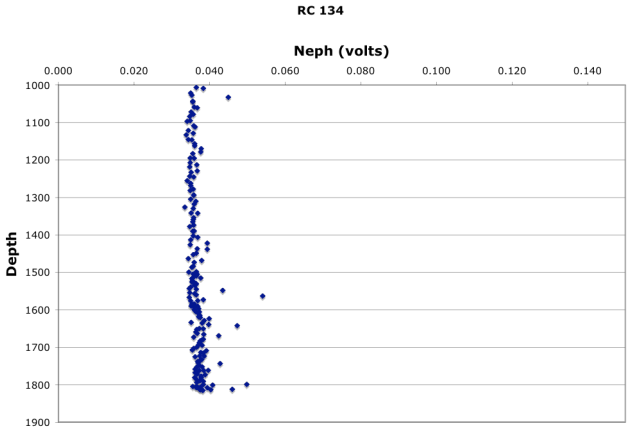
RC 134
Neph (volts)
0.000
0.020
0.040
0.060
0.080
0.100
0.120
0.140
Depth
1000
1100
1200
1300
1400
1500
1600
1700
1800
1900

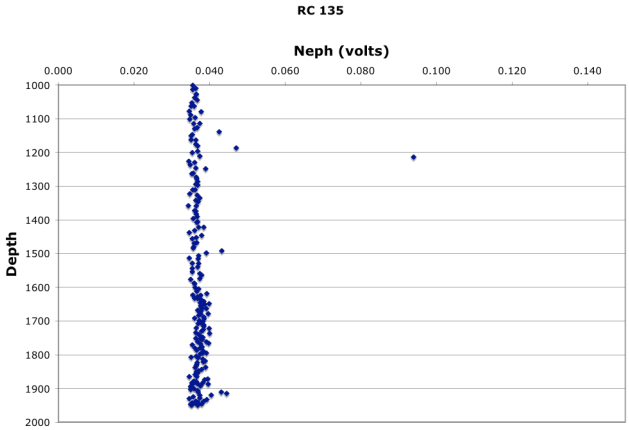
RC 135
Neph (volts)
0.000
0.020
0.040
0.060
0.080
0.100
0.120
0.140
Depth
1000
1100
1200
1300
1400
1500
1600
1700
1800
1900
2000

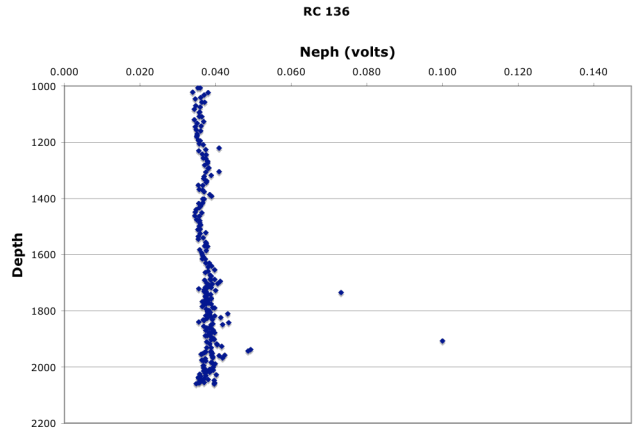
RC 136
Neph (volts)
0.000 0.020 0.040 0.060 0.080 0.100 0.120 0.140
Depth
1000 1200 1400 1600 1800 2000 2200

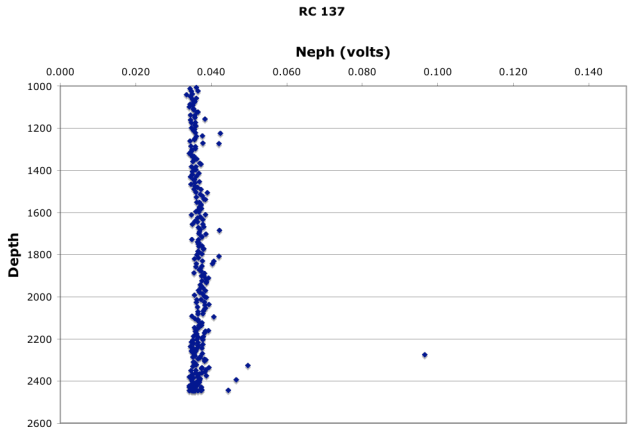
RC 137
Neph (volts)
0.000 0.020 0.040 0.060 0.080 0.100 0.120 0.140
Depth
1000 1200 1400 1600 1800 2000 2200 2400 2600

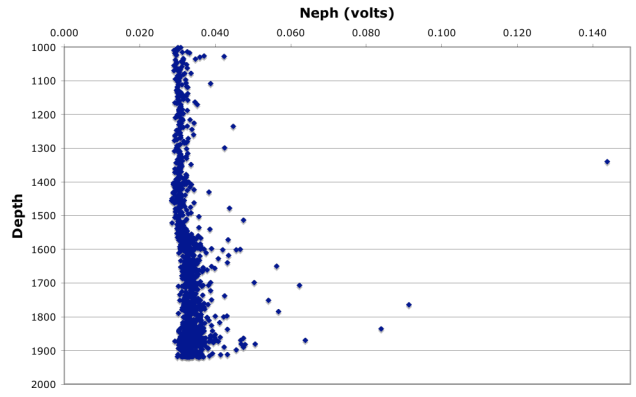
DR 060
Neph (volts)
0.000 0.020 0.040 0.060 0.080 0.100 0.120 0.140
Depth
1000 1100 1200 1300 1400 1500 1600 1700 1800 1900 2000

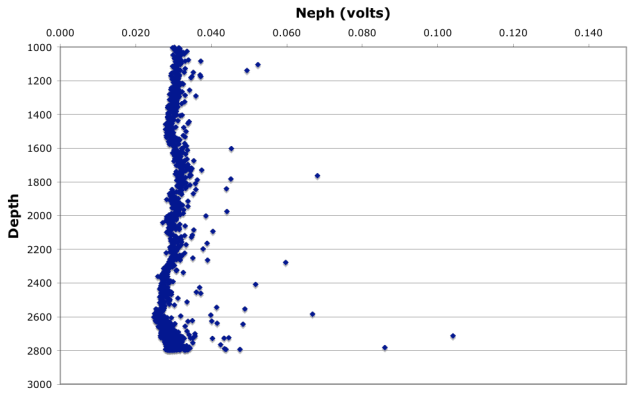
DR 061
Neph (volts)
0.000 0.020 0.040 0.060 0.080 0.100 0.120 0.140
Depth
1000 1200 1400 1600 1800 2000 2200 2400 2600 2800 3000

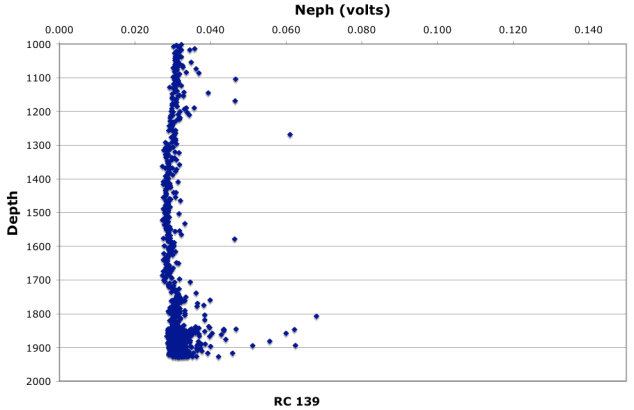
DR 062
Neph (volts)
0.000 0.020 0.040 0.060 0.080 0.100 0.120 0.140
Depth
1000 1100 1200 1300 1400 1500 1600 1700 1800 1900 2000

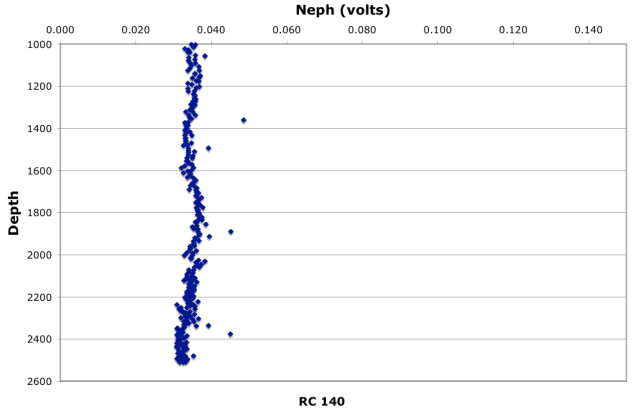
RC 138
Neph (volts)
0.000 0.020 0.040 0.060 0.080 0.100 0.120 0.140
Depth
1000 1200 1400 1600 1800 2000 2200 2400 2600

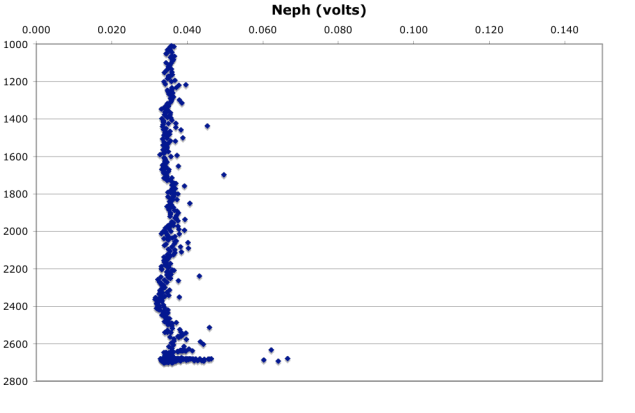
RC 139
Neph (volts)
0.000 0.020 0.040 0.060 0.080 0.100 0.120 0.140
Depth
1000 1100 1200 1300 1400 1500 1600 1700 1800 1900 2000

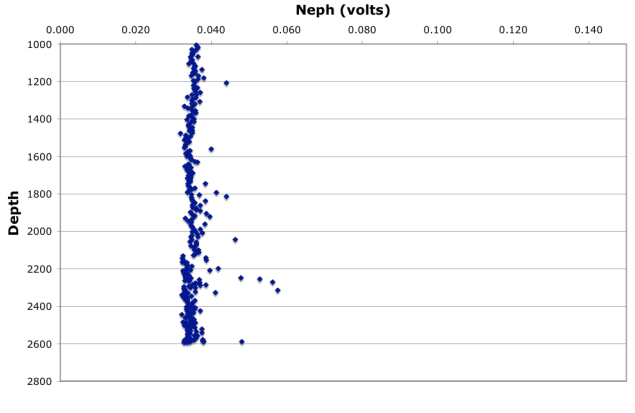
RC 140
Neph (volts)
0.000 0.020 0.040 0.060 0.080 0.100 0.120 0.140
Depth
1000 1200 1400 1600 1800 2000 2200 2400 2600

Neph (volts)
0.000 0.020 0.040 0.060 0.080 0.100 0.120 0.140
Depth
1000 1200 1400 1600 1800 2000 2200 2400 2600 2800

Neph (volts)
0.000 0.020 0.040 0.060 0.080 0.100 0.120 0.140
Depth
1000 1200 1400 1600 1800 2000 2200 2400 2600 2800

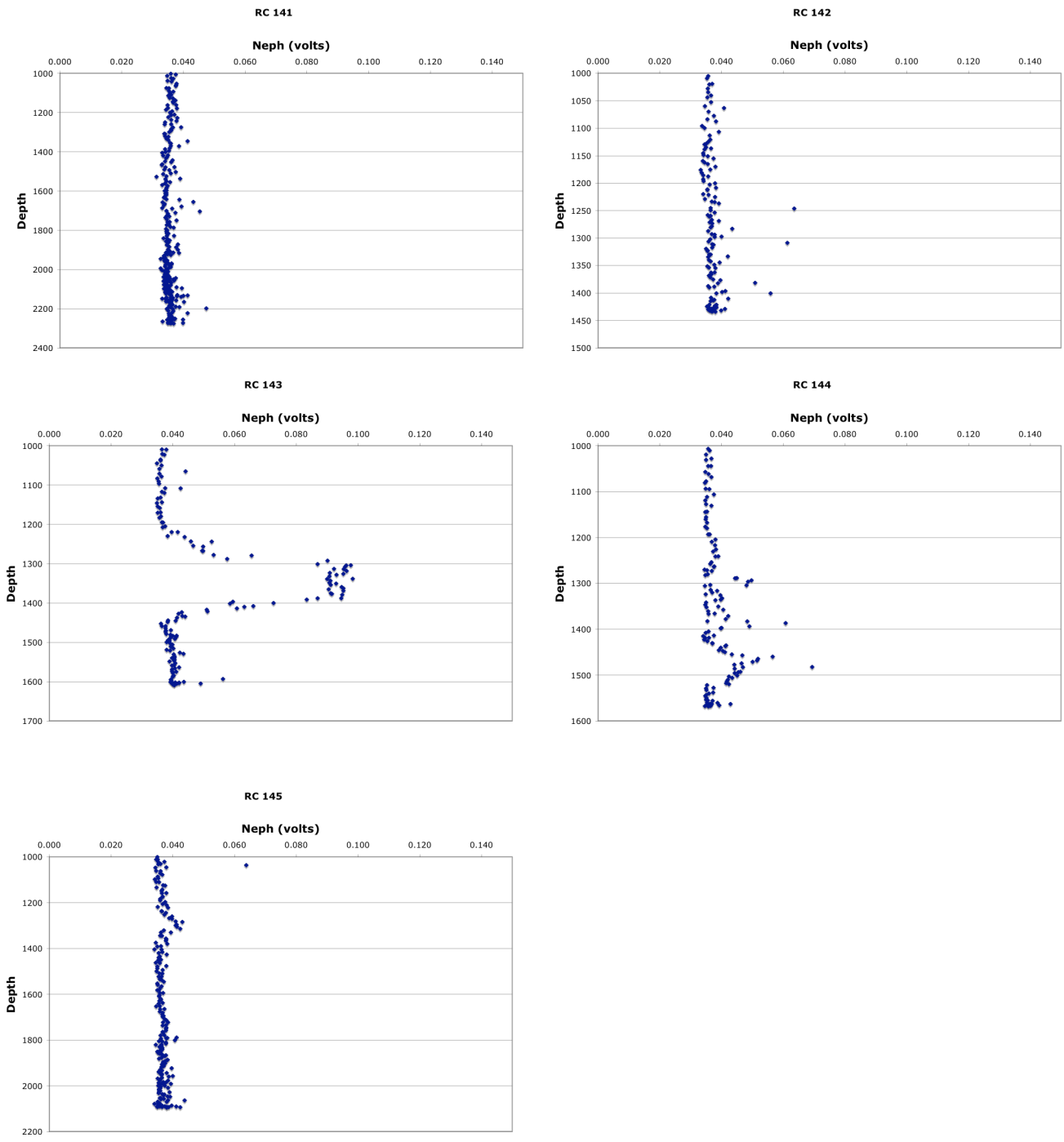

Figure 44: Deep water column profiles of nephelometry voltage recorded by the MAPR's

TOWCAM OPERATIONS

WHOI TowCam – Brief System Description

The WHOI *TowCam* was used for twelve deployments during the KM4-17 cruise to collect digital seafloor images over areas of interest based on ABE surveys, DSL-120a sidescan imagery or CTD tow-yos. *TowCam* is an internally recording digital deep-sea camera system that also permits acquisition of volcanic glass samples using up to eight (8) rock core winches, and triggering of four (4) 1.2 liter or 5.0 liter Niskin bottles, in conjunction with CTD water properties data [Fornari, 2003]. The *TowCam* was towed on the Kilo Moana's standard UNOLS 0.322" coaxial CTD sea cable. The system permits real-time acquisition of digital depth and altitude data during the tow that can be used to help quantify objects in the digital images. The use of the conducting sea cable and CTD system also permits real-time, manual triggering of any of eight rock core units and four Niskin bottles on the sled so that discrete samples of volcanic glass and seawater can be collected during a lowering from specific areas

TowCam height off-bottom is monitored in real-time using a 100 kHz altimeter on TowCam's SBE25 CTD. *TowCam* altitude is controlled by hauling-in and paying out CTD wire at the Lab #1 winch control station. Because water clarity was generally good for the Lau Basin work, the system was normally towed ~5 m above the seafloor at speeds of ~1/4 to 1/2 knot. Camera and strobe functionality are verified during the tow using the "Flashbird"; a light sensor that plugs into one of the available serial ports on the Seabird25 CTD. Each flash from the strobe produces a signal in the CTD data acquisition screen so that camera functionality can be constantly monitored and the time of each flash can be correlated to the camera time stamped on each image.

The DSPL DigiSeaCam is the imaging sensor on the TowCam (<http://www.deepsea.com>). It is a 6000 m depth rated, 3.3 Mpixel, digital camera (a Nikon 995 Coolpix is the imaging module) with a 2GB CompactFlash card for internal image storage. The camera has a corrected optical dome port that generates crisp, wide-angle photographs exhibiting a minimum of geometric distortion. For *TowCam* operations, it is used in a 'simple time lapse' mode whereby the camera is programmed to have a delay (a 60 minute delay was used during this cruise) that permits descent to the seafloor without taking photographs, thereby saving images for the seafloor traverse. The camera utilizes a DigiSnap controller board (currently a DigiSnap Model 2300 with firmware rev. 3.02-manufactured by Harbortronics (<http://www.harbortronics.com>).

Technical specifications, setup for the camera and downloading procedures, as well as other information on the WHOI *TowCam* are described in the *TowCam* Users Manual available at:

http://www.whoi.edu/marops/support_services/list_equip_towed_camera.html.

The digital images are 2048 x 1536 color, high-resolution JPEG format files, each ~900kbytes in size. Each image is date/time stamped when acquired, but the image file names are in standard Nikon format and must be converted in order for the files to be tagged with date and time as the file name. DOS and Apple Mac OSX scripts have been written and are used for converting the raw Nikon formatted files to date/time named files having the format:

"yyyy_mm_dd_hh_mm_ss.jpg".

In addition, a Perl script is used to correct image file name times based on correlation to photographs of GMT clock time at the beginning and end of each tow in order to correct for any clock drift over the course of a cruise without having to open the camera housing and manually reset the internal clock.

Table 4. Field of view in seawater for DSPL DigiSeaCam.

Altitude above Bottom	3 meters	5 meters	7 meters
Field of View in Seawater	3.49mx2.62m	6.06x4.54m	8.03x6.02
Pixels/Meter	586	338	255

KM4-17 TowCam Summaries

Brief descriptions of the TowCam dives are provided below, along with figures showing the dive tracks overlain on bathymetry. TowCam rock sample locations are given as part of Appendices 4-6. Water sample locations are given in Appendix 11.

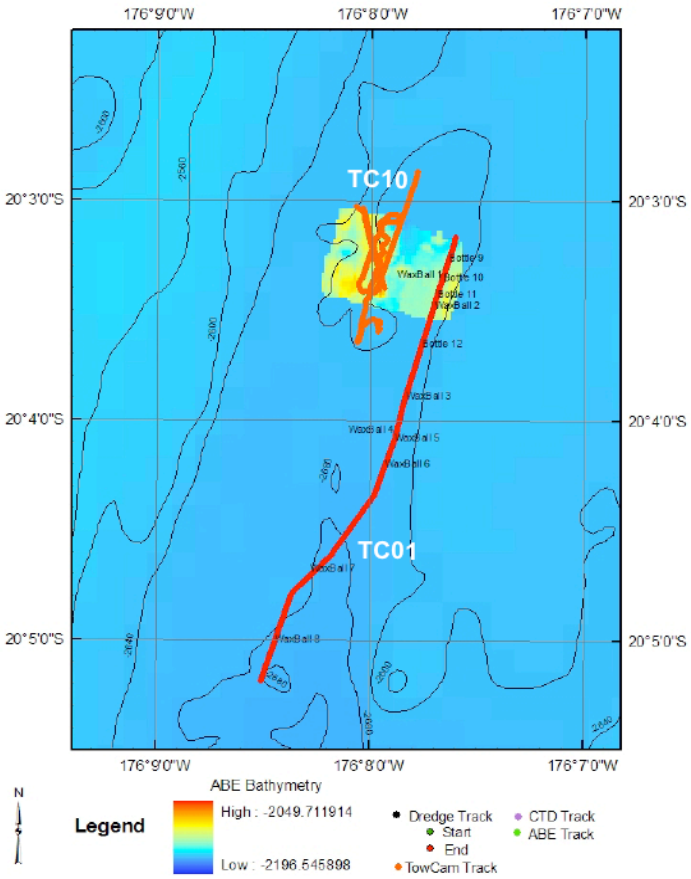

Figure 45- Tow Cam tracks for tows 1 and 10 plotted on bathymetry

TowCam #1

The first camera tow of the cruise was intended to ground-truth the DSL-120A sidescan sonar data in the rift at Site 1 between 20° 03'-05'N. Tow was from north to south and crossed the rift obliquely ending up near the western rift wall. Terrain during the first portion of the tow was heavily sediment covered lobate and pillows with large apparently tectonic fissures and scarps. Some stalked sessile animals and anemnes were imaged, usually on the edges of scarps or fissures. About 1/3 through the tow, some sedimented sheet flows were observed that transition into the lobate and pillowed flows. Occasionally the sheet lava displays a folded character. Half-way into the tow and continuing to the end of it, the lava morphology is dominantly pillows, cylindrical pillows and lobate lava; the sediment cover decreases dramatically, however when the seafloor is comprised of sheet and folded sheets, the apparent sediment cover increases because of the general

flatness of these morphologies. In addition, there are areas where apparent contacts were imaged of the fresher, largely unsedimented flows with presumably older, sediment covered lobate lava. No evidence of hydrothermal activity was observed during the tow.

TowCam #2

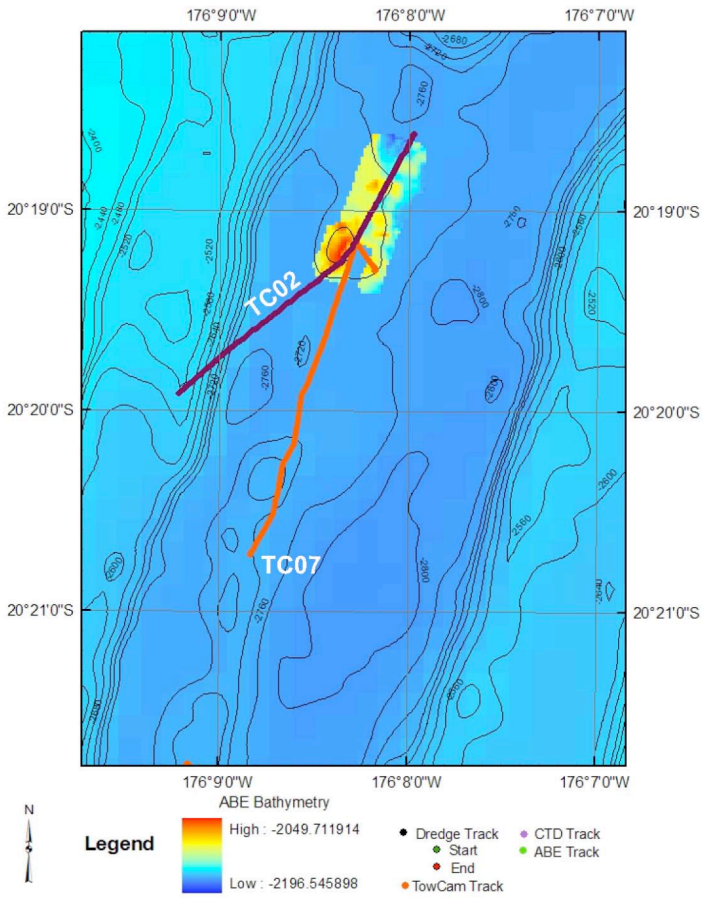

Figure 46- Tow Cam tracks for tows 2 and 7 plotted on bathymetry

Tow#2 was located at Site 2 in the rift valley between 20° 18.6'S to 20° 19.2'S. The tow proceeded from south to north, starting at the western rift wall and angling towards the axis of the rift where the tow path angled more northward to follow what was interpreted to be the neovolcanic zone – a lineament of small volcanic constructional features. Seafloor at the beginning of the tow is characterized by extensive talus, fist sized to <1 m blocks, developed on the fault scarps that define the western boundary of the rift. The talus is only dusted with sediment. Once the camera began traversing the rift floor, the talus ended and the terrain is composed of medium sized pillows and lobate terrain, with occasional fissures and constructional escarpments with talus ramps at their base. The constructional terrain is also nearly devoid of sediment. The last portion of the dive, just north of the small rifted cone in the center of the rift valley, traversed pillow and lobate lava terrain that showed evidence of distal hydrothermal vent communities, largely small white anemones, mussel chaff, barnacles, pogonophora worms, brisingid sea stars and galatheid crabs. Evidence of lowT diffuse flow was observed along cracks in the largely pillow terrain including white microbial staining. Smoke from a hiT black smoker vent was encountered at 17:25-17:27 and a >2°C temperature spike (above ambient) was also noted in the TowCam's CTD real-time data. The pillow lava around the venting areas appeared coated with a sooty (Mn?) deposit. The last part of the camera

tow continued north of the vent area, but no evidence of hydrothermal activity was observed in the unsedimented pillow and bulbous lobate flows.

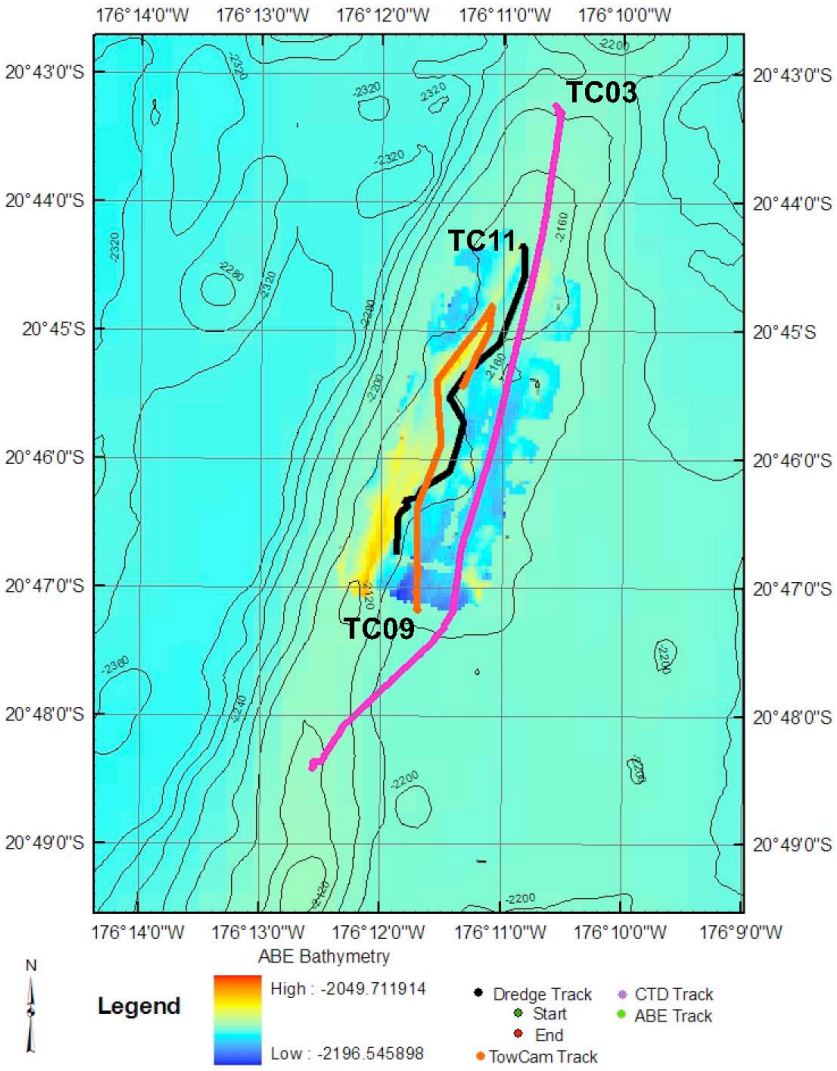

Figure 47- Tow Cam tracks for tow 3,9 and 11 plotted on bathymetry

TowCam#3

Tow#3 was located at Site 4, in the rift axis between 20° 44.65'S to 20° 47.28'S; the tow was conducted from north to south. The tow proceeded generally SSW along the axis of the rift over several constructional mounds and fissures imaged in the near-bottom sidescan data and ended near the western boundary fault of the rift valley. The constructional terrain is typified by pillow and lobate flows with variable relief on the flow fronts. Some of the flows are more heavily sedimented than others with contact relationships between pillows and lobates and a more hackly largely sediment free flow morphology. Few sheet flows were observed. Occasionally there are large vase sponges attached to the lava flow surfaces and a there are a few good shots of octopus. The second half of the tow traversed more tectonized terrain characterized by talus ramps and racks and fissures. No hydrothermal vent-endemic animals were observed during the tow.

TowCam#4

This lowering was at Site 5 and was located in the rift axis between 22° 9.1' to 22° 9.8'S, consisting of three, closely-spaced, nearly parallel lines oriented ~ NNE-SSW that traversed several acoustic facies in the DSL-120A sidescan data suspected to be fresh volcanics and possibly hydrothermal areas. The western line was run first from north to south. The terrain covered by this lowering is predominantly heavily sedimented with occasional large bulbous pillows or lobate flows outcropping, as well as some areas where more hackly flows are exposed. In a few instances small bedforms were observed in the heavily sedimented areas. Several escarpments were traversed exposing cuts through pillowed terrain with talus at the base of the scarps. No evidence of hydrothermal activity was observed during this tow.

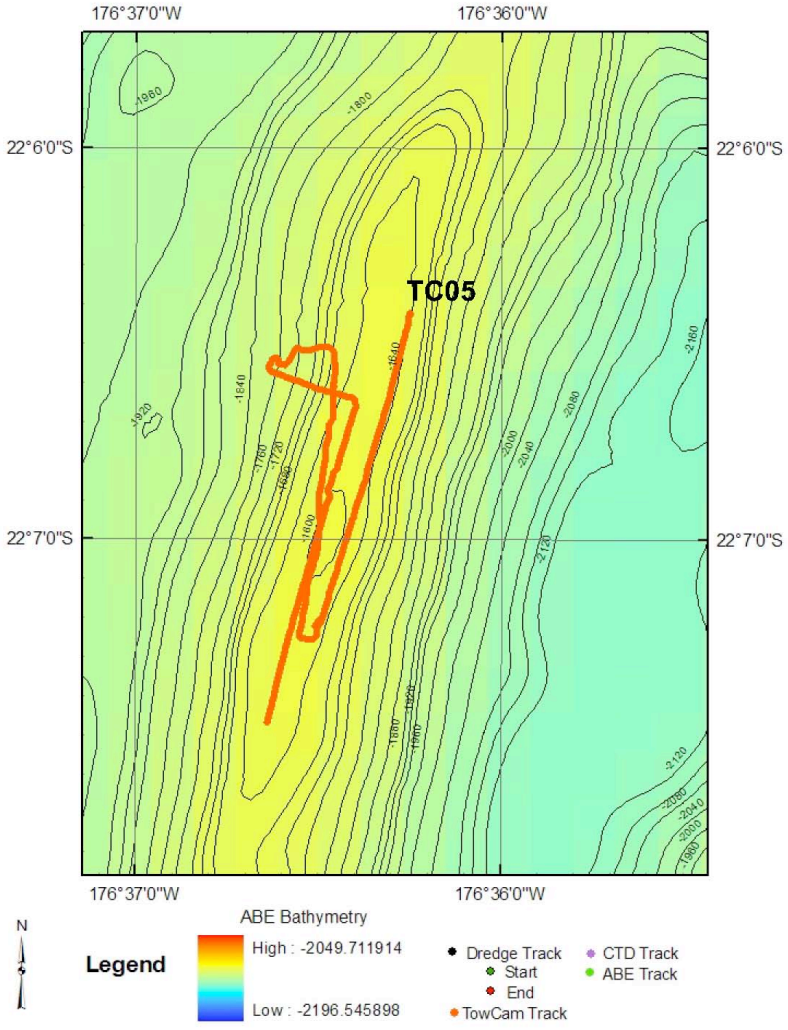

Figure 48- Tow Cam track for tows 5 plotted on bathymetry

TowCam#5

TowCam#5 was located at Site 6, at the summit of the narrow and shallow (~1600 m) ridge crest in this area near 22° 6.4'S to 22° 7.4'S to look for sites of hydrothermal activity. The tracks are approximately parallel to the NNE-SSW trend of the axis; the first track was the easternmost one and ran from N to S. The seafloor traversed is dominated by talus – fist sized and sometimes larger, with sparse outcrops of blockly (pillow?) flows surrounded by dark sediment (presumably eroded volcanic glass) that is influenced by current flow (shows evidence of streaking of dark color in the buff pelagic

sediment). Some large scarps exposing blocky flows that at times seemed welded were also observed. Sessile animal life was very sparse save some gorgonian coral, especially at the end of the dive on the shallowest part of the axis. The only evidence for hydrothermal activity was observed at 11:01 where lowT clear diffuse fluids were observed issuing from blocky/welded outcrop that was stained yellow and white. No vent endemic fauna were observed.

TowCam#6

The seafloor traversed by this camera tow was at Site 5 and involved a detailed E-W survey over a very small area near 22° 10-10.4'S and a NE-SW track at the end of the tow over an area suspected of possible hydrothermal activity based on initial ABE dives and CTD plume data. The terrain is heavily sediment covered and consists of largely blocky to hackly flows that protrude the sediment cover with occasional areas of more lobate flows. Only a few gorgonian corals were observed and no evidence of hydrothermal activity was seen in the photographs.

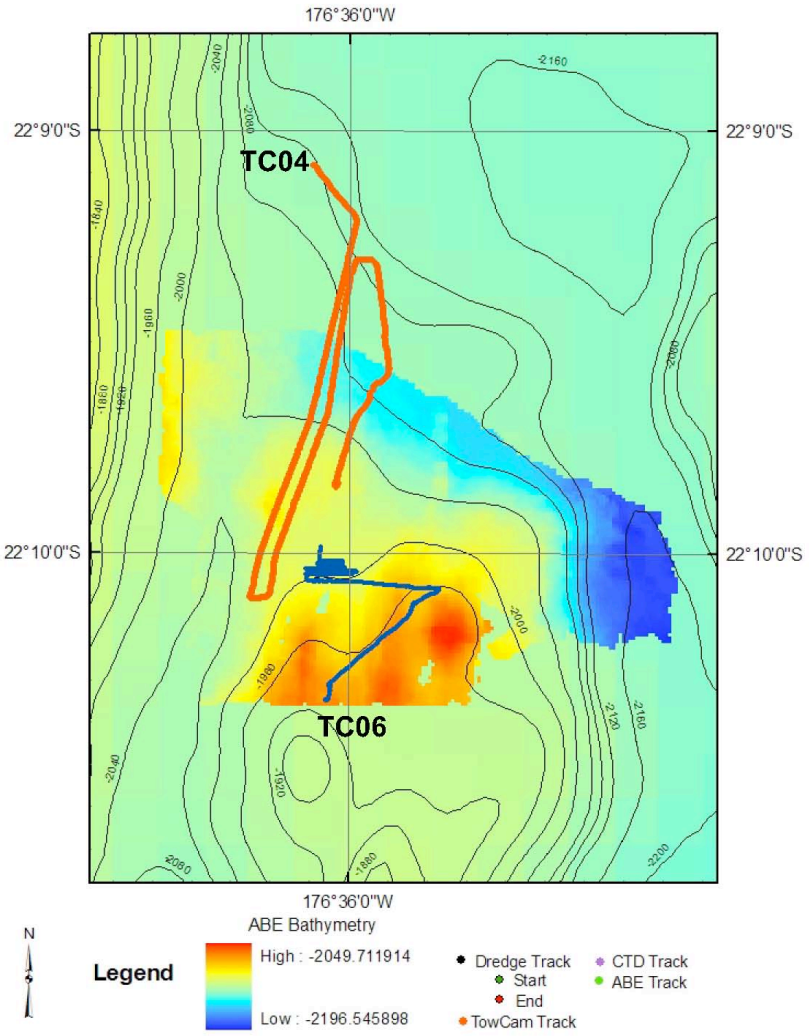

Figure 49- Tow Cam tracks for tows 4 and 6 plotted on bathymetry

TowCam#7

TowCam#7 investigated the area at Site 2 between 20° 19.7'S to 20° 20.3'S along a N to S line in the middle of the rift valley over several constructional features displayed in the DSL-120A data. The lava flows range from small pillows to occasional lobate morphologies with moderate to at times heavy sediment cover. There are also some areas of talus at the base of scarps. A few benthic fish were seen and no evidence of hydrothermal activity was observed.

TowCam#8

This bottom traverse investigated terrain at Site 3 between 20° 21.8'S to 20° 24.2'S along a N to S line in the middle of the rift valley along a small cone and a cleft mapped by the DSL-120A phase-bathymetry. The first half of the tow observed largely unsedimented talus and scarps along the cleft. Once the base of the small cone is approached, unsedimented pillow lava dominates and a series of constructional escarpments that are likely to be flow fronts were traversed. No vent endemic fauna were observed during the tow.

TowCam#9

The traverse examined the boundary faults along the west margin of the rift valley at Site 4 between 20° 46.3'S and 20° 45.8'S where Phase 2ABE data indicated possible hydrothermal vent activity. The traverse proceeded from S to N along several scarps and terraces that form the western margin of the rift. Hydrothermal activity was encountered between 8:55 and 8:58 and included sulfide and microbial staining and clear diffuse flow, shell chaff and crabs on largely unsedimented pillow and hackly flows. The tops of the terraces have abundant sediment with some outcrops of pillow and blocky flows. The edges of scarps consist of exposures of blocky and pillow lava with talus at the base of the steps. Occasional deep sea corals were observed along the scarps.

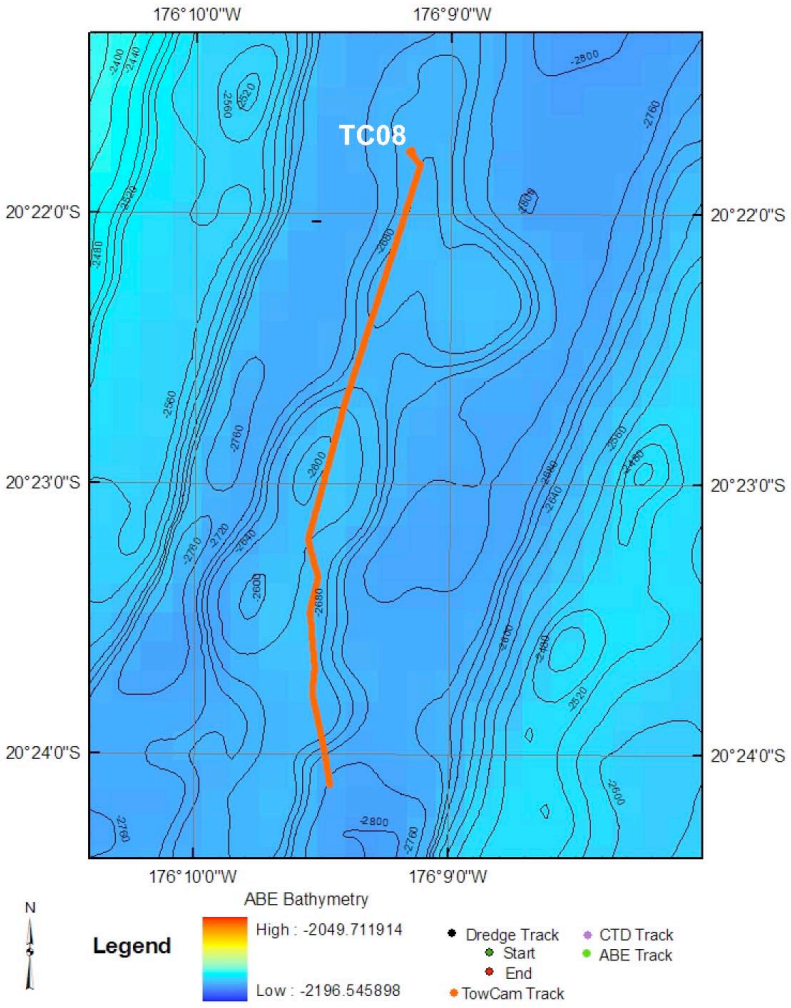

TowCam#10

TowCam#10 explored the area at Site 1 between 20° 2.8's to 20° 3.6'S along the western margin of the rift valley over scarps and a prominent constructional feature where ABE Phase 2 data showed hydrothermal activity. Lightly sedimented pillows and steep-sided scarps were traversed some sessile corals were observed on the scarps, no evidence of hydrothermal activity was observed.

Figure 50- Tow Cam track for tow 8 plotted on bathymetry

TowCam #11

This camera tow was located at Site 4, west of the traverse of TowCam #9, over well-constrained areas of ABE Phase-2 mapping, including SM2000 near-bottom multibeam that showed evidence for hydrothermal activity along the boundary scarps. The area investigated is just west of the western edge of the DSL-120A sidescan imagery. The seafloor is dominated by lightly sedimented pillow, tubular pillows and lobate flows. Hydrothermal venting was observed between 8:22 to 8:25 consisting of vent animal concentrations (crabs, pogonophoran worms, bacterial staining) and sulfide blocks within talus along the scarps. One other site of venting was observed between 9:29 and 9: 935 and consisted of mussel shells, pogonophoran worms, bacterial staining, galatheid crabs and gastropods on sulfide chimneys and blocks along the scarp.

Figure 51- Tow Cam track for tow 12 plotted on bathymetry

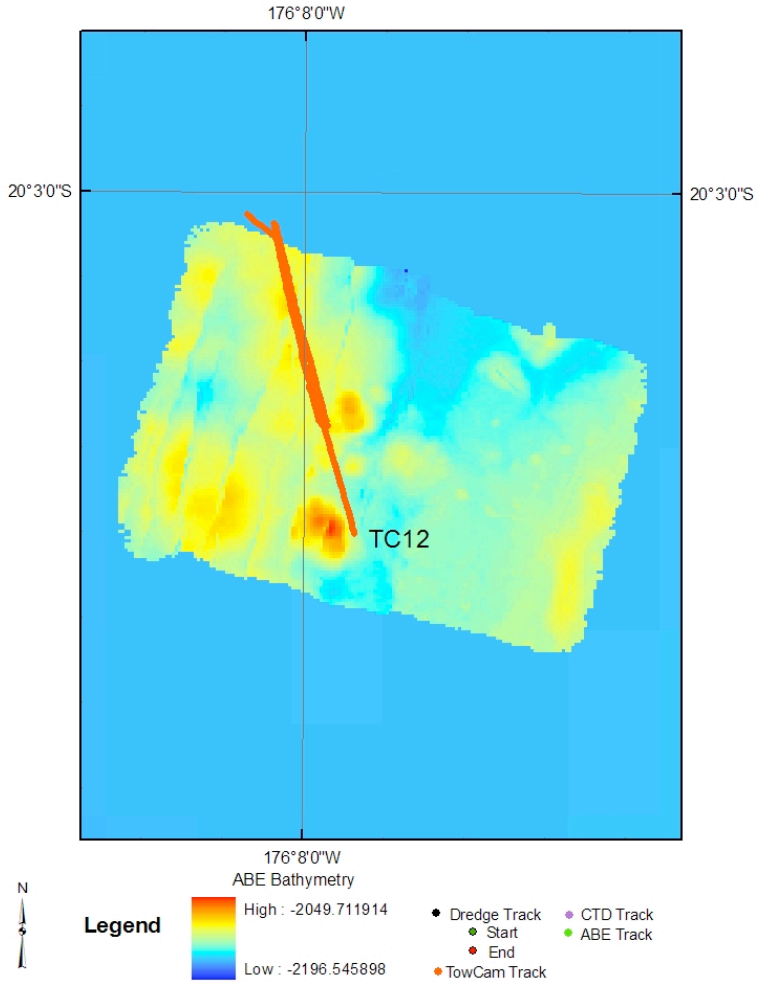

TowCam#12

TowCam#12 explored specific areas at Site 1, between 20° 3.0'S and 20° 3.4'S, where ABE Phase 2 SM2000 mapping had identified possible hydrothermal chimney spires along two intersecting cracks and scarps at the western margin of the rift valley in this area. The tow proceeded from N to S. Hydrothermal venting was first observed in pillowed terrain between 20:58 and 21:03, at the northern end of the survey area near where the two faults intersect. The venting consisted of increasing density of brisingid sea stars, anemones and mussels until a black smoker chimney was imaged at 21:03. Pillowed flows are the dominant morphology throughout the area. A second area of black smoker activity was encountered a few tens of meters south of the first one, at 21:10 to 21:11. Diffuse flow and vent-endemic biology was observed south of these chimneys until 21;28. The chimneys are ~5-10 m tall and situated along the top edge of the fissure. The terrain south of the smoker has clear evidence of lowT diffuse flow (milky water) emanating from the cracks along the fissure. Communities of anemones and barnacles line the margin of the fissure. This area is perhaps the largest concentration of vent endemic animals and black smoker activity observed at any of the sites investigated during this cruise.

BIOLOGY PROGRAM

The overall goal of the biology program was to elucidate the distribution of venting activity and habitat diversity through detailed photo-characterization of constituent communities (in part for future integrated studies) and demonstrate the utility of AUV (specifically ABE) for hydrothermal biological research through nested Phase II to Phase III approaches. Fortuitous biological collections will be used for systematic comparison (e.g., molecular and isotopic) to fauna inhabiting other deep-sea ecosystems in conjunction with ongoing studies.

Table 5. Biological samples and their dredge location.

Dredge #	Julian Day	Lat° Start End	Lat' Start End	Lon° Start End	Lon' Start End	Depth (m)	Morphospecies identification
2	256	20	3.503	176	7.670	2640	scallop
		20	4.178	176	7.911	2661	
6	257	19	37.200	175	59.163	2636	forams
		19	37.487	175	59.046	2636	
23	268	21	44.932	176	24.260	2366	gorgonian coral
		21	45.332	176	23.565	-	stalked sponge
27	270	22	6.855	176	32.499	-	shrimp
		22	7.382	176	32.489	-	
29	271	22	9.318	176	34.693	2100	brittle stars
		22	9.860	176	34.684	1900	
32	273	21	48.456	176	22.993	2470	barnacles
		21	49.259	176	23.232	2100	
41	276	20	31.175	176	12.230	-	fish
		20	31.698	176	12.178	-	
42	276	20	39.035	176	10.533	-	gorgonian coral
		20	39.489	176	10.645	-	
43	277	20	39.574	175	59.824	2193	scallop shell
		20	40.115	176	0.324	1980	brittle stars
46	278	20	17.514	176	0.012	-	solitary corals
		20	17.556	175	59.733	-	
48	279	20	10.401	175	59.913	2436	gorgonian coral
		20	10.840	175	59.470	2436	solitary corals
49	281	20	25.383	176	2.694	2379	sea stars
		20	25.410	176	3.420	-	
50	282	20	45.711	176	11.480	-	crab legs, parts
		20	46.114	176	11.583	-	sea pen; shrimp
52	283	20	3.011	176	8.044	2640	bathymodiolin mussels
		20	3.525	176	7.956		archaeogastropod limpets
							turid gastropods; polychaetes
							sulfides with microbial mats
							barnacles
60	288	15	55.992	174	36.212	2060	amphipod
		14	54.021	174	0.708	2814	

Biological Collections

Faunal specimens and microbial samples were collected opportunistically from dredge recoveries. Organisms were promptly processed, either dissected and placed in 70% ethanol for preservation or cryogenically preserved in a –80°C freezer. Typical non-vent deep-sea fauna were recovered until Dredge 52, when sulfides and vent-endemic fauna were sampled. All preserved and frozen specimens were transported by to the Woods Hole Oceanographic Institution.

Autonomous characterization of venting activity, biological communities and habitat distribution using ABE.

Phase III overlapping image surveys acquired 12bit images every 5 seconds during 5 ABE dives employing 5, 6, and 10-m trackline spacing and speeds of 0.4 to 0.6 m/sec. These imaging surveys were conducted from 4 to 7 meters altitude to permit the mosaic mapping of spatial relationships and associations among biological, hydrothermal, and geological phenomena.

Table 6. ABE biological image statistics.

ABE Dive	Area #	Processed raw images	Total # of images / dive
137	1	0000-4565	4565
138	2	1670-11958	11958
139	3	0000-14313	14314
140	1	0000-18545	18545
141	1	1540-5999	5999

ABE (and TowCam) documented fissure-dominated regions (area 1) as well as sulfide mound regions (area 2) that were observed hosting both live and dead faunal assemblages. Discrete communities were similar in composition among all three areas. Patches of mussels, large gastropods, shrimp, pogonophorans, anemones, barnacles, and fish endemic to Lau Basin vents were documented in each of the three areas co-imaged with ABE and TowCam (Fig. 52).

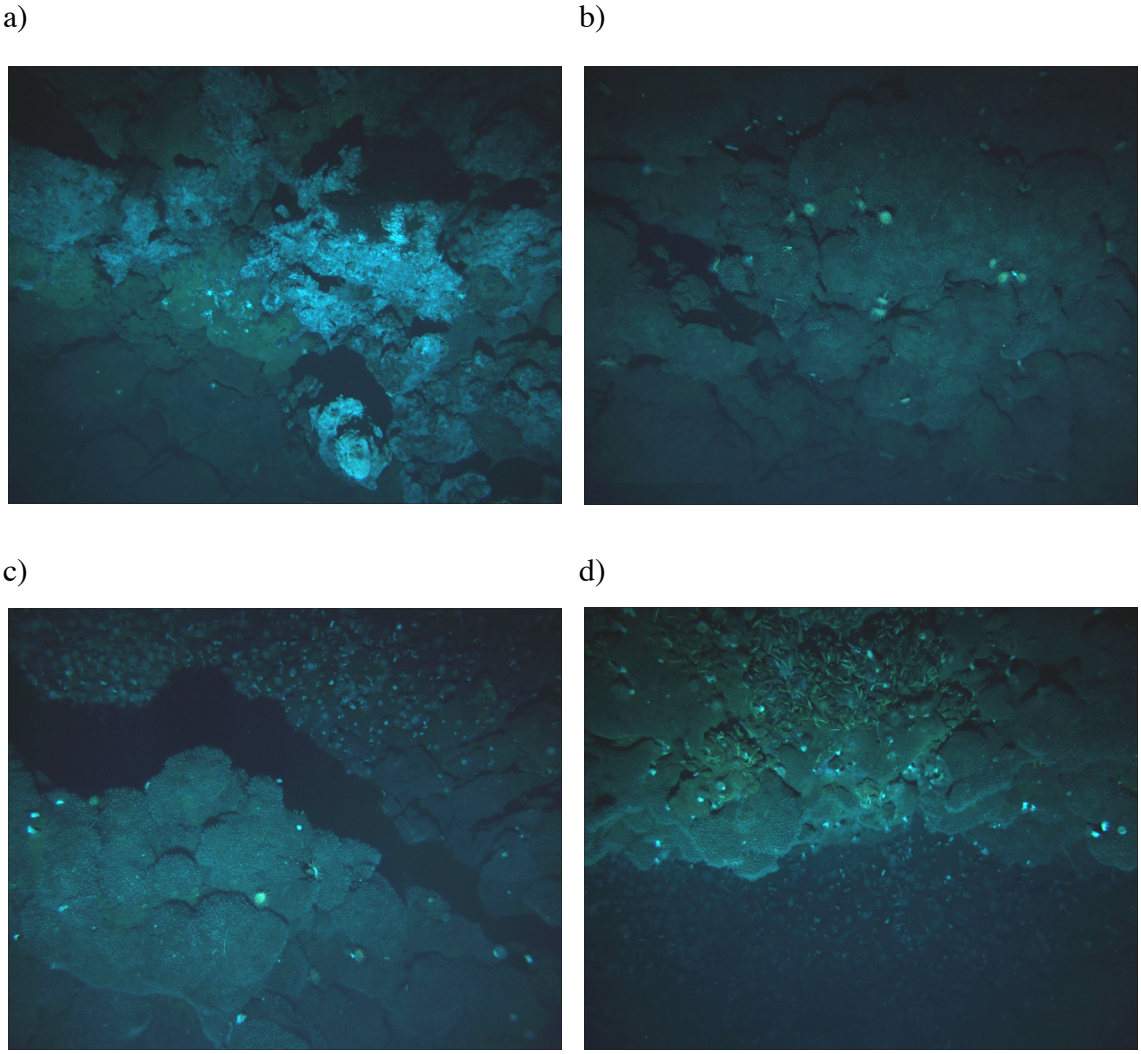

Figure 52. Examples of vent communities imaged in Area 1 (ABE dive 141) representative of the biological communities in all areas documented by ABE: a) black smoker habitats hosted clusters of gastropods (center) and mussels; b) neighboring pillow basalts supported groups of anemones (background of c), that frequently co-occurred with carpets of barnacles (foreground of c); and d) mussel communities in discrete patches on fissure margins, on the sulfide surface of active black smokers, and in cracks between lobate and pillow lavas.

High-resolution biological image surveys

Higher resolution imaging during twelve TowCam lowerings, including several towlines over the exact terrain imaged by ABE, were conducted to groundtruth images obtained from ABE- providing cross-calibration for species identification. Single pass image

swaths using TowCam were used to create linear mosaics to examine spatial relationships between venting activity and faunal assemblages.

Table 7. TowCam biological/seafloor image statistics

Tow #	Date GMT (JD / Calendar)		Start Time	End Time	Area	Start Lat./Long	End Lat./Long.	# Images (incl. water column
1	259	9-16-2004	12:41	19:52	site 1	20° 03.16'S 176° 07.60'W	20° 05.18'S 176° 08.51'W	1871
2	261	9-18-2004	13:01	19:12	site 2	20°19.91'S176° 09.21'W	20°18.62'S 176° 07.97'W	1900
3	262-3	9-19/20-2004	16:46	00:00	site 4	20°44.65'S176°11.13'W	20° 47.28'S176° 12.07'W	1876
4	268	9-24-2004	08:17	15:17	site 5	22° 09.05'S176° 36.09'W	22° 09.81'S 176° 35.98'W	1838
5	270	9-26-2004	05:05	12:31	site 6	22° 06.42'S176° 36.25'W	22° 07.43'S176° 36.63'W	1898
6	271	9-27-2004	04:38	11:52	site 5	22° 09.98'S176° 36.07'W	22°10.38'S 176° 36.08'W	1840
7	275	10-1-2004	04:23	09:44	site 2	20° 20.72'S176° 8.83'W	22°19.30'S 176° 08.175'W	1589
8	275	10-1-2004	12:01	19:00	site 3	20° 21.85'S176° 9.23'W	22° 24.21'S176° 09.42'W	1914
9	277	10-3-2004	07:08	14:33	site 4	20° 46.38'S176°11.61'W	20°45.76'S176°11.50'W	1887
10	278-9	10-4/5-2004	22:35	04:49	site 1	20° 2.870'S176° 7.78'W	22° 03.64'S 176° 08.06'W	1897
11	281	10-7-2004	05:54	12:48	site 4	20° 45.14'S176° 11.7'W	20° 46.47'S 176°11.84'W	1866
12	283-84	10-9/10-2004	19:42	00:29	site 1	20° 3.03'S 176° 8.07'W	20° 03.39'S 176° 07.96'W	1000

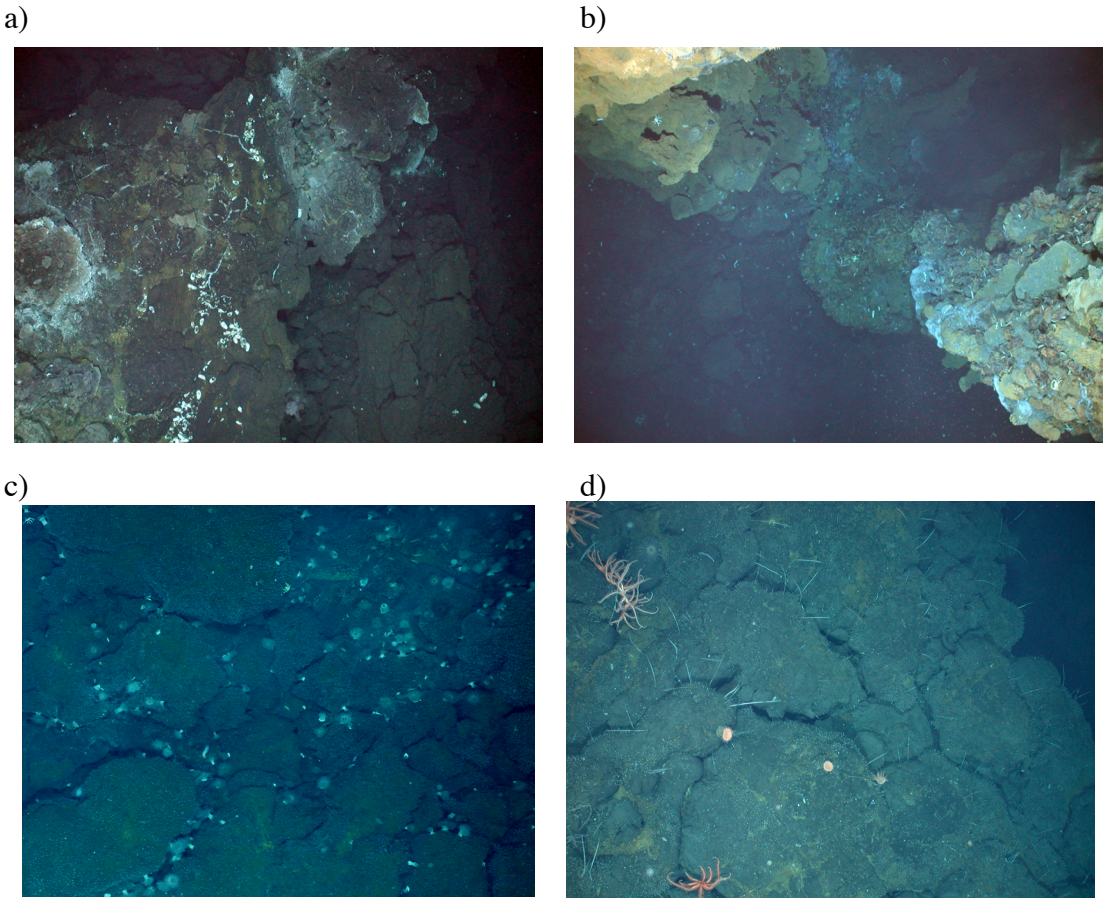

Figure 53. Examples of vent communities as acquired by WHOI TowCam representative of the biological communities documented in site 4, including (a) mussels in milky diffuse flow (upper center of a) with microbial staining, and from site 1, with (b) mussel and shrimp assemblages along the side of, and nestled between, two active chimneys, c) fields of anemones and barnacles in diffuse flow (upper right), and d) stands of pogonophoran worms attached to the margins of pillows and lobates and often accompanied by orange brisingid seastars.

PETROLOGY PROGRAM

Rock sampling took place largely during ABE dives and imposed down time. Because an ABE dive could take as long as 24 hours, this provided a potential large quantity of time for sample recovery. Locations were constrained, however, because of the need to watch ABE descend and to occasionally check on ABE to make sure it had not surfaced prematurely. This led to many samples near the target sites, and less dense sampling elsewhere. The aims of the sampling were to obtain a regular high density sampling of the ridge axis, higher density sampling of the hydrothermal target areas, and sampling of off-axis seamounts along the length of the ELSC. We hoped to obtain samples from seamounts on both sides of the ridge axis, but the Martinez data revealed no seamounts to the west of the axis, and our own bathymetric surveys a bit farther off-axis, as well as the regional maps of Taylor and Martinez, also found no seamounts. Therefore we obtained approximately 3km spacing along the ELSC, 24 dredges of off-axis seamounts east of the ELSC approximately regularly spaced between the ELSC and the Tonga arc, as well as 25 sampling stations on the Fonualei rifts. Sampling took place both by dredging and rock coring (also called wax coring).

Dredging Operations

Dredges were used at widely-spaced intervals along the axes of ELSC and Fonualei Rifts to collect larger quantities of rock that could be used for all types of geochemical and petrological analyses. Compared to wax cores, dredges took much longer and were not as precisely located, but typically returned much more material. Certain of the axial dredge targets were selected to be prominent high points along the axis or at deep rift tips. We used bathymetric and sonar backscatter data from the previous cruise of Martinez et al. to select targets. A few dredge lines were selected along the ELSC axis to characterize the substrate of hydrothermal sites. In these cases, there was a higher probability of collecting sulfides as well as the desired basalt rocks. We also attempted to preserve any biota that was caught in the dredge as a by-product. Off-axis seamounts were sampled exclusively by dredging, since their age, freshness and sediment cover made it unlikely that wax coring would be successful. We selected those targets to be located at various distances from the ridge axis, sometimes in lines that were perpendicular to the ridge axis. We concentrated on seamounts with high sonar reflectivity to increase our chances of recovering fresh and young volcanic rock instead of pumice or mud.

We used a Scripps-type dredge. It was fairly easy to bring onboard and to empty, clean and reline on deck. The chain link bag of the dredge was lined for its entire length with a heavy 6-cm fish net (tuna netting) that was replaced once during the cruise. The netting trapped smaller rocks that would otherwise have gone through gaps in the chain bag. For each dredge, a new burlap bag was tied into the bottom of the dredge bag using plastic tie-wraps to bind it to both the tuna netting and the chain links. Then a burlap-encased iron weight was tied into the burlap at the bottom of the dredge bag with several tie wraps. When the dredge arrived on deck, it was emptied of rocks, then the weight and burlap liner were cut out and any trapped material was removed from the burlap. The

dredge was raised, and the dredge bag shaken and hosed down to remove all traces of rock fragments to avoid contamination.

Dredge operations were performed using the 9/16" 3x19 torque-balanced trawl wire that is standard on most UNOLS vessels. The dredge was lowered in the water to 150 meters depth, at which point, a 12 KHz Benthos or SandyWilliams pinger was attached. The pinger's depth and height above the seafloor were monitored using a12 KHz recorder. When the pinger attained150 meters of separation from the bottom, the ship was moved forward at 0.3 – 0.8 knots while wire was laid out at 10 meters/minute until separation was 75-100 meters above the bottom. At the end of the dredge track, the dredge was brought in at 3-10 meters/minute. Most "bites" occurred in this interval. The dredge was judged free of the bottom, when pinger separation exceeded 150 meters, at which point winch speed was increased to 60 meters/minute for recovery.

Unfortunately, both the 12 kHz multibeam sonar and the ship's freshwater purification pump interfered with the reception of the direct pinger and echo returns, especially when the less intense SandyWilliams pinger was used or the Benthos pinger was not operating at full strength. Because of this inherent shortcoming of Kilo Moana, we recommend that the ship maintain at least two healthy Benthos pingers on board.

The Dynacon trawl winch was operated at a maximum speed of 60 meters/minute. This is standard for many UNOLS vessels but should be increased to improve productivity. Even at 60 meters/minute, the winch experienced problems with its level wind, which occasionally had mechanical difficulties. Kilo Moana's Engineering department did a great job of repairing the winch when the level wind failed and kept the winch operational for the duration of the cruise. Weak links were set to break at 7,500 lbs, but did not release on the occasion of a much larger pull (16,500 lbs at the winch, with <3000 m of wire out). The loss of the first dredge resulted from an improperly tightened and pinned shackle.

We made a total of 62 dredge attempts, of which 59 recovered material that could be analyzed (see dredge descriptions in Appendix 2). The amounts recovered varied widely, ranging from a few grams to over 100 kg. The amount of material recovered was crudely correlated with the number of "bites" recorded by the winch's tensiometer: i.e., increases in tension followed by a rapid release. In many cases, the burlap bag and weight in the dredge were responsible for the success of the dredge, by entrapping small shards of glass or rock: no material would have been recovered otherwise. Dredge locations and descriptions are given in Appendices 1 and 2. The photographic log (included as Appendix 16) presents images of each dredge recovery.

Rock Coring Operations

The advantages of rock coring in comparison to dredging are that station time is reduced by a factor of three, and very specific and precise locations can be targeted (Reynolds et al. 1991). Ordinarily rock coring is carried out using a free fall winch at speeds of 110-120m/min. The Kilo Moana did not have a hydrowinch, and the ship operator purchased a "moving vessel profiler" winch from Brooke Ocean Technology. This winch had a Kevlar cable rather than a wire, and could be lowered at speeds as great as 250m/min, which potentially would be of great benefit to the speed of rock coring.

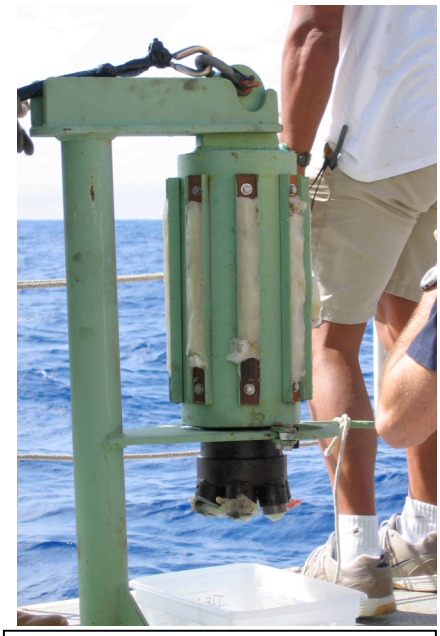

Figure 54 - Picture of new rock core design used with MVP winch on KM0417.

The geometry and payload of the winch, however, required substantial changes to the rock core design. Rather than a 300Kg rock core about 1.5 meters in length, with a multihead corer at the bottom and a large collar at the top, it was necessary to design an approximately 100kg core with a barrel less than one meter in length. For constant speed, this lessened the force of impact considerably. The tubular design and short length also prevented an effective "double hit" that is possible with the longer barrel design as the collar attached to the weight head falls to the bottom just after impact.

The modified rock core design is shown in Figure 54 . The body of the rock core is a solid steel cylinder. We attached a multi-head corer to the bottom of the cylinder, and "rails" filled with wax were attached to the sides. This design functioned satisfactorily, although average recovery per lowering was less than 5 gm, or about one quarter the recoveries we have experienced using the longer and heavier design that can be used with a hydrowinch. Some of the decreased recovery may have been a consequence of the different physical characteristics of the glass for hydrous magmas. This will not be known until rock coring with a different instrument is carried out along the ELSC.

On the first rock core, the very high speed of descent meant the impact of the rock core with the bottom was not seen clearly, and substantial wire was laid out on the sea floor. A long period of attempted recovery led to the wire being abraded on the bottom, and the loss of one of the rock cores. Subsequently, we adopted the approach of lowering at high speeds until about 100meters above the bottom and stopping the winch. Then we would lower at about 150m/minute to be sure to be able to see the impact on the tensiometer. Wire up speed was approximately 120 m/min. In the 2000 meter water depths at which we were working this permitted a complete rock core station in about one half hour. A total of 145 rock core stations were occupied, of which 140 were successful.

In addition to the rock cores deployed from the surface, the TowCam system had eight metal balls about 10cm in diameter that could be dropped by fishing wire to the bottom during the camera tow. Recoveries from the balls are small, almost always less than 1gm of glass, but provided very close spacing and high resolution with photographic documentation. Rock core locations and descriptions are given in Appendices 4 and 5.

Shipboard Sample Processing and Description

1. Dredges

When a dredge was brought on deck, all specimens were transferred to buckets and the buckets, together with the burlap sack, the dredge weight, and the burlap sheet from the deck were taken to a sorting table in the staging bay. The tables were re-covered with clean paper rolls for each dredge. All samples hand-size and larger were laid out for drying and visual examination. A photograph was taken of the entire dredge, with the cruise and dredge number marked on the brown paper; for scale in these photos, the tabletops are about 5 feet on a side. A short assessment of the overall recovery and character of the dredge was entered in the Dredge Description Log book.

a. Types

Each dredge was split into "Types" if it contained rocks that, by any criteria, appeared to be from different lava flows. Criteria included overall morphology (e.g., pillows vs. sheets), freshness, character of the glass rim (thickness, texture, etc.), vesicularity (abundance, size, shape, and distribution within the rock), phenocryst populations, color, etc. More than one unconnected rock could be merged within the same type, so a type is not the same as a working sample; however, a working sample (see below) is a subset of a type, namely a single connected or reassembled rock chosen from within a type to represent that type. To avoid confusion, type numbers are always prefixed with a capital 'T', e.g. KM0417 DR25 T2. Generally, non-working material was bagged and labeled by type, although for large dredges additional material was often archived untyped. The philosophy in assigning types was to err on the side of designating too many types, since it is easier to recombine analyses that turn out to be identical than it is to deal with an undersampled dredge with unrecognized diversity. For some dredges, loose glass fragments were treated as an additional type, "SG" standing for station glass. The list of types can be discerned from the Dredge Description log book or by examination of the list of working samples (Appendices 3 and 6), since every type yielded at least one working sample.

b. Working Samples

From each type within a dredge, one to three working samples were selected. No less than two working samples were taken from each dredge, but in dredges with more than three types generally only one working sample per type was taken. A working sample is always a single rock or pieces that could be reassembled into a single rock. When station glass fragments are taken as working samples, again a working sample is a single connected piece of station glass, never a commingling of multiple pieces. Working samples were selected on the basis of size, glass abundance and quality, and whether they represented the most typical characteristics of their type. Working samples are numbered in the format DRXX-#, where # identifies the working sample. The type from which the working sample is drawn may also be specified, e.g. KM0417 DR25-2 T2, meaning working sample 2 from dredge 25, which is from type

T2.However, the type number is not part of the official sample designation and is only affixed for clarity in sample processing.

Each working sample is photographed with a label bearing a 10-cm scale. Each working sample is described in the Dredge Description log book and also entered on a description worksheet (see working sample inventory, Appendix 6) with its approximate weight, glass rim thickness, quantity of glass, phenocryst population, alteration state, vesicularity, and comments. After thin section blank cutting and chipping (see below), the rest of the working sample (if any) was bagged (with labels in and on the bag), and all working samples from a dredge (excluding the chipped glass and the thin section blanks) were bagged or bucketed together (with labels in and on the bag and on a shipping tag) and placed in the working sample area of the science stores hold. This material will be archived at Harvard.

The remaining, non-working material was bagged or bucketed, triple-labeled, and placed in science stores in the non-working sample area. This material will be archived at the Woods Hole core repository. For most dredges, the entire recovered sample was archived. For a few very large dredges (>200 kg), several buckets or 25 kg bags were saved and the excess set aside for souvenirs or tossed overboard.

c. Sediment and pumice fraction

For several dredges that brought up a large quantity of mud or pumice, these were set aside and labeled with ‘s’ (for sediment) or ‘p’ (for pumice). Sediments were dried at room temperature or in the 80°C oven before bagging.

d. Thin section blanks

Each working sample that is big enough to yield four thin section blanks and still leave plenty of material for chipping and archiving was sawn for thin section blanks. Blanks were cut for Harvard, Tulsa, Caltech, and Oregon State. Each blank is placed in a small Ziploc bag identified by a label written on the bag as well as a duplicate label on a paper card inserted into the bag. Thin section blanks were generally cut perpendicular to the glassy rim of a sample and contained a cut through the rim where possible. The list of samples cut for thin sections is shown in Appendix 7.

e. Chipping

A wood box was lined with fresh brown paper, canvas, or a double thickness of polyethylene from a large bag. Hammer and chisel were used to break off at least 20 g of glass from the rim of each working sample, where possible. Chipping was done in sunlight for best visual recognition of glassy material, weather permitting. Chips were placed in their own labeled bag and brought into the lab.

f. Helium split

From every dredge, a glassy fraction of one sample was set aside for He measurements at Oregon State. This material was separated before any heating of the sample took place. Where possible, fragments larger than 5 mm in minimum dimension were chosen and a total of 1-5 g were placed in this split. The list of sample splits for He analysis is given as one of the columns in in Appendix 6.

2. Rock cores, Towcam wax balls, serendipitous CTD and ABE samples

Each rock core head, any side-rails observed to have glass or sediment on them, and each recovered wax ball were brought into the lab. Where possible, the largest glass pieces were removed from the wax by hand and bagged separately as the "unheated" fraction; this will allow noble gas work on many of the rock core specimens should the need arise. The rest of the material together with the wax in which it was embedded was scraped off, placed in a beaker, and covered with boiling water. When a core of mud was noted in the center hole of a wax head, this was pushed out, labeled with an 's' sample number (e.g., RC133s), dried, and saved.

When the wax was frozen, it was removed from the top of the beaker, the water poured off, and the glass (and/or rock) recovery transferred to a clean beaker for drying. From this point forward it is treated the same as a chipped glass fraction from a dredge working sample.

Each Towcam lowering results in as many as eight wax ball samples. These are labeled by the Towcam dive number and ball drop number, for example CT07-3 is the third wax ball dropped during Camera Tow 07. These samples, though frequently small in quantity, were treated the same as Rock Cores. The list of rock samples from camera tows is given in both Appendices 5 and 6.

Twice, the CTD struck the bottom and yielded glass samples that were recovered, numbered by the CTD number (e.g. TY011-1), and processed.

Four times, ABE struck the bottom and material was recovered from the fiberglass hull or from UHMW polyethylene structural members. The samples were labeled by ABE dive number (e.g., ABE135-1) and processed.

3. All samples

a. Crushing, sieving, washing

The remaining chipped glass was dried in an 80°C oven, or left to sit at room temperature long enough to be thoroughly dry. Some particularly muddy samples were washed in fresh water and ultrasonicated before drying. When dry and reasonably clean, samples were gently crushed in a steel percussion mortar and sieved into three size fractions with sieves of 10, 17, and 28 openings per inch (roughly, 2, 1, and 0.5 mm openings). Material passing through each of these sieves was labeled "Large picking", "Small picking" and "Fine" fractions, respectively [N.B. sometimes

the “Small picking” fraction that passed the 17-count sieve but was retained by the 28-count sieve was labeled “Fine picking” and the smallest fraction was labeled “ultrafine” or bagged without specific size label]. The Large and Small picking fractions were ultrasonicated in fresh water for at least 3 minutes, decanted, and placed in the 80°C oven to dry. The Fine fraction was bagged, labeled and retained.

b. Handpicking

The sieved, washed, and dried picking fractions were examined under a binocular microscope. Where possible, clean glass was picked from the Large picking fraction; only if the Large picking fraction was unsuitable would the Small picking fraction be used as a backup. About ten of the cleanest glass chips from each working sample were chosen for electron probe work and split between plastic vials for the Harvard and Tulsa probe mounts. The Tulsa probe glass chips will also be used for FTIR analysis. About 30 minutes of additional separation of clean glass was performed on each sample, and the picked material bottled separately from the discards and the unpicked material. If enough picked material resulted, a split of a few hundred mg was set aside for Tulsa and the rest kept for DCP, ICP-MS, isotope, and other work at Harvard. In other cases, a split of the unpicked material was set aside for Tulsa. Where numerous phenocrysts were observed, loose phenocrysts or glass chips with big phenocrysts in them were added to the Tulsa probe mount vial for potential melt inclusion work. When sulfide material was observed, it was picked also and placed in separate vials for probe work and mineral identification; this material was frequently magnetic and presumed to be pyrrhotite. A log was kept of each picked sample and whether sufficient material was found for two probe fractions, additional picked material, Tulsa fraction, and shipboard DCP. Rock core samples were described (quantity, phenocrysts, alteration state, and vesicularity) during the handpicking stage. Additional notes were taken on dredge samples, which generally supersede hand-sample scale observations taken during working specimen identification.

c. Probe mounts

Probe mounts were prepared aboard ship for the Harvard probe sample suite, ready to polish upon return to land. Polycarbonate disks were premade, 1” in diameter, 5 mm thick, with 16 2 mm holes predrilled in a standard pattern. Each disk was inscribed on the back and side with the probe mount number (e.g., KM0417-5) and stuck to double-stick scotch tape on a glass side. A single 2 cm chunk of standard glass VE32 was crushed and handpicked, and one chip was placed in the top hole of each probe mount. Then a single chip from the probe-picks vial of a particular working sample was stuck to the tape at the base of the remaining fifteen holes. An attempt was made to achieve maximum contact area with the tape. As the samples were loaded, a “back-side” map was kept showing which sample was placed in each hole, as viewed from the loading side of the probe mount. Then a “front-side” map was created, which is a mirror image of the backside map and shows the arrangement of the glass chips as they will appear on the polished side of the mount in the electron probe. Also, the fifteen slots were numbers (by rows, top to bottom, left to right, as viewed from the

front side) and the glass processing log shows mount number and position (e.g. 5-12 for 12th position in mount KM0417-5) for each sample. When all the positions were filled, the disks were heated to 65°C on a griddle, and Epo-fix epoxy was injected into each hole, trying to minimize the formation of bubbles. After the epoxy was set, the disk was removed from the tape and placed in a labeled bag. The remaining glass chips in the Harvard probe-picks fraction were saved in groups according to which mount the chosen chip went into.

d. Final disposition

After picking and removal of a DCP split, the part of the working sample that went through the various stages of processing was bagged and stored in a final disposition location. This material is likely to include the dried sediment fraction, chipped but uncrushed material, the ultrafine fraction, the small picking fraction unprocessed, extra large picking material not examined, picking discards, and clean picked glass left over after removal of probe and DCP splits.

Sample Analysis using the DCP Multi-Channel Spectrometer

Instrument Setup

Previously, major element of rock samples analysis at sea was carried out using the single channel DCP (ARL). A single run produced data for only one element (wavelength); samples were analyzed 10 times to obtain the desired major elemental concentrations.

The multi-channel DCP (Spectrametrics) was used instead on this cruise, for the first time at sea. The benefits turned out to be significant on many fronts. Up to twenty elements could be analyzed simultaneously using a fraction of the acid required for the single channel instrument, and major element data from rock dredges/cores were generally returned within 24-36 hours of being pulled from the ocean.

The instrument resided in the radiation van (free standing) aboard the Kilo Moana which was air conditioned and had a fume hood. The stainless steel shelving allowed the argon regulation unit and the AdaM unit to sit well above the DCP, ensuring a constant temperature around it (Figure 55).

Figure 55 – Multi-channel DCP layout

As shown in Figure 56, approximately five feet of flexible 4” aluminum dryer hosing was used prior reaching to the plastic duct hose.

Figure 56 – DCP Ducting aboard the Kilo Moana

The aluminum tubing was essential because of the high heat production of the plasma, even with the fume hood fan operating. The fume hood in the van had a very poor air flow, thus it was necessary to use the portable fan to exhaust the jet area which was placed within the fume hood – Figure 57, below.

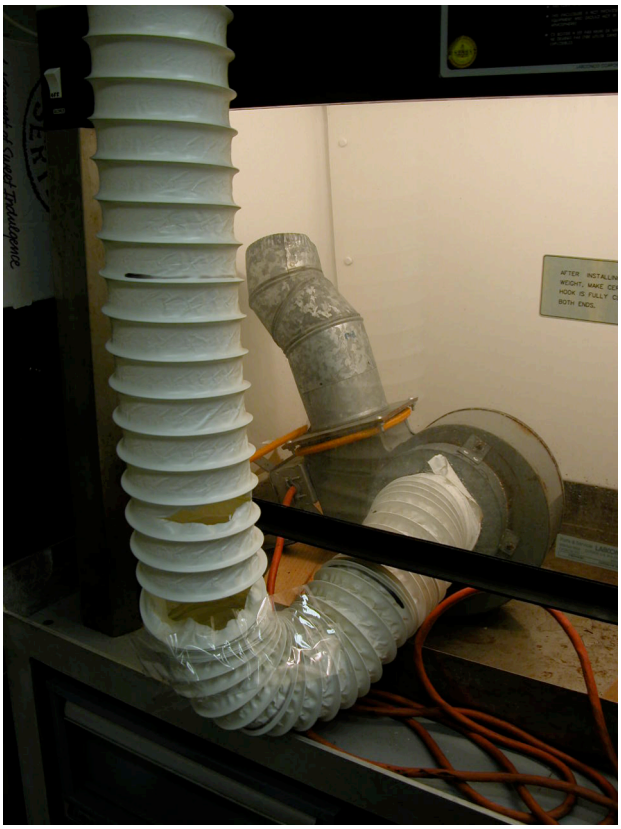

Figure 57 – Portable exhaust fan in fume hood

In order to maintain an optimal exhaust rate around the jet, it was necessary to puncture the plastic hosing in several places and introduce a cardboard flow baffle just beyond the section of aluminum hosing. These air flow modifications were made after it was apparent that the plasma signal was very noisy in the initial sample analyses.

The single channel DCP was unpacked onto the bench opposite as a backup instrument.

One dewar of liquid argon (180L) and twelve high pressure argon cylinders (300 cubic feet) were ordered from Gas Pro in Honolulu for use on the Kilo Moana. With only 2 days of the cruise left, the argon dewar read 1/8 full, and the cylinders were unused. (It was unclear how the multi-channel instrument would perform on a moving platform, and in the event that the single channel instrument had to be used, more argon would be necessary.) The quality of the dewar is a large factor in determining how much argon is retained with time, and we are fortunate to have a good quality dewar on the ship. The dewar resided in the van throughout the cruise which greatly enhanced its shelf life as was maintained at

72F. The dewar came attached to a trolley, and being relatively tall and thin, was the only reason we were able to manipulate it into the van; dimension of trolley plus dewar: 21"W x 21"D x 75"H.

Though smaller in volume, the high pressure cylinders have the advantage that they maintain their pressure and do not vent over time as the dewar does. To minimize down time, we have a "spider" arrangement for the regulator whereby up to 6 high pressure cylinders can be attached to the regulator simultaneously, or the spider can simply attach to the dewar.

The argon regulator needs to be dual stage, 0-3500 psi on the high pressure side and 0-100 psi on the low pressure side. The DCP will not light without a pressure of at least 60 psi on the low side of the regulator.

Sample Preparation

When using the multi-channel DCP, internal standard elements Ge and Co are used. It was convenient to make up 8L of internal standard solution at a time at 3% acidity (close to 1N) with Ge at 10 ppm and Co at 20 ppm. (To make the internal standard solution, add 320mL of concentrated (70%) trace metal grade nitric acid, 8 mL of 10,000 ppm Ge and 16 mL of 10,000 ppm Co to a total volume of 8L in 18.2 MΩ water.)

Weighing samples and standards is not possible while at sea, so the standards and flux were weighed prior to the cruise. Rock powder standards (MAR, NBS688, AGV2, CHEPR25, BCR2 and BHVO-2) were added to lithium metaborate, $LiBO_2$, to make the analytical standards for all of the runs (50 mg of a standard + 200 mg of $LiBO_2$). Samples were generated by using a coke spoon to estimate 50 mg of picked glass chips and then added to 200 mg of pre-weighed $LiBO_2$. <u>It is very important that all of the lithium metaborate used is from the same jar for ALL of the samples and standards!!</u> Allow 15 minutes to fuse in the muffle furnace at 1100°C, then swirl the molten bead in the graphite crucible prior to pouring it into 50 mL of internal standard solution. For each run, the internal standard solution is dispensed into the sample bottles at one time using a re-pipette.

The standards and samples were prepared at a dilution of 1:1000 i.e. 50 mg standard (or sample) + 200 mg $LiBO_2$ flux in 50 mL of internal standard solution. This dilution certainly conserved acid, as only 2.5L of trace metal grade concentrated nitric acid was used during the entire cruise. This amount of acid was sufficient to prepare about 300 bottles of samples/standards as well as 3 liters of bottle washing solution, made by adding 750 mL of concentrated nitric to a total volume of 3 L in 18 MΩ water (about 4N solution). Only two hundred 100mL bottles were brought to sea, making bottle washing an additional task which could have been avoided. Four hundred bottles when using the multi-channel DCP at sea in the future is recommended and it is also important

to use only wide mouth Nalgene bottles. Two other types of polyethylene bottles used on this cruse (made in Germany, brand unknown) often leaked.

Sample Analysis

A dilution factor of 1000 provides good signal to noise for the majority of the major elements that can be analyzed with the 20 channel cassette in the multi-channel DCP in a rock matrix. However, the signal for some elements is low and/or there are interfering wavelengths close by to the wavelength of interest. Figure 57 shows a scan of 19 peaks using the 20 channel cassette in a combined sample solution, prepared by the fusion technique above at a dilution of 1:1000 (i.e. Ge is present at 10 ppm, and Co at 20 ppm). (The zinc channel was turned off early during the cruise as the signal to noise provided meaningless data.) Clearly, the signal to noise for Ni, V and Sc, in particular, is very poor and for Cr and Cu, the background is quite high in this matrix. Although the peak for Ba is quite pronounced, the peak to background ratio is much worse than for Ti, which has a comparable signal.

This problem was addressed earlier in the cruise, and increasing the PMT voltages for several of the elements (Ba, V, and Ni) improved the data somewhat. The PMT settings used are shown below in Figure 58.

The software used for the DCP, Adam v10 for Windows, experienced a corrupted sample file half way through the cruise. This problem was worked around by calling all samples "standards", and collecting standard data to update calibration graphs. After the software was uninstalled then re-installed all was well. The cassette files were still in tact i.e. elements and their respective wavelengths.

Data from the DCP had to be exported into Excel for data reduction. In order to do this, the data collection window in Adam must be left OPEN – closing this window means all data is lost without any warning messages. Simply use "control A", then "control C" once in Excel, then "control V" to paste. The right mouse click in Adam 10 does not work, hence the keyboard shortcuts.

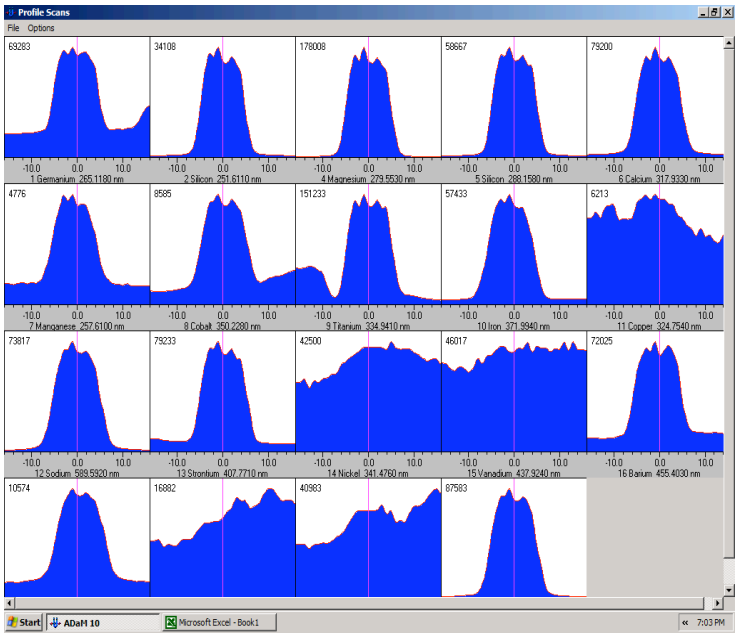

Figure 58 – Spectra across 19 peaks in a 1:1000 rock fusion solution using the DCP

Potassium, Scandium, Chromium, Aluminum

The DCP should be allowed to warm up and equilibrate for at least 20 minutes prior to tuning. It was very useful to tune on a mixed, or "junk", fusion solution

made by combining old fusion solutions together (without the blanks). This solution thus had 10 ppm of Ge and 20 ppm of Co as well as the matrix elements which allowed more precise tuning within the digested rock matrix.

Once a sample solution reached the plasma during the run, a 15 second delay was used in the Adam 10 software to allow the solution to stabilize in the plasma. Fifty acquisitions were used to generate four intensity readings per element, and these 4 readings were then averaged within Adam10 to yield the final intensity for each element in every sample. Fewer than 50 readings produced very noisy and unusable data.

During the final day of sample analysis, it was discovered that the probe that is placed in each sample bottle was becoming constricted as a result of particulate buildup. The graphite crucibles generally produce small graphite particles which then reside at the bottom of each sample bottle. This buildup produced more spurious data as time went on during the cruise. Therefore, the probe tip should be changed before each run.

Figure 59 – PMT settings used for the multi-channel DCP

Data

Data were obtained by running one standard (K1919) as a drift correction standard, and in addition having the internal standards Co and Ge added to all solutions. Three standards were run in each run to calibrate the samples. The three standards in addition to blanks were a depleted ocean ridge basalt (MAR), an arc tholeiite (NBS 688) and an ocean island tholeiite equivalent to BHVO-1 (K1919). In addition, AGV-1 was run in most runs to ensure that andesitic rocks were being adequately standardized. The basalt standard CHEPR 25, a basalt from the East Pacific Rise, was run as an unknown in each batch to be able to compare data quality throughout the cruise. Table 8 presents the replicate data for all the standards and for CHEPR 25. Data quality can be evaluated by the replicate analyses of CHEPR 25. Percent standard deviations for the major elements are generally less than 1%, and for the trace elements are 2-5%. Transition metal trace elements in the runs towards the end of the cruise degraded in quality for unknown reasons, and therefore several of these runs did not provide useable data for these elements.

More than 300 samples were analyzed during the cruise, producing an essentially complete data set for stations where there was sufficient sample. As far we are aware, this is the highest quality and most complete chemical data set on rocks that has been obtained at sea during an underway oceanographic expedition. The cruise was ideally set up to take advantage of these data. Because of the multiple passes that were taken up and

down the ridge to carry out the various phases of the ABE program, we were able to select stations on the basis of systematics that were apparent in the data. For example, the data enabled us to map out in detail separate petrological domains in some of the target areas, and to identify the region between Sites 2 and 3 as where the major geochemical changes took place. We were then able to focus in much more detail on this region to establish the nature of the chemical gradient and how it relates to the tectonics and segmentation of the ELSC.

Table 8- Precision of Shipboard DCP Analyses and of Standard Samples*

BATCH	SAMPLE	SiO2	SiO2	Al2O3	MgO	FeO	CaO	MnO	TiO2	Na2O	K2O	Sc	V	Cr	Ni	Cu	Sr	Ba	WEIGHT
Batch "4"	CHEPR25	49.79	50.24	15.56	7.62	9.71	11.27	0.179	1.91	3.05	0.298	39	264	253	94	70	179.6	32.8	49.0
BATCH 10	CHEPR25	50.30	50.12	15.90	7.39	9.73	11.21	0.179	1.93	3.08	0.298	39	294	252	99	70	184.6	33.7	49.9
BATCH 11	CHEPR25	50.34	50.39	15.87	7.42	9.61	11.03	0.173	1.95	3.06	0.310	40	285	232	94	70	183.6	35.0	48.3
BATCH 12	CHEPR25	50.67	50.24	15.67	7.48	9.67	11.28	0.179	1.93	3.07	0.301	39	284	250	94	69	187.7	34.2	49.0
BATCH 13	CHEPR25	50.21	50.21	15.79	7.45	9.60	11.31	0.180	1.93	3.06	0.298	40	286	253	97	70	182.2	33.0	53.3
BATCH 14	CHEPR25	50.59	50.30	15.71	7.47	9.78	11.07	0.181	1.94	3.09	0.303		294			76	182.8	33.0	49.1
BATCH 15	CHEPR25	50.13	50.19	15.69	7.51	9.79	11.11	0.181	1.94	3.08	0.307	39	294	259	100	72	181.3	33.9	47.7
BATCH 16	CHEPR25	50.50	50.26	15.71	7.53	9.82	11.02	0.184	1.92	3.08	0.299	40	297	250	106	75	182.7	34.1	48.8
BATCH 17	CHEPR25	49.97	50.31	15.62	7.53	9.74	11.15	0.178	1.93	3.03	0.302	40	280	253	100	69	188.4	34.7	48.3
BATCH 18	CHEPR25	50.63	50.28	15.76	7.42	9.82	10.98	0.178	1.93	3.17	0.306	40	295	265	95	74	182.1	32.7	47.9
BATCH 19	CHEPR25	50.26	50.46	15.78	7.41	9.72	11.05	0.178	1.92	3.00	0.298	37	272	251	95	71	183.5	33.9	49.0
BATCH 2	CHEPR 25 b	50.45	50.38	15.78	7.41	9.89	10.90	0.180	1.92	3.06	0.305	40	304	254	96	70	178.3	33.3	49.0
BATCH 3	CHEPR 25	50.65	50.18	15.75	7.39	9.70	11.35	0.175	1.93	3.08	0.293	37	256	251	100	63	181.6	32.3	50.0
BATCH 4	CHEPR25	50.07	50.11	15.69	7.57	9.70	11.23	0.181	1.94	3.10	0.305	40	300	255	100	70	181.0	33.6	48.0
BATCH 5	CHEPR25	50.39	50.34	15.80	7.35	9.74	11.10	0.179	1.94	3.06	0.301	38	297	251	96	68	182.9	34.1	48.3
BATCH 6	CHEPR25	51.04	50.36	15.67	7.43	9.72	11.15	0.180	1.94	3.08	0.294	39	305	252	101	72	184.4	35.7	47.5
BATCH 7	CHEPR25	50.24	49.94	15.85	7.53	9.79	11.17	0.180	1.96	3.13	0.307	40	302	262	100	68	183.8	34.3	50.2
BATCH 8	CHEPR25	50.24	50.13	15.90	7.46	9.73	11.12	0.180	1.96	3.05	0.302	39	293	252	98	69	185.4	34.3	51.0
BATCH 9	CHEPR25	50.16	49.63	15.75	7.46	10.22	11.04	0.195	1.89	3.13	0.292	36	275	244	112	77	174.6	34.0	50.6
BATCH R1	CHEPR25	50.15	50.25	15.51	7.58	9.73	11.23	0.184	1.95	3.08	0.303					81	182.1	33.2	48.0
BATCH R2	CHEPR25	50.53	50.07	15.70	7.57	9.80	11.23	0.182	1.94	3.03	0.307					76	181.8	33.8	48.4
BATCH16(	CHEPR25	49.91	50.17	15.72	7.51	9.78	11.13	0.180	1.94	3.09	0.308	39	303	257	101	77	182.0	35.3	48.9
AVERAGE		50.34	50.19	15.73	7.47	9.79	11.13	0.18	1.93	3.08	0.30	38.6	290.2	253.8	99.5	72	182.27	33.94	
%STDEV		0.6	0.4	0.6	1.0	1.4	1.0	2.5	0.9	1.49	1.8	3.5	5.4	2.2	4.6	6	1.7	2.7	

		SiO2	SiO2	Al2O3	MgO	FeO	CaO	MnO	TiO2	Na2O	K2O	Sc	V	Cr	Ni	Cu	Sr	Ba	WEIGHT
Batch "4"	NBS688	49.0	48.5	17.53	8.52	9.40	12.11	0.166	1.14	2.18	0.190	37	265	308	143	96	171	168.8	49.4
BATCH 10	NBS688	48.4	48.3	17.40	8.80	9.37	12.23	0.168	1.15	2.15	0.187	37	253	321	140	93	166	167.9	45.2
BATCH 11	NBS688	48.4	48.3	17.36	8.83	9.38	12.30	0.168	1.14	2.14	0.187	36	246	320	145	94	167	164.8	47.8
BATCH 12	NBS688	48.2	48.2	17.34	8.80	9.39	12.33	0.167	1.15	2.16	0.185	37	266	324	144	92	166	166.4	49.8
BATCH 13	NBS688	48.1	48.3	17.46	8.75	9.33	12.24	0.165	1.14	2.17	0.188	37	250	320	142	93	168	168.0	50.9
BATCH 14	NBS688	48.2	48.3	17.54	8.68	9.34	12.23	0.164	1.15	2.17	0.187		239			94	167	167.4	48.3
BATCH 15	NBS688	48.4	48.4	17.49	8.71	9.33	12.23	0.165	1.14	2.17	0.189	36	247	318	139	102	168	170.6	47.0
BATCH 16	NBS688	48.4	48.4	17.56	8.61	9.32	12.17	0.163	1.15	2.16	0.192	37	250	319	131	91	171	167.8	47.9
BATCH 18	NBS688	48.3	48.2	17.47	8.77	9.38	12.21	0.167	1.15	2.19	0.191	37	256	324	149	96	166	172.6	47.5
BATCH 19	NBS688	48.2	48.2	17.41	8.78	9.37	12.33	0.166	1.16	2.17	0.190	38	269	318	145	96	167	169.8	47.4
BATCH 2	NBS 688 a	48.2	48.3	17.42	8.77	9.31	12.28	0.167	1.16	2.15	0.189	37	250	308	137	93	165	173.2	47.9
BATCH 2	NBS 688 b	48.4	48.3	17.31	8.81	9.30	12.38	0.164	1.14	2.16	0.190	37	229	314	141	89	169	152.3	47.5
BATCH 3	NBS 688	48.6	48.4	17.55	8.64	9.27	12.23	0.162	1.13	2.14	0.187	36	221	316	141	94	172	171.1	47.4

* CHEPR 25 was run as an unknown in each run. NBS688, MAR and K1919 were used in the standard regressions.

Table 8 - Precision of Shipboard DCP Analyses and of Standard Samples*

BATCH 4	NBS688	48.4	48.3	17.36	8.76	9.26	12.42	0.165	1.14	2.11	0.186	37	226	315	135	89	169	163.6	47.7
BATCH 5	NBS688	48.4	48.4	17.42	8.79	9.41	12.13	0.166	1.14	2.16	0.188	37	239	323	142	92	166	170.4	45.1
BATCH 6	NBS688	48.2	48.4	17.48	8.70	9.42	12.08	0.165	1.14	2.16	0.187	37	251	324	143	98	166	163.2	45.2
BATCH 7	NBS688	48.4	48.4	17.38	8.76	9.27	12.37	0.165	1.15	2.13	0.184	36	244	314	143	93	167	167.6	48.1
BATCH 8	NBS688	48.5	48.2	17.47	8.80	9.35	12.23	0.166	1.16	2.15	0.187	38	249	331	142	91	167	166.9	47.1
BATCH 9	NBS688	48.1	48.4	17.44	8.74	9.20	12.34	0.165	1.16	2.13	0.189	36	271	327	134	91	171	164.1	48.3
BATCH R1	NBS688	48.2	48.3	17.50	8.70	9.32	12.27	0.164	1.14	2.19	0.187					88	167	161.9	47.5
BATCH R2	NBS688	48.2	48.3	17.42	8.74	9.37	12.25	0.165	1.15	2.21	0.188					86	167	169.8	47.3
BATCH16(	NBS688	48.6	48.4	17.41	8.70	9.29	12.33	0.167	1.15	2.15	0.197	38	243	324	139	94	168	167.8	48.1
AVERAGE		48.4	48.3	17.44	8.74	9.34	12.26	0.165	1.15	2.16	0.188	37	248	319	141	93	168	167.1	
%STDEV		0.4	0.2	0.4	0.8	0.6	0.7	0.8	0.7	1.06	1.5	1.7	5.4	1.9	3.0	4	1.2	2.7	

		SiO2	SiO2	Al2O3	MgO	FeO	CaO	MnO	TiO2	Na2O	K2O	Sc	V	Cr	Ni	Cu	Sr	Ba	WEIGHT
Batch "4"	MAR	49.3	49.7	15.19	9.28	9.99	11.63	0.180	1.24	2.55	0.086	39	244	331	139	75	91	6.1	51.1
BATCH 10	MAR	49.8	49.9	15.25	9.10	10.02	11.45	0.181	1.22	2.56	0.087	38	258	312	145	76	94	6.7	47.6
BATCH 11	MAR	50.0	50.0	15.29	9.04	10.00	11.35	0.180	1.23	2.58	0.088	38	264	307	141	74	93	6.4	48.0
BATCH 12	MAR	49.7	50.0	15.40	9.00	9.97	11.42	0.179	1.23	2.56	0.087	38	248	312	140	73	94	6.0	49.1
BATCH 13	MAR	50.0	49.8	15.34	9.10	10.01	11.47	0.181	1.23	2.56	0.085	39	272	313	146	76	94	6.2	51.5
BATCH 14	MAR	49.8	49.9	15.15	9.14	10.03	11.52	0.181	1.24	2.54	0.084		259			73	93	5.6	49.1
BATCH 15	MAR	49.8	50.1	15.27	9.02	10.06	11.35	0.181	1.23	2.55	0.087	38	260	314	140	72	93	6.2	48.0
BATCH 16	MAR	49.9	49.9	15.18	9.16	10.03	11.51	0.182	1.24	2.55	0.085	39	260	316	148	70	92	6.0	47.8
BATCH 17	MAR	50.0	49.9	15.16	9.13	10.04	11.51	0.181	1.22	2.57	0.086	39	268	323	147	75	92	6.4	48.0
BATCH 18	MAR	49.9	50.0	15.19	9.09	9.96	11.57	0.180	1.22	2.51	0.084	38	253	308	139	73	95	6.9	48.9
BATCH 19	MAR	49.7	50.1	15.21	9.06	10.00	11.37	0.180	1.23	2.56	0.087	38	253	316	143	75	93	6.1	47.8
BATCH 2	MAR	50.2	50.0	15.40	9.02	10.08	11.30	0.180	1.22	2.56	0.087	38	259	323	148	72	94	6.7	49.1
BATCH 2	MAR	49.5	50.0	15.15	9.23	10.06	11.36	0.185	1.24	2.52	0.084	39	278	306	131	80	91	7.4	48.6
BATCH 3	MAR	49.8	49.9	15.27	9.16	10.06	11.33	0.184	1.23	2.55	0.085	39	281	314	146	69	93	5.9	48.8
BATCH 4	MAR	49.9	49.9	15.31	9.09	10.06	11.33	0.181	1.22	2.57	0.087	38	267	317	148	75	92	6.3	47.9
BATCH 5	MAR	50.1	50.0	15.38	8.99	10.01	11.43	0.181	1.22	2.55	0.086	38	262	314	145	72	94	6.3	48.1
BATCH 6	MAR	49.9	49.8	15.19	9.18	9.99	11.57	0.181	1.22	2.53	0.086	38	257	302	142	72	94	5.9	47.1
BATCH 7	MAR	50.1	50.0	15.27	9.06	10.07	11.35	0.182	1.22	2.57	0.088	38	267	313	143	76	94	6.1	49.8
BATCH 8	MAR	49.8	50.0	15.22	9.05	9.99	11.48	0.182	1.21	2.56	0.087	38	261	307	145	74	95	6.0	49.4
BATCH 9	MAR	50.6	50.1	15.22	9.08	10.05	11.31	0.181	1.21	2.58	0.087	38	232	302	147	73	92	6.4	47.6
BATCH R1	MAR	50.0	49.9	15.27	9.09	10.04	11.44	0.182	1.23	2.53	0.084					76	94		48.8
BATCH R2	MAR	50.1	50.0	15.30	9.02	10.03	11.47	0.182	1.21	2.51	0.091					75	94	6.5	49.4
BATCH16(	MAR	49.8	49.9	15.29	9.12	10.02	11.47	0.181	1.22	2.55	0.083	38	266	311	146	75	93	6.0	47.8
AVERAGE		49.9	49.9	15.26	9.10	10.02	11.43	0.181	1.23	2.55	0.086	38	260	313	144	74	93	6.3	
%STDEV		0.5	0.2	0.5	0.8	0.3	0.8	0.7	0.7	0.79	2.0	1.1	4.3	2.2	2.9	3	1.3	6.2	

* CHEPR 25 was run as an unknown in each run. NBS688, MAR and K1919 were used in the standard regressions.

Table 8 - Precision of Shipboard DCP Analyses and of Standard Samples*

	SiO2	SiO2	Al2O3	MgO	FeO	CaO	MnO	TiO2	Na2O	K2O	Sc	V	Cr	Ni	Cu	Sr	Ba	WEIGHT
Batch "4" K1919	50.3	50.3	13.81	7.21	11.06	11.59	0.171	2.73	2.40	0.547	32	293	251	114	142	399	135.4	50.3
BATCH 10 K1919	50.4	50.3	13.97	7.03	11.07	11.57	0.171	2.73	2.38	0.542	33	305	251	109	146	404	136.7	50.0
BATCH 11 K1919	50.1	50.2	13.95	7.13	11.06	11.63	0.175	2.75	2.38	0.544	33	315	261	112	147	397	139.0	49.9
BATCH 12 K1919	50.4	50.3	13.84	7.16	11.10	11.48	0.172	2.73	2.40	0.546	33	305	250	114	148	402	137.9	50.0
BATCH 13 K1919	50.1	50.1	13.79	7.23	11.16	11.60	0.175	2.79	2.43	0.545	33	332	260	115	145	397	135.8	50.0
BATCH 14 K1919	50.4	50.3	13.89	7.14	11.09	11.46	0.173	2.73	2.41	0.546		319			145	401	137.4	50.0
BATCH 15 K1919	50.1	50.2	13.84	7.21	11.12	11.52	0.172	2.74	2.39	0.542	33	313	254	116	142	400	133.0	50.0
BATCH 16 K1919	50.3	50.3	13.84	7.17	11.11	11.52	0.174	2.75	2.40	0.546	33	318	255	118	150	402	136.8	50.0
BATCH 17 K1919	50.3	50.3	13.87	7.18	11.12	11.45	0.174	2.75	2.15	0.544	32	317	252	111	145	408	133.8	50.0
BATCH 18 K1919	50.3	50.3	13.88	7.10	11.14	11.51	0.171	2.75	2.40	0.540	33	310	253	112	146	398	129.7	50.0
BATCH 19 K1919	50.3	50.3	14.00	7.10	11.09	11.50	0.171	2.73		0.543	32	297	252	111	145	400	133.7	50.0
BATCH 2 K1919	50.2	50.3	13.77	7.17	11.10	11.63	0.172	2.73	2.40	0.544	33	311	256	113	147	402	129.4	50.0
BATCH 3 K1919	50.1	50.2	13.75	7.15	11.15	11.65	0.172	2.74	2.42	0.545	34	311	258	111	148	399	132.0	50.0
BATCH 4 K1919	50.3	50.3	13.89	7.15	11.04	11.60	0.171	2.72	2.38	0.542	33	306	250	110	146	401	138.7	50.0
BATCH 5 K1919	50.3	50.3	13.85	7.12	11.12	11.57	0.172	2.73	2.41	0.545	33	320	251	113	148	401	133.1	50.0
BATCH 6 K1919	50.4	50.2	13.94	7.08	11.09	11.60	0.172	2.74	2.40	0.544	33	315	261	117	146	399	141.0	50.0
BATCH 7 K1919	50.1	50.2	13.96	7.14	11.14	11.49	0.171	2.74	2.41	0.545	34	310	260	112	146	401	136.6	50.0
BATCH 8 K1919	50.3	50.4	13.87	7.09	11.12	11.49	0.173	2.73	2.40	0.547	33	308	246	112	149	403	138.7	50.0
BATCH 9 K1919	50.3	50.0	13.91	7.12	11.31	11.55	0.176	2.74	2.38	0.543	33	288	249	115	149	399	141.6	50.0
BATCH R1 K1919	50.2	50.3	13.77	7.21	11.12	11.52	0.174	2.75	2.19	0.544					150	397	140.9	50.0
BATCH R2 K1919	50.3	50.2	13.88	7.21	11.09	11.50	0.172	2.74	2.40	0.545					149	399	133.5	50.0
BATCH16(K1919	50.2	50.3	13.84	7.18	11.11	11.50	0.172	2.74	2.40	0.544	32	315	256	114	146	400	136.9	50.0
AVERAGE	50.3	50.2	13.87	7.15	11.12	11.54	0.172	2.74	2.38	0.544	33	310	254	113	###	400	136.0	
%STDEV	0.6	0.4	0.6	1.0	1.9	1.0	2.5	0.9	1.5	1.8	3.5	5.4	2.2	4.6	6.4	1.7	2.7	

* CHEPR 25 was run as an unknown in each run. NBS688, MAR and K1919 were used in the standard regressions.

Education and Outreach

A comprehensive educational website developed for the Ridge2000 "South Pacific Odyssey" program made its debut during Cruise KM0417. Kristen M. Kusek, a science writer who has worked as a consultant with Liz Goehring (coordinator, education outreach) and team at the Ridge2000 office since November 2003, joined the expedition. The website was intended to reach a general public audience, and will cover the remaining cruises in the Lau Cruise series sponsored by Ridge2000. A combination of dispatches (science updates) and feature stories were emailed regularly to the Ridge2000 office every 2-3 days throughout the 37-day expedition, as were images highlighting the action. Members of the science crew were also encouraged to submit articles.. The site material is included as Appendix 15 of this report. The Ridge2000 office is hosting the site and is responsible for maintaining all web-related statistics. Key pieces of information on the website will likely be repackaged subsequent to the cruise for use by various learner groups (http://www.venturedeepocean.org/).

GIS

Data from this cruise was imported into ArcMap, a geographic information system (GIS), to aid in the visualization and consolidation of complex and diverse data sets. Martinez et al. collected both hull mounted (Simrad EM120) and deep tow (DSL120) sonar. These maps served as a guide for our sampling and a base on which to overlay our data. Onboard the ship we collected three distinct types of data: (1) Rock samples/chemistry, (2) Water samples/chemistry, as well as (3) sonar and imagery data. Putting the information into a geospatial database gives the data created by diverse instruments a common reference frame and standardizes the format in which the data is reported. Below is a summary of the information contained in the database.

Rock Sampling and Rock Chemistry

Wax Cores

The database contains the latitude and longitude of the point at which the core was deployed from the ship, the Julian day, comments about the core, wire out upon impact, as well as a chemical analysis (if available). The chemical analyses were conducted onboard using a direct current plasma (DCP) system. Information about silicon, titanium, aluminum, iron, manganese, magnesium, calcium, sodium, and potassium are reported as weight percent oxides, while scandium, vanadium, chromium, nickel, copper, strontium and barium are reported in parts per million.

Dredges

The information for dredges is split into two databases. The first contains the latitude, longitude, Jday, and wire out for both the on and off bottom locations for each dredge. This database also contains the DCP chemistry in an identical format to that of the wax cores. The second part of the database contains the ship's navigation, sampled every minute, while the dredge was on bottom.

TowCam
Latitude, longitude, wire out, Jday, and a comment are recorded for each rock samples obtained during a TowCam run.

Water Sampling and Water Chemistry

CTD
To correct for the horizontal distance between the ship and an instrument in tow Dr. Paul Asimow constructed a program that uses the wire out as reported by the winch, instrument depth, and ship position at a given point in time and calculates a corrected position for the instrument, the horizontal distance that separates the instrument and ship is also known as the layback. All CTD information in the database is "layback corrected" and reported every second. A description of the calculation and code of the program is in Appendix 9). To smooth navigational jitter as recorded by the POS-MV, the navigation files were first smoothed using a median filter followed by a Gaussian filter. The smoothed navigation was then input to the layback calculation. While this calculation dramatically improves instrument position, it does not give the accuracy provided by a relay transponder. This layback corrected position is the first column in all of the CTD tables located in Appendix 10. The tables combine the data recorded by the CTD with the day, date, wire out, latitude and longitude of the ship at that point in time.

TowCam
The same layback correction that was applied to CTD casts was also used on all TowCam runs. The tables for each camera tow are similar in structure to those of the CTD. Instrument latitude and longitude, operation (i.e., firing of bottles or waxballs), ship navigation and winch information, are combined with all data recorded by the Seabird system aboard the Towcam at one second intervals. The last column of the table contains the filenames of the pictures taken, effectively assigning each picture an x,y,z location.

ABE
The information that ABE records during a dive was also included in the geospatial database. Position, depth, time, pressure, heading, temperature, conductivity, current information, and iron counts (where applicable) are all recorded for each ABE dive. Two tables were made for each dive; the first is an average of the instrument readings averaged every second, while the second is a five second average of instrument readings.

Sonar Data

The Simrad hull mounted sonar was used to collect data during the cruise. After a SABER area-based editor was used to process this data it was put into ArcMap.

ABE also has the ability to make very high resolution maps using its sonar system. Abe successfully mapped portions of sites 1-5 with one to two meter resolution, and these maps are included in the GIS.

Data Integration

The various data that were put into the GIS enabled diverse views of the data products from many different perspectives. Examples of the data visualization made possible by the GIS are illustrated in the following figures.

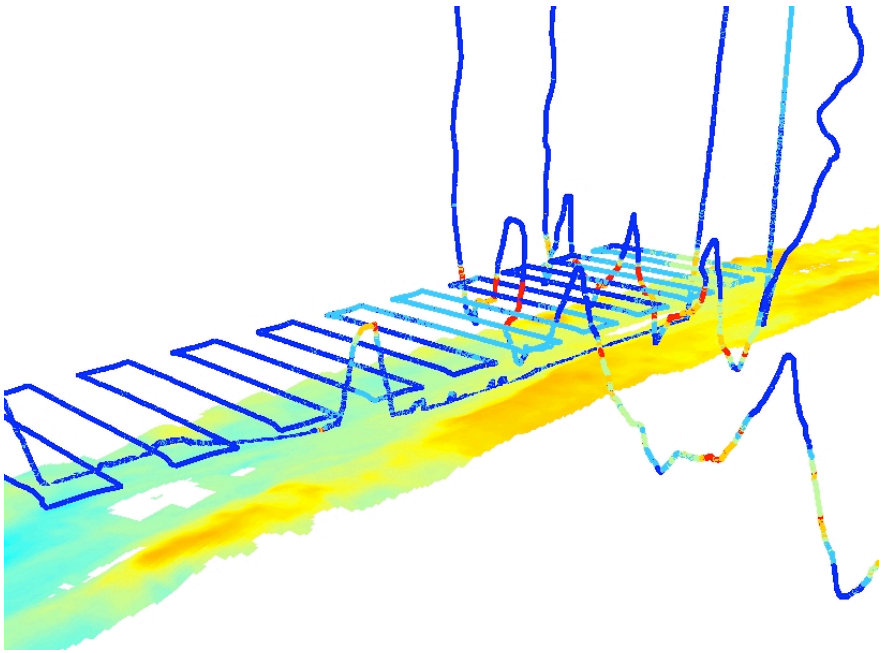

Figure 60: Water column data from both ABE dive and CTD tow-yo shown over multibeam bathymetry

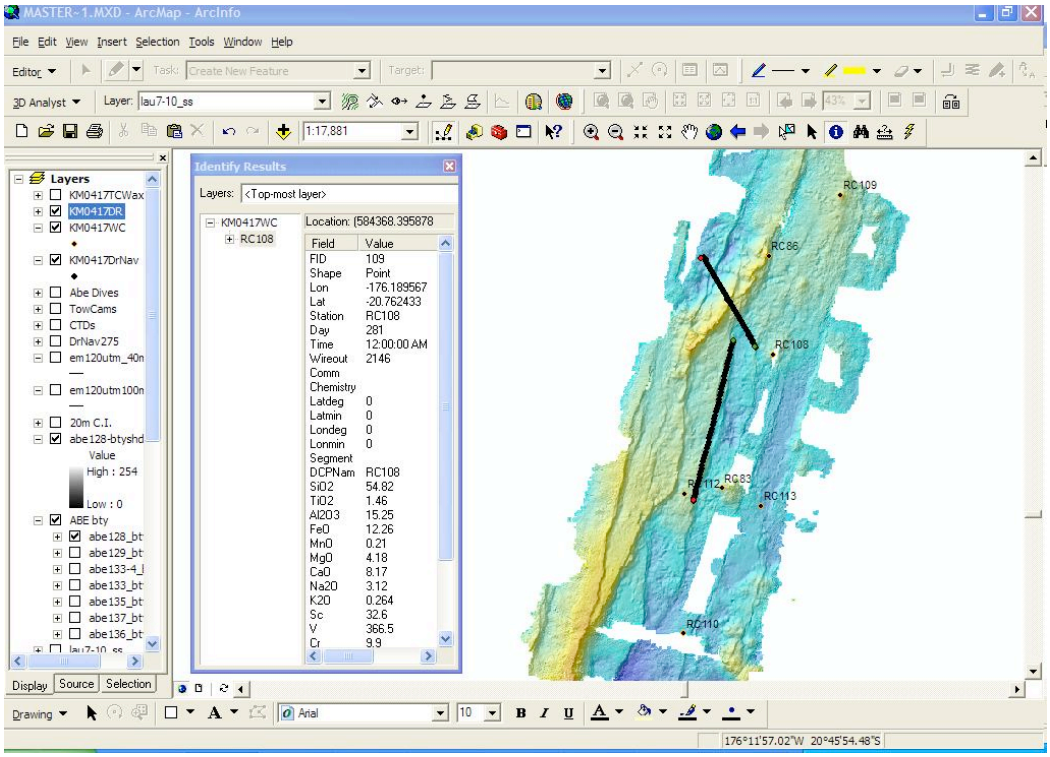

Figure 61: Dredge tracks and rock chemical compositions shown over SM2000 bathymetry from Site 3.

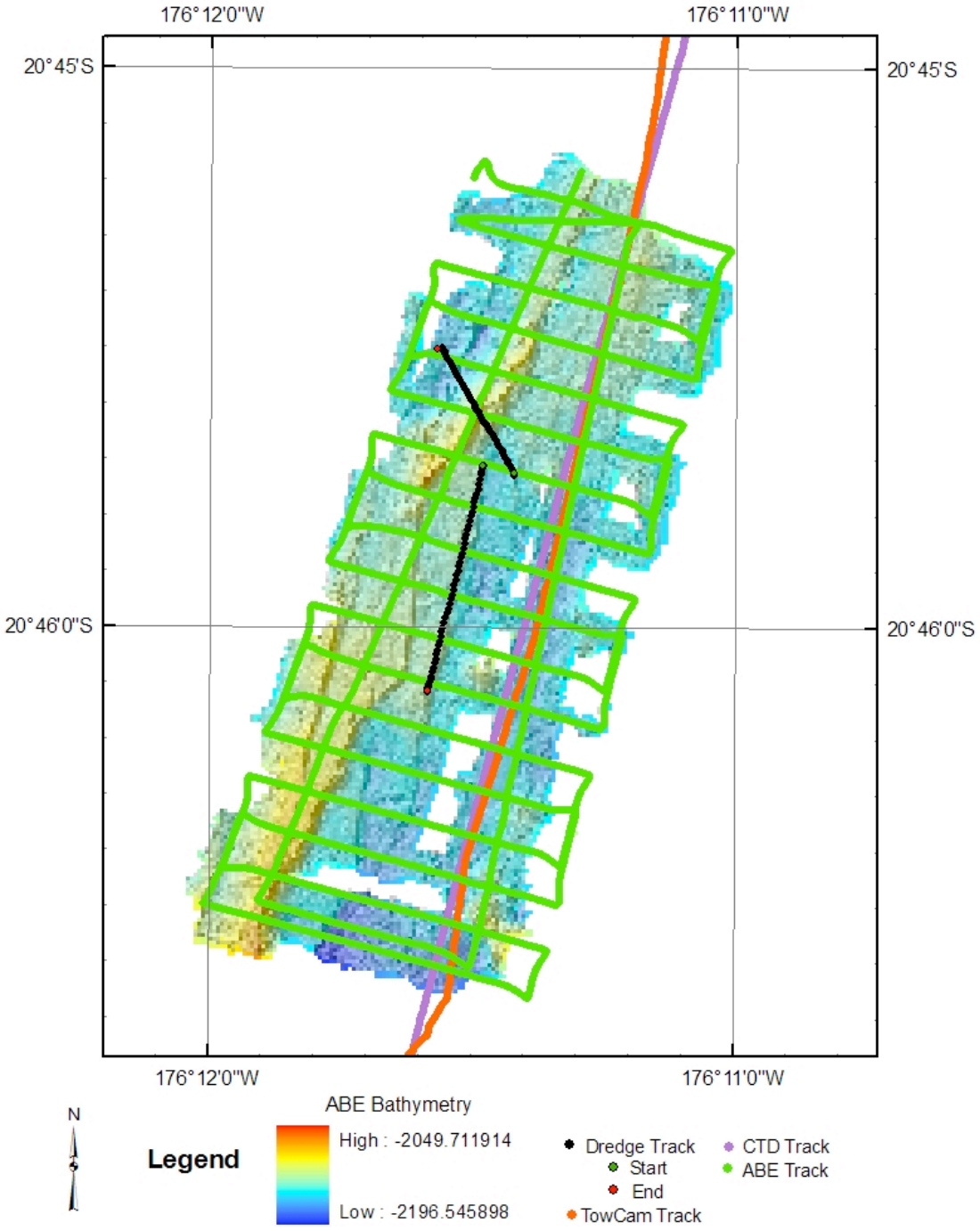

Figure 61: Dredge, TowCam, ABE navigation and CTD tracks shown over the ABE SM2000 bathymetry for Site 3.